School of Mining Engineering

UNIVERSITY OF THE WITWATERSRAND, JOHANNESBURG

GEOZONE DEFINITION OF THE UG2 REEF FOR IMPROVED MINERAL RESOURCE ESTIMATION BASED ON STATISTICS AND GEOSTATISTICS AT AMANDELBULT PLATINUM MINE, THABAZIMBI

Maja Ruddy Maakamedi

Student Number: 605153

Supervisor: Clinton Birch

Co supervisor: Professor Christina Dohm

A research report submitted to the Faculty of Engineering and the Built Environment, University of the Witwatersrand, Johannesburg, in partial fulfilment of the requirements for the degree of Master of Science in Engineering.

Johannesburg, 2020

DECLARATION

I declare that this report is my own, unaided work. I have read the University Policy on Plagiarism and hereby confirm that no plagiarism exists in this report. I also confirm that there is no copying nor is there any copyright infringement. I willingly submit to any investigation in this regard by the School of Mining Engineering and I undertake to abide by the decision of any such investigation.

_______________________________ 30 October 2020

Signature of Candidate Date

ABSTRACT

The economic viability of any mine is underpinned by its Mineral Resource estimation. Crucial to this is the utilisation of all relevant and available data, to ensure that the resource evaluation process is comprehensive and carried out to the highest standard possible. There is always the case, where, in the initial development stages of a mine project limited data is available however, as the project progresses information regarding the orebody usually also increases. The increase in information opens an opportunity to assess whether the existing estimation method remains suitable and also allows for the modification of the current estimation method to better suit the behaviour of the orebody based on the additional new information.

Standard procedure when carrying out a Mineral Resource estimate is to split the orebody into zones that show statistical and geostatistical homogeneity i.e. similar characteristics for example grade and or reef thickness. Of course, when data is limited this privilege might not be possible. The reason being that geostatistics rely of an assumption of second order stationarity which means that the mean and co-variance is consistent irrespective of the location within the orebody, an assumption that cannot be validated with limited data.

In recent years the Amandelbult UG2 reef database increased in terms of both surface borehole intersections and underground channel sampling. Splitting the UG2 orebody into homogeneous zones for resource estimation using statistics as well geostatistics is outlined in this research report. Statically the orebody thickness, density and platinum grade show variation across the area of interest, this allowed for subdivision of the orebody into several homogeneous geozones. Both the descriptive statistics and graphical data summaries confirmed local variation in these three variables. The geostatistical analysis involved the creation of two sets of variograms, one for each identified geozone and a global variogram ignoring the individual identified geozones within the project area. Ordinary kriging was used to estimate the UG2 orebody thickness, density and platinum grade using these variograms. A comparison was conducted to check if the quality of the estimates improved by comparing the true values and estimated values and the correlation coefficient of the two indicated that the estimates were improved when using individual variograms rather than a global variogram. Additionally, comparisons of the errors from the true values and estimated values indicate that the Mean Absolute Error and Root Mean Error are reduced when using separate variograms rather than using a global variogram when solving the kriging solutions. In conclusion this research study has shown that by delineating the orebody into homogeneous zones for thickness, density and platinum grade and applying ordinary kriging using the relevant individual geozone variograms resulted in improved block estimates for Amandelbult UG2 reef.

ACKNOWLEDGEMENTS

First and foremost, I would like to thank God for giving me the strength and persistence to complete my studies. The support and understanding of my wife Pertunia Maakamedi and daughter Neo-Entle Maakamedi, is well appreciated especially for the times when I was away and when I had to go into seclusion to study. My love for mathematics ultimately led me into the world of geostatistics, am grateful for the passion and time my high school teacher (Mr. A .Horn) took in making me enjoy the subject. Mrs Nawaal Tendaupenyu is acknowledged for being a mentor and introducing me to Resource Estimation. Prof. Christina Dohm is highly thanked for the time, abundance of knowledge shared and guidance. My supervisor Mr. Clinton Birch is thanked also for the time and suggestion that have gone into the completion of this research report. Lastly, I would like to thank Anglo American Platinum and its great employees (past and present) and my amazing colleagues who have given assistance, guidance, understating, patience and many opportunities for me to grow into the person I am today, for this I will forever be indebted.

TABLE OF CONTENTS

DECLARATION i

ABSTRACT ii

ACKNOWLEDGEMENTS iv

LIST OF FIGURES ix

LIST OF TABLES xvi

1 INTRODUCTION 1

1.1 Background 1

1.2 Project location 1

1.3 Geological Setting 4

1.3.1 The Bushveld Complex 4

1.3.2 Geology of the Bushveld Complex Western Limb 6

1.3.3 Mine geology 13

1.4 Problem Statement 19

1.5 Research Motivation 21

1.6 Research Objectives 21

1.7 Overview of the Research Report 22

2 LITERATURE REVIEW 24

2.1 Introduction 24

2.2 Random and Regionalised Variables 24

2.3 Statistics in Earth Sciences 25

2.4 Geostatistics 27

2.5 Variography 28

2.6 Estimation of Mineral Resources 31

2.7 Kriging 32

2.8 Ordinary Kriging 34

2.8.1 Kriging variance 35

2.8.2 Block variance 36
2.8.3 Kriging efficiency 36
2.8.4 Slope of regression.. 37
2.9 Orebody Domaining.. 37
2.9.1 Case studies on orebody domaining 39
2.10 Conclusion.. 44
3 RESEARCH METHODOLOGY 45
3.1 Introduction.. 45
3.2 Data Assembly.. 45
3.3 Global Data Analysis and Classed Data Posting 45
3.4 Exploratory Data Analysis.. 46
3.5 Geological Study.. 47
3.6 Variography 47
3.7 Kriging Neighbourhood Study.. 48
3.8 Estimation and Results Comparison.. 48
3.9 Conclusion.. 49
4 DATA DESCRIPTION 50
4.1 Introduction.. 50
4.2 Data Acquisition and Sources.. 50
4.2.1 Channel samples.. 51
4.2.2 Borehole Information 52
4.2.3 Assay and Density Determination Techniques 52
4.3 Data Validation 53
4.3.1 Channel and borehole validation 53
4.3.2 QA/QC... 55
4.4 Conclusion.. 56
5 ANALYSIS OF THE DATA SET... 57

5.1 Introduction 57
5.2 Orebody Thickness 61
5.2.1 Thickness (cm) analysis 61
5.2.2 Thickness statistics 64
5.2.3 Influence of geology on the thickness of the orebody 71
5.2.4 Thickness variography 73
5.3 Density 81
5.3.1 Density (t/m^3) analysis 81
5.3.2 Density statistics 85
5.3.3 Influence of geology on the density 88
5.3.4 Density variography 90
5.3.5 Re-assessment of D-Zone 3 92
5.4 Platinum 98
5.4.1 Platinum (g/t) analysis 99
5.4.2 Platinum statistics 102
5.4.3 Influence of geology on the platinum grade 105
5.4.4 Platinum variography 107
5.5 Optimum Block Size Determination Based on the Zone Variograms 110
5.5.1 Optimum block size for the orebody thickness study 111
5.5.2 Optimum block size analysis for the orebody density 116
5.5.3 Optimum block size analysis for the orebody platinum grade. 120
5.5.5 Conclusion of the block size study 124
5.6 Block Estimation 124
5.6.1 Thickness estimation 129
5.6.2 Density estimation 134
5.6.3 Platinum estimation 138
5.7 Conclusion 140

6 RESULTS AND DISCUSSION 142
6.1 Introduction 142
6.2 Data Posting 142
6.3 Statistical Analysis 142
6.4 Geology 143
6.5 Geostatistical Analysis 144
6.6 Optimum Block Analysis 145
6.7 Kriging Estimation Results 145
7 CONCLUSION 146
8 RECOMMENDATIONS 148
RERERENCES 151
APPENDIX 159

LIST OF FIGURES

Figure 1: Map of the platinum mines operating in the Bushveld complex. Source: Makgato and Laubscher (2018). 2

Figure 2: Topographical-cadastral map showing extend of the Amandelbult complex and constituting farms. Source: Makgato and Laubscher (2018). 3

Figure 3: Arial distribution of the Bushveld Complex, indicating the distribution of the Lebowa Rashoop, RLS and the Rooiberg volcanics. Modified from Eales (1996); Eales *et al.* (1993). 5

Figure 4: Stratigraphic column of the RLS Mafic and Ultra Mafic sequence of the Bushveld Complex. Source: Zientek et al. (2010). 7

Figure 5: Geological map of the Western Limb RLS of the BC. Modified from Hatton and Gruenewaldt (1985); Viljoen *et al*. (1986); Scoon and Teigler (1994). 10

Figure 6: Geology map of the Bushveld complex north of the Pilanesberg Complex, showing the gab areas between Union and Amandelbult compartments. Source: Geological Survey, South Africa, in Coertze (1958). 11

Figure 7: Section through the northern gab area. Modified from Wilson *et al.* (1994). 12

Figure 8: Stratigraphic column of Amandelbult Section. Modified after Sibiya (2017). 13

Figure 9: Geological structure plan of Amandelbult complex showing the main structures across the property. Source: Dishaba Mine (2019). 17

Figure 10: The PGE distribution of the UG2 chromite orebody across the Bushveld complex. Source: Maier and Barnes (2008). 18

Figure 11: An example of an experimental and modelled variogram. Source: Dohm (2018a). 29

Figure 12: Geozones plan of the different facies of the UG2 identified from exploration data. Source: Davey (1992). 43

Figure 13: PGE grade profile of two UG2 facies at Rooikoppies. Source: Davey (1992). 44

Figure 14: Spatial plot of the dataset. 51

Figure 15: Examples of histograms. Source: Doane and Seward (2011). 59

Figure 16: An examples of a colour coded map to illustrate levels of phosphorus levels for a season and year. Source : Zapata-Rios *et al*. (2012). 60

Figure 17: Colour coded map showing levels of arsenic in drinking water in eastern Michigan. Source AvRuskin *et al*. (2004). 61

Figure 18: Histogram and summary statistics of the orebody thickness. 62

Figure 19: Cumulative plot of the orebody thickness. 63

Figure 20: Thickness (m) classed post map. 64

Figure 21: Stacked cumulative plot of the orebody thickness of the various zones. 66

Figure 22: Histogram of the various zones and global zone. 67

Figure 23: Box plot of the thickness of the orebody of the various zones. 68

Figure 24: Q-Q plots of the orebody thickness of the various zones. 70

Figure 25: Thickness zones and data superimposed onto geological structures. 72

Figure 26: Illustration of the influence of increased internal waste within the reef on orebody thickness. 73

Figure 27: An example of how lag tolerance and direction tolerance is applied to select samples to pair with the point at (x, y) in practice. A sample falling within the shaded are will be paired with the sample at (x, y). Source: Isaaks and Srivastava (1989). 75

Figure 28: Example of a variogram with experimental points and model fitted. Source: Course exercise for Dohm (2018a) 75

Figure 29: An example of a variogram and its features. Modified from Guibal (2001). 76

Figure 30: Influence of the nugget effect on the various kriging performance measures. Source: assignment for Dohm (2018a).................................. 77

Figure 31: Types of variogram models, modified after (Clark, 1979). 78

Figure 32: Experimental variograms of the orebody thickness with fitted models. 79

Figure 33: Theoretical variograms of the thickness zones. 80

Figure 34: Histogram of the density data (t/m3)... 82

Figure 35: Cumulative frequency plot of the orebody density. 82

Figure 36: Classed data post of the orebody density (t/m^3). 84

Figure 37: Density histograms (UG2). 86

Figure 38: Cumulative frequency plot of the density. 87

Figure 39: Density box plots. 87

Figure 40: Q-Q plot of the density for the various zones.................................... 88

Figure 41: Geology superimposed onto the density zones 89

Figure 42: Comparison of two borehole density profiles where the internal waste is minimal and where it is excessive. 90

Figure 43: Experimental variogram of the orebody density of the various zones. 91

Figure 44: Data posting of D-Zone 3 with subsequent split into D-Zone 3-1 and D-Zone 3-2. 92

Figure 45: Histogram of the D-Zones 3-1, 3-2, 3 and the global area. 94

Figure 46: Combined cumulative frequency plot of the various zone. 95

Figure 47: Box plot of the density of the various zones. 95

Figure 48: Q-Q plot of density zone 3-1 and 3-2. 96

Figure 49: Experimental variogram of the orebody density of the various zones. 97

Figure 50: Theoretical variograms of the density. 97

Figure 51: Histogram of the platinum grade. 99

Figure 52: Cumulative frequency plot of the platinum grade (g/t). 100

Figure 53: Classed post map of the Platinum grade g/t. 101

Figure 54: Platinum Histograms of the various zones. 103

Figure 55: Cumulative frequency of the Platinum grade for the various zones. 104

Figure 56: Platinum box plots for the various zone. 104

Figure 57: Q-Q plots of the platinum zones. 105

Figure 58: Platinum zones in comparison with geological structures 106

Figure 59: Grade profile comparison of two boreholes with one having minimal internal waste and the other extensive. 107

Figure 60: Experimental variograms of the Platinum and fitted models. 108

Figure 61: Stacked theoretical variograms of the Platinum grade. 108

Figure 62: KNA test blocks with data distribution for the thickness zones. 112

Figure 63: Results of the block size analysis for the well informed thickness areas. 113

Figure 64: Results of the block size analysis for the moderately informed thickness areas. 114

Figure 65: Results of the block size analysis for the poorly informed thickness areas. 115

Figure 66: Selected test blocks with data distribution for the density zones. 116

Figure 67: Results of the block size analysis for the well informed density areas. 117

Figure 68: Results of the block size analysis for the moderately informed density areas. 118

Figure 69: Results of the block size analysis for the poorly informed density areas. 119

Figure 70: selected test blocks with data distribution for the Platinum grade zones. 120

Figure 71: results of the block size analysis for the well informed platinum areas. 121

Figure 72: Results of the block size analysis for the moderately informed platinum areas. 122

Figure 73: Results of the block size analysis for the poorly informed platinum areas. 123

Figure 74: An example of a block model. Source: Poniewierski (2019). 125

Figure 75: 2D 250m x 250m and 500 x 500m block model (blue blocks) over the study area with the data (red) location plot. 126

Figure 76: Thickness zones estimates for the global area and the zoned areas for 250x250m-500x500m blocks. 130

Figure 77: Histogram of residuals showing a case where there is negative bias, positive bias and no bias in the estimation errors. Source: Isaaks and Srivastava (1989). 131

Figure 78: Scatter plot of true values and estimated values. A closer cloud of points is preferred (b) as opposed to a more spread of points (a). Source: Isaaks and Srivastava (1989). 132

Figure 79: Scatter plots of the true value and estimates for the global and T Zones area. 133

Figure 80: Block estimates of the density (t/m^3) for the global area and zone areas. 136

Figure 81: Scatter plots of the density true value and estimates for the global and D-Zone area. 137

Figure 82: Platinum grade block estimates for the global and the Pt-Zones. 139

Figure 83: Scatter plots of the true value and estimates for the global and Pt-Zone area. 140

Figure 84: Zones identified for the orebody thickness, density and platinum grade with the respective mean (m) and variance (m^2) of each zone. 159

Figure 85: Post maps of the orebody thickness (m) at various intervals. 160

Figure 86: Post maps of the density (t/m^3) at various intervals. 161

Figure 87: Post maps of the platinum grade (g/t) at different intervals. 162

Figure 88: Scatter plot of the true values and estimated values using T-Zone 1 variogram (a) and Global variogram (b). 163

Figure 89: Scatter plot of the true values and estimated values using T-Zone 2 variogram (a) and using the Global variogram (b). 163

Figure 90: Scatter plot of thickness the true values and estimated values using T-Zone 3 variogram (a) and using the Global variogram (b). 164

Figure 91: Scatter plot of the thickness true values and estimated values using T-Zone 4 variogram (a) and using the Global variogram (b). 164

Figure 92: Scatter plot of the density true values and estimated values using D-Zone 1 variogram (a) and using the Global variogram (b). 165

Figure 93: Scatter plot of the density true values and estimated values using D-Zone 2 variogram (a) and using the Global variogram (b). 165

Figure 94: Scatter plot of the density true values and estimated values using D-Zone 3-1 variogram (a) and using the Global variogram (b). 166

Figure 95: Scatter plot of the density true values and estimates values using D-Zone 3-2 variogram (a) and using the Global variogram (b). 166

Figure 96: Scatter plot of the platinum grade true values and estimated values using Pt-Zone 1 variogram and using the Global variogram (b)............. 167

Figure 97: Scatter plot of the platinum grade true values and estimated values using Pt-Zone 2 variogram and using the Global variogram (b)............. 167

Figure 98: Scatter plot the platinum grade true values and estimated values using Pt-Zone 3 variogram and using the Global variogram............................ 168

LIST OF TABLES

Table 1: Summary statistics of the orebody thickness for the various thickness zones. 65

Table 2: Values used in experimental variogram calculation. 78

Table 3: Thickness variogram model parameters for the various zones. 81

Table 4: Summary statistics density (t/m^3) for the various zones. 85

Table 5: Experimental variogram calculation values for the density. 91

Table 6: Density variogram model parameters. 91

Table 7: Summary statistics of D-Zone 3 redefined. 93

Table 8: Values used for the calculation of the density experimental variogram. 98

Table 9: Density variogram model parameter values. 98

Table 10: Summary statistics of the Platinum grade for the various zones. 102

Table 11: Platinum experimental variogram data input values. 109

Table 12: Platinum variogram model parameter values. 109

Table 13: Variogram parameter file. 128

Table 14: Statistics of the estimation errors of the Global and T-Zone area estimates. 134

Table 15: Comparison of the model results and the data of the density. 137

Table 16: Comparison of the model result and the data of the platinum grade. 140

1 INTRODUCTION

1.1 Background

The main objective of resource estimation in mining is to obtain a best estimate of the resource that is envisaged to be extracted or is in the process of extraction. Failure to meet this objective leads to either over or underestimation of the potential of the orebody which in turn has a spiral effect affecting every stage of extraction, from ore breakage cost expectations to beneficiation.

Additional information regarding the orebody will in most instances improve the interpretation of the orebody, quality of the estimates and their confidence. As this information increases it is necessary to validate and determine whether the assumptions that were made prior to acquiring the new information are still valid. This process gives one an opportunity to adjust certain parameters during estimation in order to improve estimates.

In this research the effect of domaining the orebody prior to resource estimation is investigated on a platinum deposit at Amandelbult Mine focusing on the Upper Group 2 reef (UG2) in the Western Limb of the Bushveld Complex using ordinary kriging as the estimator. The source of data comprises of assays from drill holes (surface and underground), underground channel samples and geological logging and mapping data. The following variables are available from the different data sources: assay results of platinum, palladium, rhodium, gold, nickel, copper, chrome oxide, width of orebody, rock density and geological lithological data. Due to time constraints only the orebody thickness, density and platinum data will be used for investigation in this research.

Glacken and Snowden (2001); Coombes (2008); Rossi and Deutsch (2014) cover the necessity to domain the deposit during a Mineral Resource estimation. Domaining results in more homogenous grade zones and this then allows for improved variography which ultimately results in robust estimates if the domaining in correct and reflects the true behaviour of the variable under study.

Variability of the orebody Platinum Group Elements (PGE) grade, width, density and local geology necessitates the need for geozoning. This allows for separate populations to be grouped together based on similarity or differences when analysed statistically and geostatistically. Estimation can then be conducted on these separate populations which can result in improved block estimates, specifically in terms of estimation confidence. Appropriate geozoning is likely to increase confidence in estimates as variability is reduced and consequently a reduction in resource risk.

Since geostatistics depends on probabilistic modelling and the utilisation of variograms, the stationarity of the random function is critical for meaningful variography and as such domains showing noteworthy differences in the population mean and variance should be dealt with separately.

"The identification of geological homogeneous zones is important in that it goes a long way towards ensuring stationarity" (Dohm, 2003, p. 351).

1.2 Project location

Amandelbult Complex is situated in Limpopo province and falls within the Waterberg District Municipality and is divided into two mines namely Tumela Mine and Dishaba Mine (Figure 1). The two mines are approximately 12km apart on the strike of the orebody. The stretch of the orebody is ~22km on strike within a 14134 hectares lease (Figure 2) formed by the farms Moddergat 389 KQ, Ellandsfontein 386 KQ, Schildpadnest 385 KQ Middlellaagte 382 KQ, Amandelbult 383 KQ, Elandskuil 378 KQ and Haakdoringdrift 374 KQ (Makgato & Laubscher, 2018). Tumela mine is 16km north of Northam whilst Dishaba Mine is 25km south of Thabazimbi. The topography is flat except for two small mountains west of Tumela mine (Viljoen *et al*., 1986). Production is from the Merensky Reef and Upper Group (UG2) reefs, with production emphasis shifting to the UG2 orebody due to a depletion of the Merensky Reef. A system of two vertical shafts and declines are utilised to access the orebody via the conventional drill and blast mining method (Anglo American Plc, 2018). A small-scale open cast operation which goes to 40-80m down dip is used to extract the two orebodies along the sub-outcrop close to surface

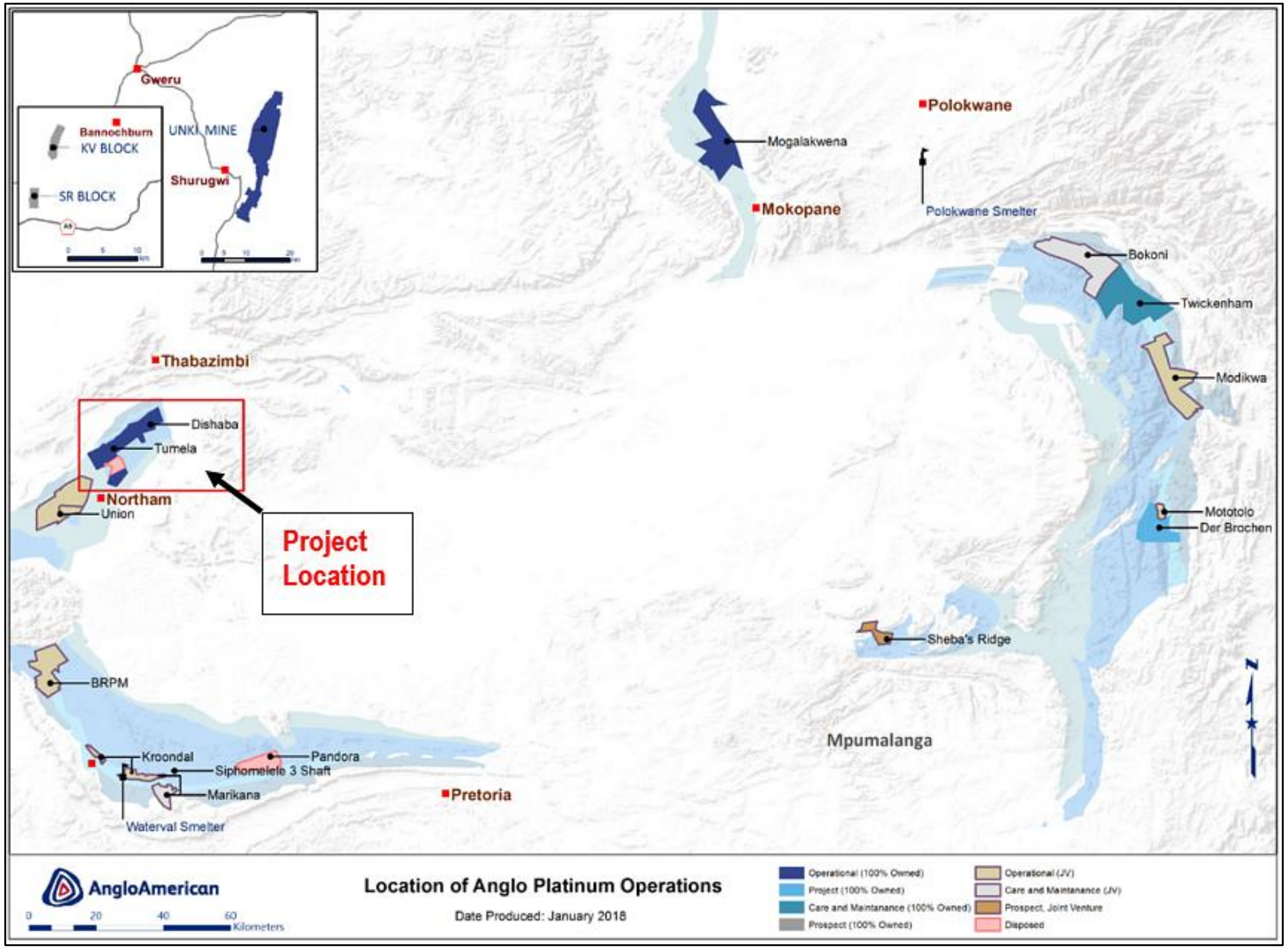

Figure 1: Map of the platinum mines operating in the Bushveld complex. Source: Makgato and Laubscher (2018).

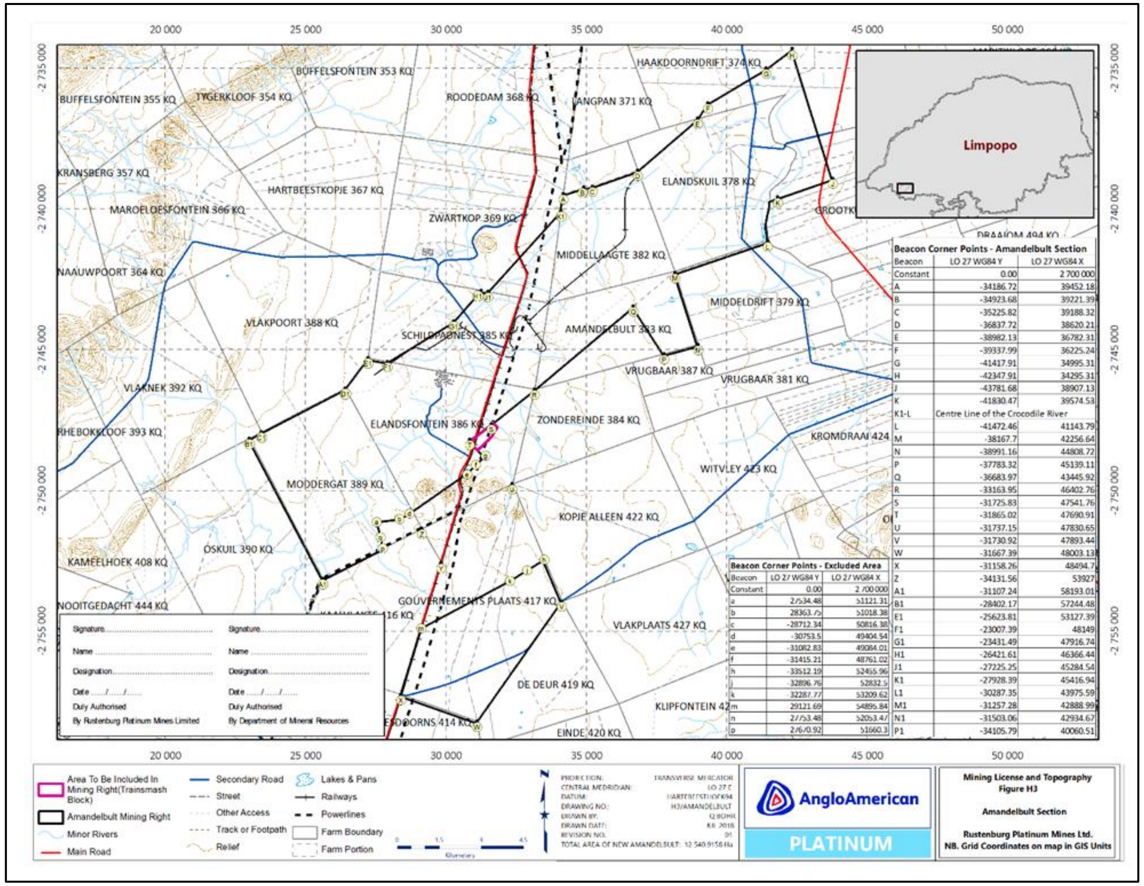

Figure 2: Topographical-cadastral map showing extend of the Amandelbult complex and constituting farms. Source: Makgato and Laubscher (2018).

1.3 Geological Setting

1.3.1 The Bushveld Complex

The formation of the complex is dated to be approximately 2050 Ma (Scoates & Friedman, 2008) when magma made its way onto the surface of the earth and resting on older rocks through three main events: a volcanic event, a first intrusive event and lastly a second intrusive event (McCarthy & Rubidge, 2005). The magma crystalized through cooling forming new igneous rocks whilst the older existing rocks underwent metamorphism as a result of the interaction with hot magma. The Bushveld Complex (BC) is divided into 5 major lobes or limbs (Figure 3), a far-western lobe, an eastern and western lobe, a north lobe and lastly the Bethal Lobe (Teigler & Eales, 1993). The three events resulted in the formation of the BC dividing it into three main parts the Rooiberg Group, the Rustenburg Layer Suite (RLS) and the Lebowa Granite Suite which all sit on the sedimentary rocks of the Transvaal Supergroup.

One of the most well studied formation of all the BC is the RLS. The reason for the interest in the RLS is that it hosts considerable amounts of chromite, platinum, palladium, rhodium and vanadium. The RLS is an approximately 9km thick succession of layered mafic and ultramafic rocks subdivided in six major zones (Marginal, Lower, Lower Critical, Upper Critical, Main and Upper Zones) with the zones divided by the dominant minerals and rock type found that particular zone (Eales, 2001).

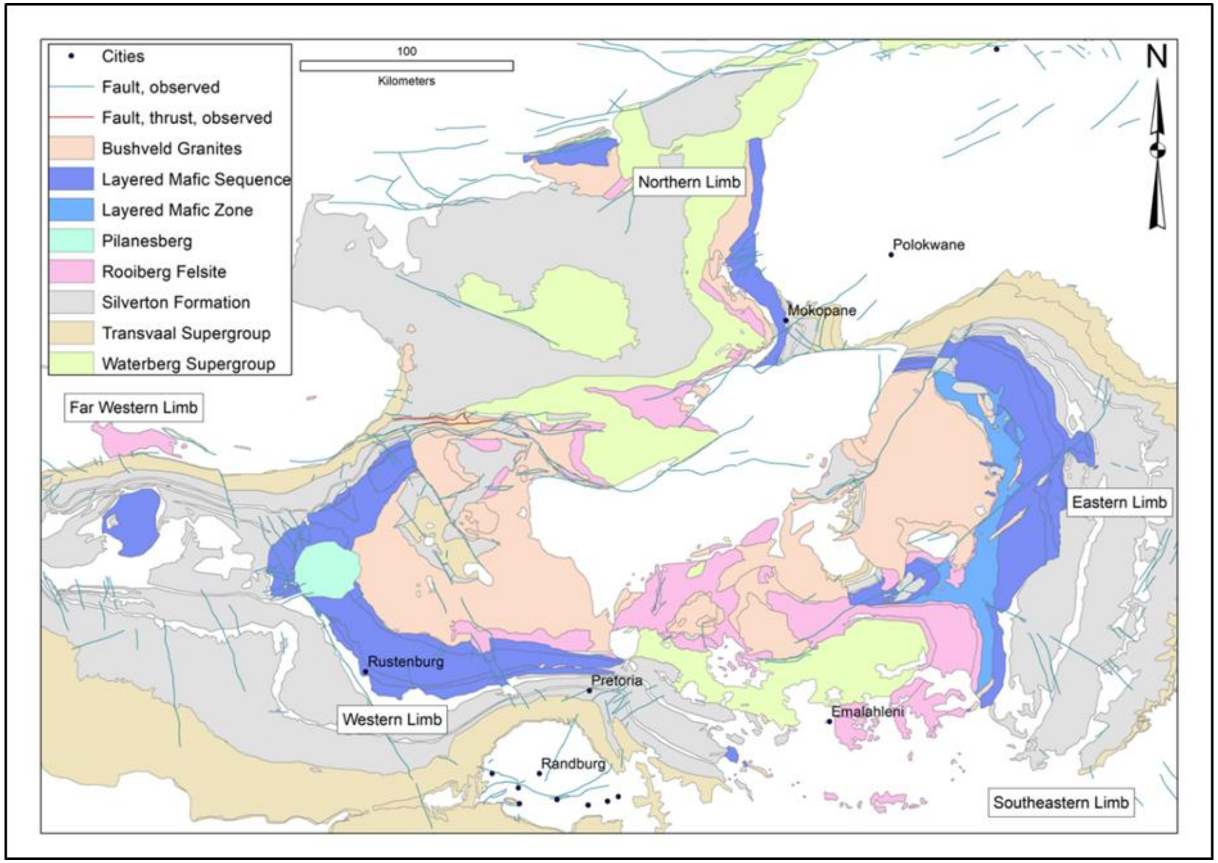

Figure 3: Arial distribution of the Bushveld Complex, indicating the distribution of the Lebowa Rashoop, RLS and the Rooiberg volcanics. Modified from Eales (1996); Eales *et al.* (1993).

Vanadium deposits are confined to the Upper Zone, whilst significant chromite and Platinum Group Elements (PGE) are found in the Critical Zone where the well-known Merensky Reef and UG2 occur in the Eastern and Western Limbs of the BC. Another major deposit of PGE is found on the Northern Limb, the Platreef, which unlike the narrow UG2 and Merensky Reef reaches thicknesses of >250m complexly inter-related sequence of mafic and ultramafic rocks (Mitchell & Scoon, 2012).

1.3.2 Geology of the Bushveld Complex Western Limb

Although there are some similarities between the Eastern Limb and Western Limb of the BC, some disparities are also found which necessitates a separate account of each and thus in this context only the Western Bushveld is discussed in detail. The presence of the BC in the Western Limb extents 200km from Pretoria in the south forming an arc structure which passes through the town of Rustenburg with Thabazimbi on the northern end (Eales, 1996).

The RLS in the Western Limb of the BC is approximately 7.2km thick (Eales, 1996) and has been divided into four major units in sequence top to bottom (Figure 4): the Upper Zone, Main Zone, Critical Zone, Lower Zone and Marginal Zone (South African Committee of Stratigraphy [SACS], 1980).

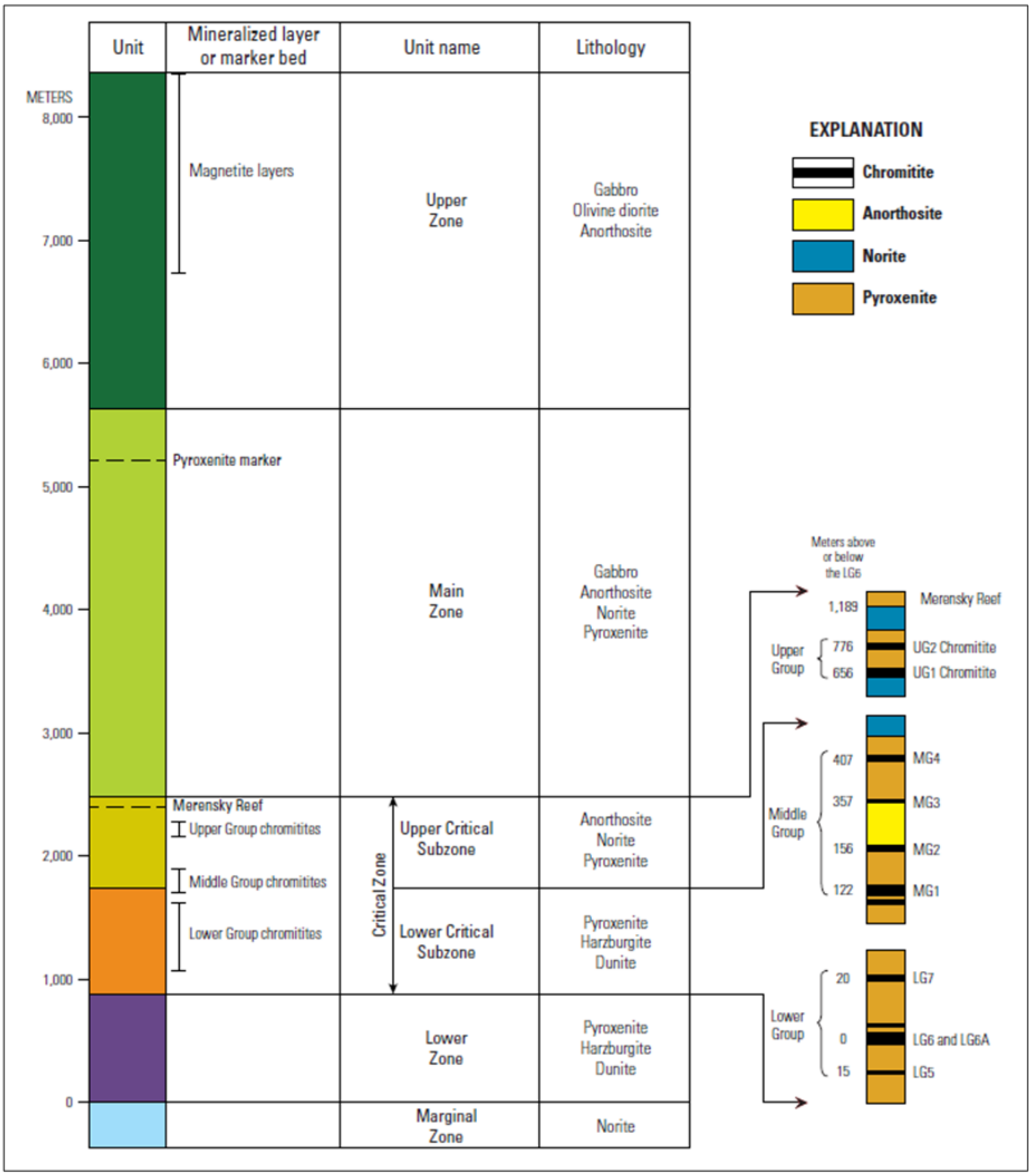

Figure 4: Stratigraphic column of the RLS Mafic and Ultra Mafic sequence of the Bushveld Complex. Source: Zientek *et al*. (2010).

The Upper Zone is ca. 2.4km thick (SACS, 1980) and dominated by ferrogabbro with anorthosites, Ti-magnetites, magnetite-olivine gabbros, diorites and olivine –diorites (Scoon & Mitchell, 2012).

The Main Zone is approximately 2.5km (Von Gruenewaldt, 1973) with gabbronorite, anorthosites and pyroxenite being the featured rocks in the Main Zone.

Below the Main Zone is the economical significant Critical Zone which host one of largest stratified deposits of PGE's within the Merensky orebody and PGE's and chromitite in the UG2 orebody. The Critical Zone is further divided into two zones, an entirely ultramafic Lower Critical Zone and an ultramafic and noritic-anorthositic Upper Critical Zone (Scoon & Teigler, 1994). Anorthosite, norite, pyroxenite, harzburgite, dunite, pegmatoidal pyroxenite/harzburgite and chromitite are the major rocks found in the Critical Zone.

Besides the high PGE content of the UG2 and Merensky reef, economical chromitite layers, though of lower PGE content, are found in what are classified as the Lower Group, Middle Group and Upper Group chromitites by Cousins and Feringa (1964). Overlying the Critical Zone is the Lower Zone which is up to 2km thick (Karykowski & Maier, 2017) where olivine cumulates (dunite and harzburgite) and pyroxenite are the dominating rocks (Eales *et al*., 1990). The Marginal Zone forms the base of the Bushveld Complex and underlays the Transvaal Group. It is however not always present and whenever it is developed it ranges in thickness from 0m to hundreds of meters (Kinnaird, 2005). Common rocks in the zone are orthopyroxenes, harzburgite and norite.

Regionally the Western BC is divided into five compartments; the Marikana compartment, the Rustenburg compartment, the Boshoek compartment, the Union compartment and the Amandelbult compartment (Figure 5). The Amandelbult and Union compartments are on the north and are both separated by breaks which are known as “Gap” areas (Figure 6) where for a strike distance of 16km on the north and 11km on the south the Merensky Reef and the UG2 are missing (Coertze, 1958).

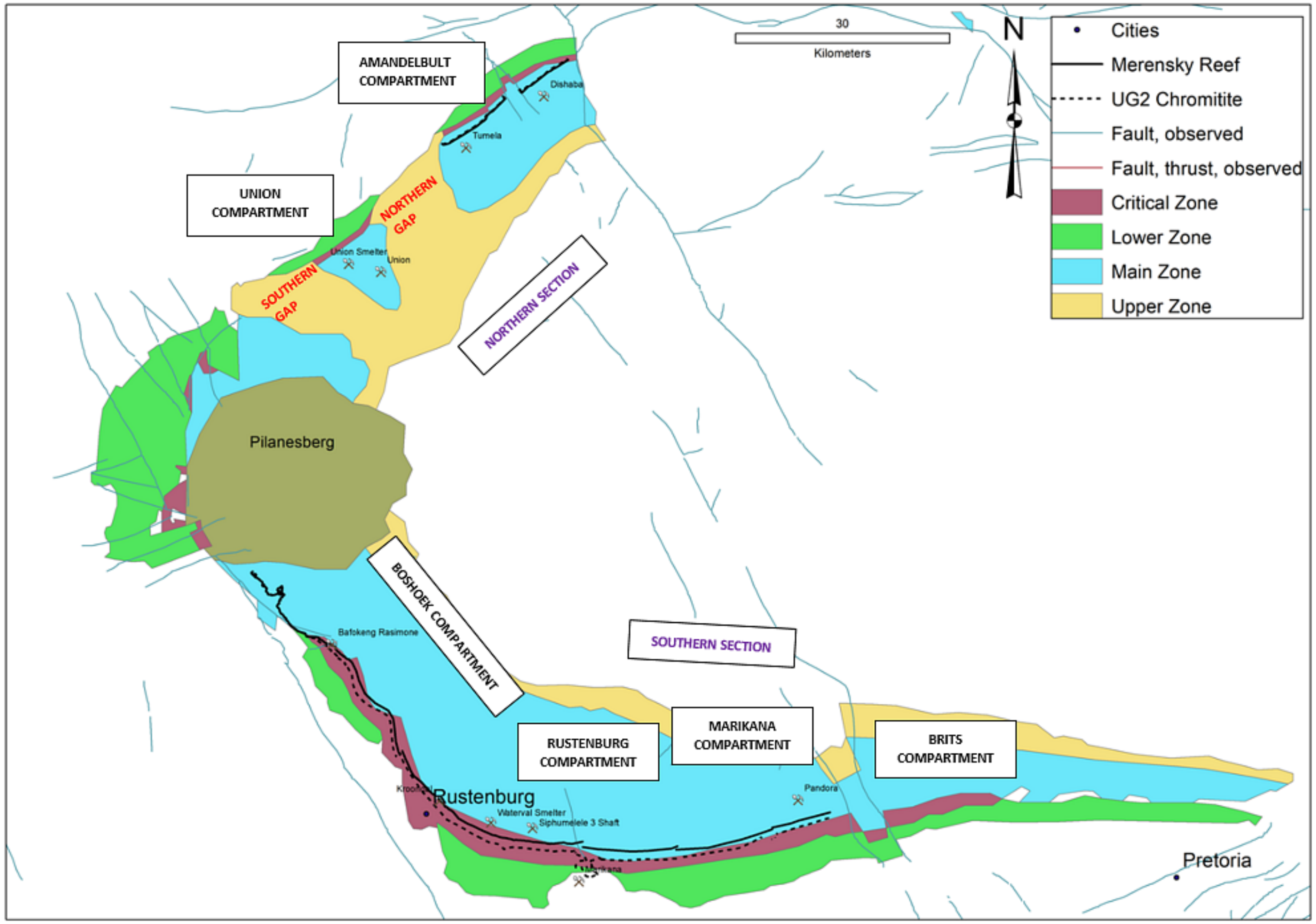

Figure 5: Geological map of the Western Limb RLS of the BC. Modified from Hatton and Gruenewaldt (1985); Viljoen *et al*. (1986); Scoon and Teigler (1994).

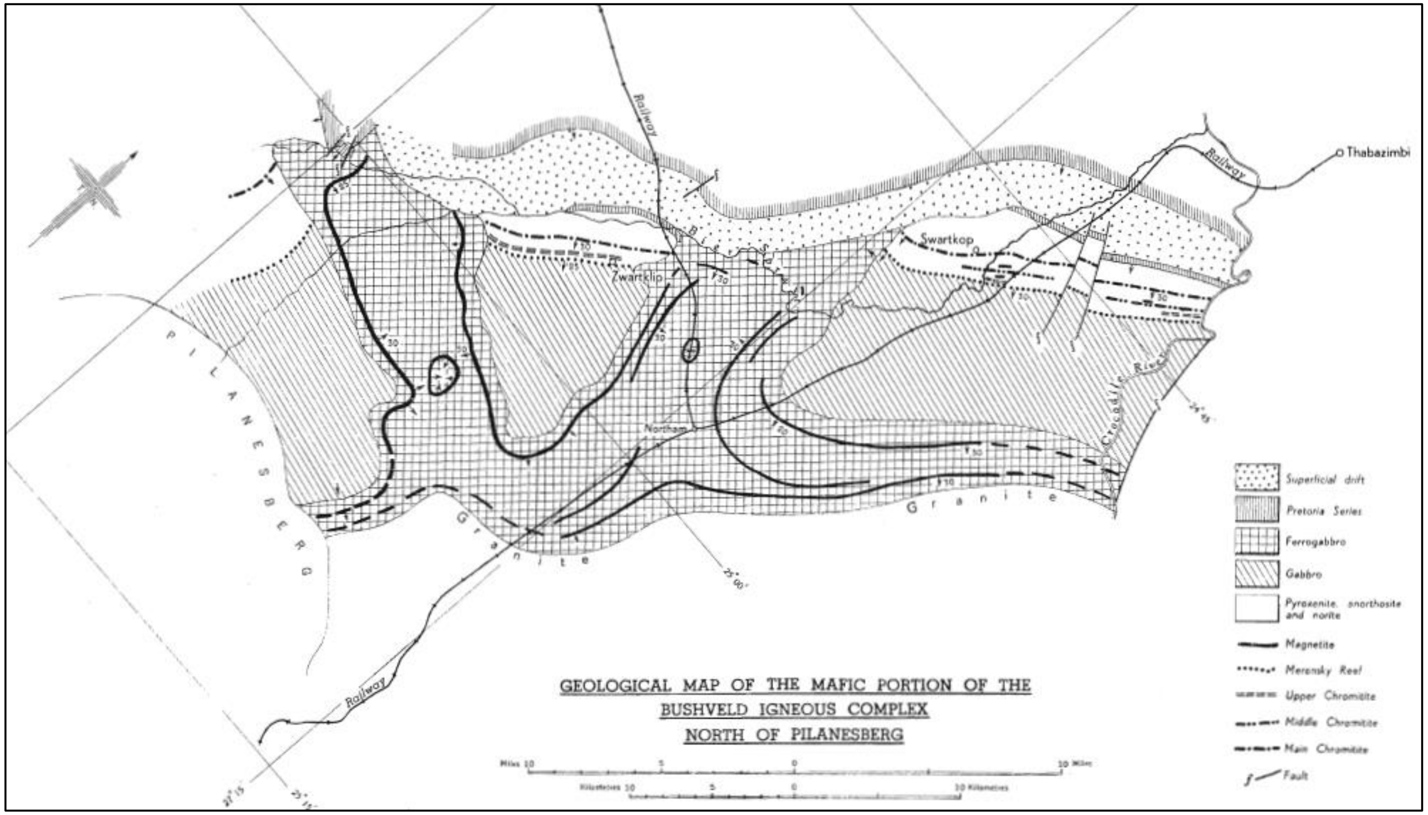

Figure 6: Geology map of the Bushveld complex north of the Pilanesberg Complex, showing the gab areas between Union and Amandelbult compartments. Source: Geological Survey, South Africa, in Coertze (1958).

Instead of the normal layering of the Main, Critical and Lower Zone, these units are rather transgressed by the overlaying Upper Zone which cuts through all these units until to the Transvaal Sequence see Figure 7 (Wilson *et al*., 1994).

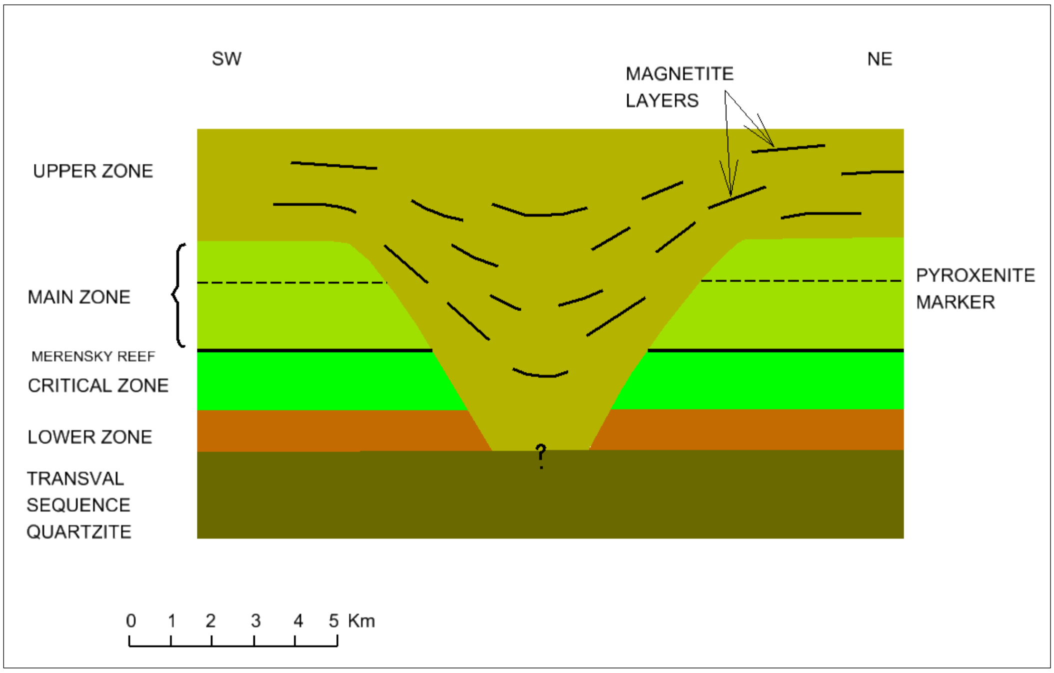

Figure 7: Section through the northern gap area. Modified from Wilson *et al.* (1994).

Also to the east the orebodies terminate on a transgression of the Upper Zone gabbros and magnetites called the far northern gap with the Amandelbult Sector and the Bushveld granite forming a wedged sliver with the Upper Zone rocks (Viljoen *et al*., 1986). The other three compartments to the south are separated from the two northerly compartments by the Pilanesberg Complex, a circular 25km diameter lopolithic alkaline intrusion (Cawthorn, 2015) into the Bushveld Complex with major rocks consisting of red, white, grey and green foyaites (Shand, 1932).

1.3.3 Mine geology

Stratigraphy

Through drilling and trenching a stretch of the Merensky and UG2 reef can be traced for a strike distance of ~23km. The Upper Critical Zone rocks have been exposed via underground excavations, underground drilling and surface boreholes where both the UG2 and Merensky Reefs are found. The main stratigraphic units from bottom to up are the UG1, UG2, Pseudo 1 Reef (P1), and Pseudo 2 Reef (P2), Lone Chrome (LCR), Footwall Marker, Merensky Reef and Bastard Reef which show lateral variation along the 23km strike (Figure 8).

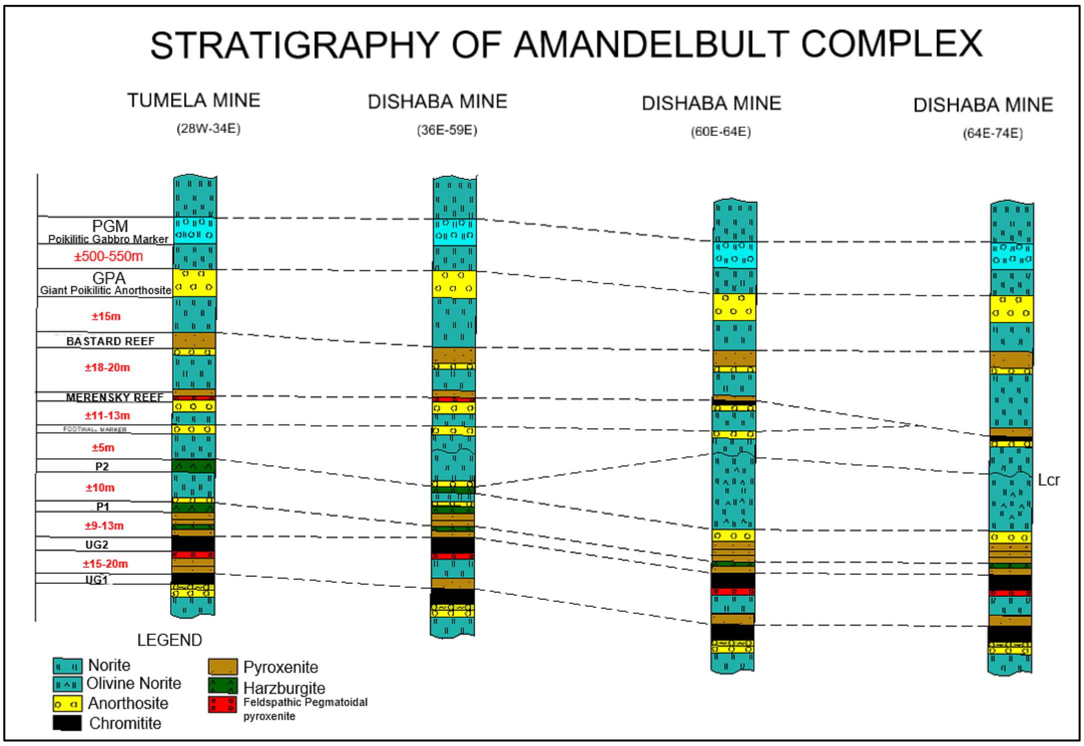

Figure 8: Stratigraphic column of Amandelbult Section. Modified after Sibiya (2017).

A brief description of each unit is summarised below as referenced from Viljoen et al. 1986; Snyman (2002); Sibiya (2017); Anglo American Plc (2018); Makgato and Laubscher (2018).

The UG1 is a chromatic layer with interlayered pyroxenite and is on average 1.5m. The UG1 is 15-20m below the UG2, with pyroxenite and norite forming the main rocks between them. The UG2 is also mainly chromatic and has interlayering of pyroxenite. It is between 25-50m from the Merensky Reef across the property (Makgato & Laubscher, 2018) and is currently mined for its elevated PGE content with chromitite as a by-product.

The P1 consists of a combination of harzburgite/pegmatoidal with a mm scale chromite stringer at the top contact. The typical mean grade of the P1 is around 3.98g/t PGE + Au as determined by Snyman (2002) . Above the P1 a second pseudo reef the P2 is developed and made up of a ~4m thick harzburgite layer bounded by a mm scale top and bottom chrome contact and is separated from the P1 by a norite and anorthosite. Towards the east of the mine though, the harzburgite changes to an olivine norite and the anorthosite/norite separating the P1 and P2 also reduces till the P2 sits directly on the P1. No significant PGE values are associated with the P2. The LCR is a persistent 1-5mm thick chrome stringer ~17m below the Merensky Reef but is only developed at Dishaba Mine (Sibiya, 2017).

The Footwall Marker (FWM) is a ~70cm anorthositic band within a norite and stratigraphically 11m below the Merensky Reef. Due to its persistence it is used as a guide for developing travelling ways to access the Merensky

Reef. The Merensky Reef at Amandelbult mine has a top and bottom chrome contact with Feldspathic Pegmatoidal pyroxenite the top portion and a Feldspathic Pegmatoidal harzburgite at the bottom. The typical grades of the Merensky Reef is 5-7g/t (Anglo American Plc, 2018) and has a thickness of ~1.5m on average (Viljoen *et al*.,1986). Most of the Merensky Reef at Amandelbult has been mined and is being replaced by the UG2 mining.

Approximately 15m above the Merensky Reef is a 10m thick pyroxenite called the Bastard Reef. Although the text “reef” may be misleading, the Bastard reef has no economical PGE’s (Viljoen *et al*., 1986). Above the Bastard Reef Unit is a 15m thick mottled anorthosite known as the giant mottle which marks the end of the Critical Zone and the start of the Lower Zone.

Geological structures

The main geological features at Amandelbult are faults, dykes, slumps, potholes and pegmatite replacement/Iron rich ultramafic replacement (Figure 9). These structures affect the orebody at varying extents throughout the property. A major graben structure with a throw of 500m separates Tumela Mine and Dishaba Mine. Other faults with varying throws traverse the property and pose challenges during mining.

Most of the major dykes across the mine have been detected by an aero-magnetic survey and mapping with the thickest measuring 20m (Makgato & Laubscher, 2018). Potholes and slumps also affect the orebody which result in dilution as these structures usually affect the elevation of the reef in the case of slumps or have no reef developed in the case of potholes.

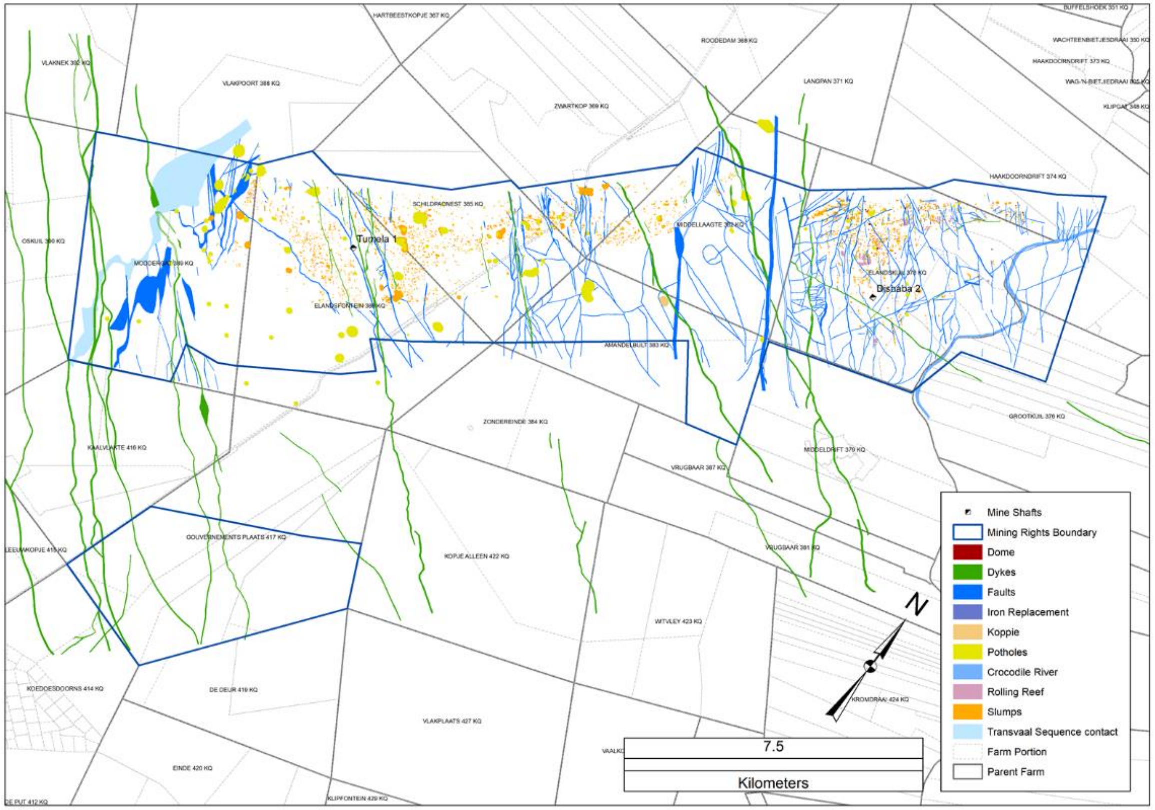

Figure 9: Geological structure plan of Amandelbult complex showing the main structures across the property. Source: Dishaba Mine (2019).

1.3.4 UG2 orebody

The UG2 exist as a 0.4m to 2.5m thick (Schouwstra *et al*., 2000) layered mass of cemented chromitite grains in a plagioclase matrix with a distinctive blackish sparkle appearance. The layer is regarded as holding the largest deposit of PGEs in the world (Kinnaird, 2005; Junge, *et al*., 2014).The UG2 can be traced persistently with few disturbances on the Eastern Limb for a stretch of almost 400km (McLaren & Villiers, 1982) and for approximately 200km on the western limb of the BC (Teigler & Eales, 1993). Of the Critical Zone chromitite layers prescribed by Cousins and Feringa (1964) the UG2 has the highest PGE concentration with a range of 4-7 g/t which varies locally across the BC (McLaren & Villiers, 1982; Schouwstra *et al*,. 2000). Figure 10 shows the grade profile and UG2 variations on some sites of the both the Western and Eastern BC. The mineral composition of the UG2 is 60-90% chromitite (by volume), 5-25% orthopyroxene and 5-15% plagioclase (McLaren & Villiers, 1982; Vermaak, 1985).

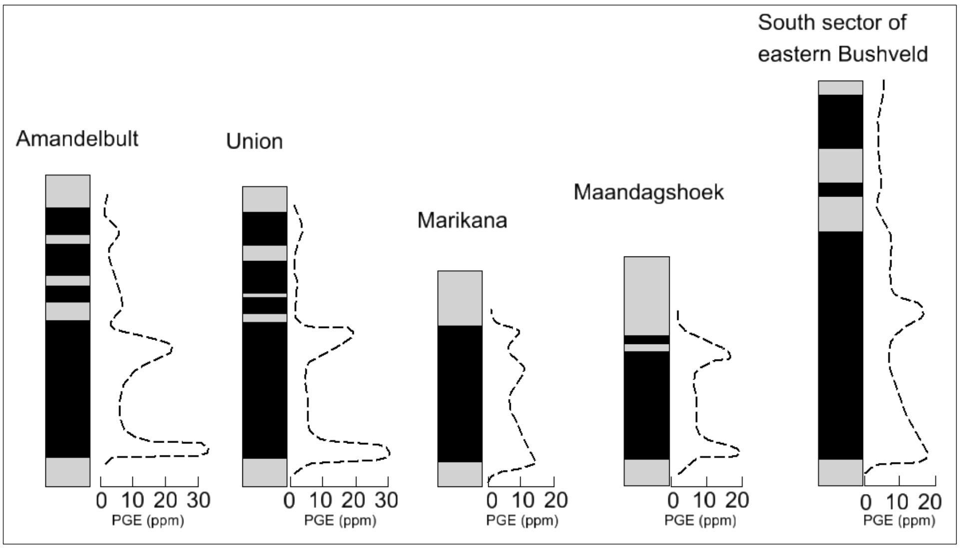

Figure 10: The PGE distribution of the UG2 chromite orebody across the Bushveld complex. Source: Maier and Barnes (2008).

The main PGE's are Pt, Pd, Rh and Au with enrichment at the middle and bottom of the UG2 main band (Maier & Barnes, 2008; Junge *et al*., 2014). The dominant PGMs are laurite, Pt-Fe alloy and cooperate-braggite (Junge, *et al*., 2014). Depending on the location (See Figure 10), the UG2 can be a one layered single mass or coexist with pyroxenite partings within smaller chromatic layers in the hanging wall of the main band called leaders seams (Junge *et al*., 2014). At the Amandelbult Section the pyroxenite separating the main UG2 band and the leader's package can reach thicknesses >2.5m in some areas and is locally called Internal Waste (IW) which poses economical mining challenges (Moyo, 2012; Makgato & Chingobo, 2019).

The hanging wall of the UG2 is pyroxenite and the footwall is usually a coarse grained feldspathic pegmatoidal pyroxenite or a melanorite or an anorthosite (Vermaak, 1985; Cawthorn, 2011) . The formation of the chromitite layers of the BC remain unsolved (Junge, *et al*., 2014) though a number of models exist with magma replenishment and mixing model, Irvine (1975) been the mostly accepted model (Teigler & Eales, 1993; Mathez & Mey, 2005; Cawthorn, 2011).

1.4 Problem Statement

Most ore deposits are large in size with the initial challenge being to establish the characteristics of the deposits from a few numbers of available drill holes or other information. As a deposit is mined and orebody knowledge is developed, understanding of the deposit increases and from time to time as this information and understanding increases the initial model needs to be reviewed and adjusted with this new information to assist in the predictability of the orebody grades, widths and tonnages (Rossi & Deutsch, 2014).

Currently, the UG2 orebody at Amandelbult is considered as having similar spatial characteristics throughout however, mining experience is indicating that this is not the case and that a distinction of the orebody characteristics needs investigated to improve estimation confidence and planning expectation across the UG2 orebody.

Some issues that can be encountered when the orebody is not domained prior to resource estimation and identified in the literature review are:

1. Misinterpretation and smearing of grades across geological boundaries (Rossi & Deutsch, 2014).
2. The resource model can be of inferior quality with an overestimation or underestimation of the grades and other variables including tonnages (Rossi & Deutsch, 2014).
3. The mineralisation controls of the orebody can be wrongly interpreted (Coombes, 1997)
4. The variogram parameters can be misinterpreted with larger nuggets and short ranges and this can lead to the interpolation of data with a high nugget effect resulting in over smoothed resource models (Coombes, 1997).

All the above-mentioned issues have a detrimental impact on the resource confidence.

1.5 Research Motivation

The focus on UG2 reef in the orebody has increased due to the progressive depletion of the Merensky Reef at Amandelbult. As such collection of UG2 data has increased over time resulting in a better understating of this orebody. At present, the UG2 orebody is not geologically zoned, with the increased data availability this research investigation was initiated in an attempt to define different homogenous regions in order to improve the estimates and provide more information with regards to the different zones and expectancies.

The expectation is that the outcomes of the domaining will have a positive effect on long term and short-term planning as the confidence of the estimates will be improved.

1.6 Research Objectives

The objectives of the research were to:

(i) Determine whether the UG2 orebody at Amandelbult complex consists of different geozones using information from boreholes, channel samples and mapping observations. To address this objective a study involving statistics was conducted on the orebody thickness, density and Pt grade to identify areas where these variables are higher or lower compared to other areas.

(ii) Determine the unique characteristics of each geozone. Application of statistical inferences using summary statistics and graphical statistical tools were used to meet this objective. From there on spatial analysis was done for each geozone using variography. The UG2 grade profile of each domain was also instigated for comparison to other zones.

(iii) Determine whether kriged block estimates improve if the geozones are used as opposed to one domain. To meet this objective two estimates were generated, one estimate was done using a global variogram and another estimate was done using a variogram in an individual zone. A cross validation exercise was conducted to determine whether the estimates improved by using the individual zone variograms.

1.7 Overview of the Research Report

Chapter 1 is an introductory chapter and discusses the background of the study, study location, motivation and objectives. Literature reviews of both the study area and the relevant geology are presented in this chapter.

Chapter 2 provides a reflection of the literature covered on Mineral Resource estimation, geozoning and some of the methods used in the process. The benefits of using domains when doing a resource estimate as well as pitfalls to be taken caution of are also highlighted.

Chapter three gives a brief on the approach of research methodology used in order to achieve the research study objectives.

Chapter 4 is an overview of the of the research data and includes a discussion of the data sources as well as validation processes in place.

Chapter 5 focuses on analysis of the data. Spatial plots of the data classed post maps were computed in Datamine™ software to provide an overview of any trend of the data values and hint on high-value and low-value locations. From this, a decision to domain was then made on variables that show geozones. Exploratory data analysis (EDT), variography, kriging neighbourhood study and finally block estimates are covered in this chapter and also comparison of the kriged estimates (without domains and with domains) is covered in this chapter mainly looking at the scatter of the average block grade vs estimated, the correlation coefficient of the average block grade vs estimated, Mean Absolute Error (MAE) and Root Mean Error (RME) to see if there was any improvement in the kriged estimates.
The grade profile of the UG2 was investigated to determine if there is a spatial correlation between grade values and the UG2 reef intersection thickness in boreholes/channel samples with the sample location.

Chapter 6 covers the results from the data analysis.

Conclusions of the study results are presented in Chapter 7 followed by recommendations for future implementation.

2 LITERATURE REVIEW

2.1 Introduction

To assist in meeting the objectives of the research study, a literature review was conducted to cover and summarise the use utilisation of statistics and geostatistics in earth science. The application of the variogram in geostatistics is also demonstrated in this chapter. Since mine projects are usually long-term activities that cover large areas of ground, some form of estimation is required to demonstrate the feasibility of undergoing the process of mining. This estimation process is conducted using kriging and other methods depending of the type of deposit. Since ordinary kriging will be used in this study a subsection has been dedicated to describing its application. Lastly orebody domaining is covered and some case studies on its implementation are discussed.

2.2 Random and Regionalised Variables

Random variables are outcomes of a random process in a numerical context. Examples are measuring the height of a bouncing ball thrown from height, an outcome of a flipped coin or a thrown die (Isaaks & Srivastava, 1989). In each of these cases there exists a process which produces outcomes that can be translated into numerical values. These are processes that can easily be described, and their predictability modelled.

In the context of mining and specifically resource evaluation random variables are the measured attributes of the orebody including width, density or grade acquired via drilling or exposure by excavation. The process by which the orebody is produced and its specific attributes, width/density/grade, are not as obvious as the examples of Isaaks & Srivastava (1989). The uniqueness of these attributes within the orebody in their location is termed regionalised variables.

A regionalized variable is a variable that exists in space having a value for example metal grade (x) at a specific location with x, y, z coordinates in three dimensions (Journel & Huijbregts, 1991). At sampled locations the metal grades are known, the challenge then becomes one where knowledge of metal grades or other attributes of interest are required at un-sampled locations as input into mine planning. One solution is to resort to some modelling of the random variable process in order estimate the value of the regionalised variable at un-sampled locations.

2.3 Statistics in Earth Sciences

Statistics are tools employed in various industries with the main objective being that of obtaining information from captured data and in mining the same concept applies from the start of a mine through to actual production. Applications of statistical analysis in earth sciences are briefly summarised by Miller and Kahn (1962) with the first records of this application spanning from approximately 1890 to the early 1930's. A sample/samples are collected from the population (orebody in a mining case) and inference is made using statistical tools which ultimately inform whether a project is feasible or not and also to inform whether assumption made in the project stage are still valid during production. A large portion of statistics deals with the organisation, presentation and summary of data (Isaaks & Srivastava, 1989).

In mining resource evaluation the data source is usually core from boreholes that have been drilled either underground or from surface and channel samples that have been cut along exposure of the orebody in an underground excavation and have undergone some form of analysis to determine the quantity of mineralisation, usually expressed in grams/tonnes (g/t) for PGE grades or million ounces (Moz) for content. The aim is to obtain characteristics including the average/mean grade, density and width of the deposit and to produce frequency tables, histograms and probability plots of the variables of interest to allow for analysis which will enable adequate planning and decision making.

A detailed example of application of statistics in earth science is illustrated by Mosobalaje, *et al.* (2019) whereby statistics was used to provide an understanding of the characteristics of data obtained from a heavy oil and bitumen deposit in Nigeria. The authors demonstrate using descriptive statistics, histograms, quartile-quartile plots (Q-Q plots), hypothesis testing and box plots that statistics applied in earth sciences can be an effective tool in determining characteristics of a potential economical deposit.

Dodge (2008) notes that the term histogram was first used by Karl Pearson, in1895 and also describes its use being that of graphically representing data into an easy form of understanding, furthermore the shape of the histogram can be used to detect the probability model of the data thereof.

The box plot was introduced by Tukey (1977) and is a useful tool for comparing two or more distributions by looking at their data location, spread and quartiles (Pierce & Chick, 2012). Additionally, to a box plot, an alternative method to compare two distribution can be done through a Q-Q plot. A Q-Q plot can be used to mainly check (i) if a data set follows a normal distribution (ii) compare distributions of two populations for similarity (Latha & Shribharathi, 2017; Dohm, 2018b).

2.4 Geostatistics

Some improvements to statistical methods in ore evaluation arose from geostatistics. Schaeben (1988) states that geostatistics arose due to a need to deal with problems of reserve estimation, providing confidence limits to the estimates and quantification of spatial variability of the ore grade for example.

Geostatistics was theorised by Matheron in the 1960's to describe the study of distribution of values in space such as grades of ores and thicknesses based on the practical and research of Krige, (Krige, 1976). Most of the underlying principles have remained unchanged since then with literature on the subject available explaining the concepts of application in ore evaluation in mining for example David (1977), (Clark, 1979) and Goovaerts (1997) in environmental pollution studies. The advantage of geostatistics compared to pure statistics alone is that geostatistics takes into account the relevance of the spatial position of each sample relative to other samples into consideration and not just the grade or width value for instance. When applying geostatistics the sample is referred to a regionalised variable. “A regionalised variable is, *sensu stricto*, an actual function, taking a definite value in each point of space ”,(Matheron, 1963).

2.5 Variography

Variography is a process whereby the spatial variability of phenomena under study is investigated with the end results being the variogram model which is required in geostatistical studies (Gringarten & Deutsch, 2001). Other tools such as the covariance and correlogram function can also be used for this purpose. An elementary statistical analysis of the available sample data is advised to be carried out prior to carrying out a variography exercise and compare the results with the geological hypothesis (Journel & Huijbregts, 1991).

The basis of the semi-variogram is to distinguish the difference in values of a regionalized variable between two sampled locations using a mathematical formula:

$$\gamma^*(h) = \frac{1}{2N_h}\sum_{i=1}^{N_h}\left[Z(x_i) - Z\left(x_{(i+h)}\right)\right]^2 \qquad \text{Eq 1}$$

were h is the separation distance between the samples, N_h is the total number of pairs, $Z(x_i)$ is the grade value at point (x_i), and $Z(x_i + h)$ is the grade value of the sample at the distance h from $Z(x_i)$.

The outcomes of the calculated values are plotted for each h and these are termed the experimental variogram points and a variogram model is then fitted to it, see Figure 11. As the distance h increases the differences between the two sample values usually also increase. The point at which this rise levels is termed the sill of the variogram and indicates that there is no longer any spatial correlation between the samples. The distance h at which the samples no longer show correlation is called the range of influence (Dohm, 2018a).

One would expect that samples taken very close together would be similar in value, but such a situation is rare in earth sciences. The nugget is used to describe this difference between samples that are infinitely close to each other.

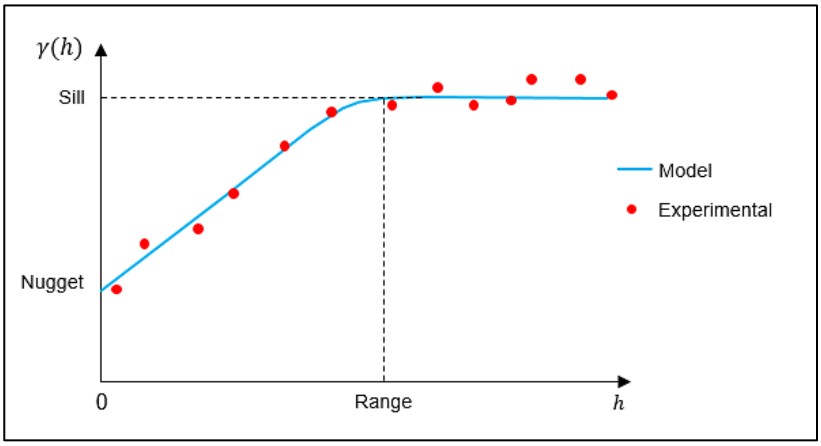

Figure 11: An example of an experimental and modelled variogram. Source: Dohm (2018a).

A semi-variogram can reveal isotropy or anisotropy. Isotropy is observed when the semi-variogram displays the same shape in all directions and takes a shape of a circle. On the other hand, anisotropy is when the variogram is ellipsoidal with longer continuity in one direction and shorter continuity in the other direction. In this way a variogram reflects the continuity of the ore deposit and reveals the preferred direction of mineralisation of the ore deposit, (Dohm, 2018a).

To complete the variography analysis, one would have to fit a model to the experimental semi-variogram. The most common variogram model used is the spherical model (Isaaks & Srivastava, 1989). The exponential model is also often used. The Gaussian model is used for modelling highly continuous occurrences whilst linear models are used in phenomena that never reach a sill but increase with distance h. The mathematical formulas for spherical, exponential and Gaussian models are shown below:

Spherical Model

$$\gamma(h) = \begin{cases} 0 & if\ h = 0 \\ C_0 + C_1\left[\frac{3h}{2a} - \frac{h^3}{2a^3}\right] & if\ 0 < h \leq a \\ C_0 + C_1 & if\ h > a \end{cases} \qquad \text{Eq 2}$$

Exponential Model

$$\gamma(h) = \begin{cases} 0 & if\ h = 0 \\ C_0 + C_1\left[1 - e^{(-h/a)}\right] & if\ h > 0 \end{cases} \qquad \text{Eq 3}$$

Gaussian Model

$$\gamma(h) = \begin{cases} 0 & if\ h = 0 \\ C_0 + C_1 \left[1 - e^{\left(-h/a\right)^2}\right] & if\ h > 0 \end{cases} \qquad \text{Eq 4}$$

Where h is the distance between the samples and a is known as the range of influence. *Co* is the nugget effect C_1 the sill, total sill of the variogram is C_0+C_1.

Rossi and Deutsch (2014) highlight the critical steps to be completed before initiating calculations of experimental variograms. The steps include: (i) visualisation of the data and developing a comprehension of the data from a geological point of view, (ii) establishment of a suitable coordinates and (iii) an analysis to deal with outliers and determining whether any data transformations are required. Additionally, the maximum lag distance analysed should not be more than the half of the domain size.

2.6 Estimation of Mineral Resources

Estimation of Mineral Resources is the process by which the main attributes of ore deposits tonnage, grade, size, shape and location are estimated (Noble, 2011). The estimates are used as input into the mine planning. The steps involved in producing resource estimates begins with data collection and subsequent input of the data into a geological database, data validation, subdividing the area to be estimated based on geological characteristics, array formation in three dimension using known grade values and other geological information which are then interpolated to areas that have no data (Dewing, 2007).

Early estimation of mining Mineral Resources were based on different types of polygonal estimation methods, which were superseded by geostatistical kriging methods and with current increased computer power and advances estimation now commonly involve conditional simulation methods (Glacken & Snowden, 2001).

Kriging methods are standard in Mineral Resource estimation, mainly due to the advantage that these methods are based on the data available and also include the spatial behaviour of the variable/s under study and produce measures of confidence in the estimates, a drawback of polygonal methods (Dohm, 2018a).

2.7 Kriging

The basis of mine development is often initially based on borehole information. An obvious problem which arises is that when mining eventually does happen, mining occurs in blocks or polygons and not on the boreholes. To address this problem a way of converting the borehole values to block values of reasonable size is required and an estimation method such as kriging provides a solution.

Kriging is a procedure where estimation of grades of a panel is carried out by computing the weighted average of available sample values, some of these samples being inside the panel and others outside the panel (Matheron, 1963). The mathematical formula of the kriging estimator is:

$$T^* = w_1 z_1 + w_2 z_2 + w_3 z_3 + \ldots + w_n z_n \qquad \text{Eq 5}$$

Where w_i is the weight and z_i *i*s the value of the sample associated with sample *i*. The weights are calculated using a variogram which must be calculated and modelled prior to a kriging exercise.

The weights must sum to one and if there is no local trend then it an unbiased estimator (Clark, 1979).

Several kriging methods namely ordinary kriging (OK), simple kriging (SK), indicator kriging (IK) are available and their application would depend on the objective of the estimation procedure and the shape of the distribution of the data.

The advantage of kriging over other methods for example polygonal or inverse distance is the fact that through utilising of the variogram, the error associated with the estimate is minimised and quantifiable through the estimation variance:

$$\sigma_\epsilon^2 = 2\sum_{i=1}^{n} w_i \; \overline{\Upsilon}(z_i, A) - \sum_{i=1}^{n} \sum_{j=1}^{n} w_i \; w_j \, \overline{\Upsilon}\left(z_i \, , z_j\right) - \overline{\Upsilon}(A, A) \qquad \text{Eq 6}$$

Where w_i is the weights assigned to each sample, $\overline{\Upsilon}(z_i, A)$ is the average variogram using the distance between the available samples and the area(A) to be estimated, $\overline{\Upsilon}(z_i, z_j)$ is the average variogram value of the distances between the sampled points $i \,\&\, j$, z_i is the grade at location i and A is the area of the block being estimated. Ordinary Kriging will be used in this study and a dedicated further discussion is outlined in the next section.

2.8 Ordinary Kriging

OK is the most popular of the various kriging methods although other variants that model trends have become more popular recently (Rossi & Deutsch, 2014). Its associated acronym is B.L.U.E. translating to “Best Linear Unbiased Estimator” (Isaaks & Srivastava, 1989). Estimation of blocks from borehole or channel sample data using ordinary kriging involves: (i) statistical analysis of the data to produce histograms and to carry out classical statistics that can be interpreted. Ordinary kriging can accommodate normal distributions, positively skewed distribution and negatively skewed distributions; (ii) dividing the area of interest in geozones depending on the amount of available data, (iii) constructing variograms, at this stage the maximum distance at which samples can be used to estimate a block A can be determined, (iv) determining the adequate block size using a kriging neighbourhood study, (v) and lastly solving kriging solutions to estimate the grade of the block.

Detailed literature on OK has been covered by a number of authors Journel and Huijbregts (1991) p 303, Isaaks and Srivastava (1989) p 278 and 323 and David (1977) p 275.

The goal of an OK exercise in ore evaluation is to provide estimates of ore grades on a block. The performance of the OK exercise can be checked by determining the error of the estimate which is the difference between the true value and the estimated value:

$$Error \ = \varepsilon = z_i - z_i^* \qquad \text{Eq 7}$$

where ε is the error, z_i^* is the estimate and z_i is the true value and for a perfect estimate, the error would be equal to zero.

Other important checks for estimation performance and comparison include the mean square error (MSE), mean absolute error (MAE), kriging variance, slope of regression, block variance, estimation variance and kriging efficiency. These methods are well documented by authors such as Isaaks and Srivastava (1989), Asli and Marcotte (1995), Deutsch (2007), Heuvelink and Pebesma (2002) and Clark (2015) , discussed below.

2.8.1 Kriging variance

An advantage of kriging methods as opposed to classical methods such as polygonal or inverse distance is that kriging methods produce estimates that have with them attached a minimum estimation error. The kriging variance is dependent on the spatial distribution of the samples and the distance of the available samples from the point or block being estimated. A low kriging variance indicates a higher confidence in the estimate as the variance in the error is reduced. This is versa for a higher kriging variance, (Dohm, 2018a).

2.8.2 Block variance

For block estimation, the block variance is used as one of the qualitative measures of the estimate. The block variance is a measure of the variance of all the block estimates, if they were to be mined and it is the same for blocks of the same size and the same variogram used in the estimation. If the block size for estimation changes, the block variance will change but for similar block sizes and a similar variogram, the block variance is constant.

The block variance is determined from the average variogram of the discretization points used to estimate a block of a certain size.

2.8.3 Kriging efficiency

According to (Deutsch *et a*l, (2014) the kriging efficiency was first presented by Krige, (1997) and provides a degree of the efficiency of block estimates. It is expressed as a percentage were 100% will represent a perfect block. The kriging efficiency is calculated using the kriging variance and block variance using the following formula:

$$KE = (BV - KV)/BV \qquad \text{Eq } 8$$

Where BV is the block variance and KV is the kriging variance. Blocks with a high KV will have a low score kriging efficiency whilst blocks with a high KV will score a high kriging efficiency.

2.8.4 Slope of regression

The slope of regression (SLOR) is defined by Deutsch *et al.* (2014) as an assessment tool for the measure of conditional bias in the estimated value. During estimation it is commonly the case that most estimation methods will underestimate low values and overestimate high values. This is referred to conditional bias and indicates the amount of smoothing in the estimate (Isaaks & Srivastava, 1989).

A SLOR of 1 indicates that there is no bias while a SLOR of less than 1 indicates a degree of smoothing. Simple kriging has a SLOR of exactly 1 and has no conditional bias whilst OK always has a SLOR of less than 1 and always has some degree of bias (Deutsch, 2007).

2.9 Orebody Domaining

Coombes (2008) defines a domain for resource estimation as a spatial volume where the geology is consistent across the domain i.e. homogeneous, the volume has a single grade population and has a single search orientation. Domaining is thus a process whereby the ore deposit is subdivided into zones and the data is grouped based on similarities and dissimilarities in orebody characteristics. For the purpose of Mineral Resource estimation two types of domains are found namely geological domains and grade domain. Geological domains are grounded on the known geology i.e. mineralisation or rock types whilst grade domains are based on some cut-off grade which differentiates between ore and waste (Guibal, 2001).

From a statistical point of view determining and using domained data has the benefit of decreasing the variability which in turn reduces uncertainty as predictability is higher and thus increases the confidence of estimates. Common geostatistical methods of estimation for example kriging Gaussian or indicator simulation are depended on domains that fulfil the assumption of stationarity, in particular second stationarity whereby the mean, variance and covariance is constant across domains without dependency on location but the distance between the support points (Larrondo & Deutsch, 2005).

Stegman (2001) highlights the fact that not all deposits have mineralisation control that show clear domains. Domaining is justified if the resulting variogram is improved compared to the un-domained variogram (Guibal, 2001).

The process of domaining the orebody is well known to improve estimates when these zones are correctly defined, and estimation of the orebody is conducted within the boundaries of such zones. In most instances during the early stages of the development of a mine, it can be difficult to identify these zones due to limited available data but as more information is collected a review of the data can reveal whether such zones do exist. A combination of statistical and geostatistical means can be used to determine domains which can include using or not using a cut-off grade (Glacken & Snowden, 2001).

A discussion on nonstationary covariance by Chilès and Desassis (2018) p 601 notes:

> *"If a stationary covariance is often a reasonable assumption when limited number of samples is available, large data sets usually show some lateral variations in the covariance or variogram, so that a global model with a stationary covariance would be a crude approximation. This problem is obviously not new. A simple solution is to split the study domain into several subdomains, to determine a specific variogram is each sub domain, and to krige each subdomain with its own variogram."*

The process by which geological domaining is determined as outlined by Rossi and Deutsch (2014) p3 with the importance of this process also emphasised:

> *"The determination of the estimation domains to use in based on geologic knowledge and should be supported by extensive statistical analysis (exploratory data analysis, or EDA, including variography. The procedure can take a significant amount of time, particularly when all possible combinations of the available geologic variable are studied, but it is typically worth the effort. Estimates are improved when carefully constrained by geological variable."*

2.9.1 Case studies on orebody domaining

Porphyry copper deposit, Chile.

A methodology of estimating Mineral Resources using grade domains is discussed in Emery and Ortiz (2005). Here a porphyry copper deposit is studied using a dataset consisting of 2000 samples of diamond drilled holes and 20000 blast-hole samples. The study compares four cases, one where ordinary kriging is used without any domaining, the second where ordinary kriging is performed using three domains, the third where ordinary kriging is used also on three domains using a cut-off grade to define the domains and a fourth case where five domains are used also using a cut-off grade. A separate variogram is used for each of the domains when doing the estimation.

From these copper deposit case studies, Emery and Ortiz (2005) identified 6 limitations of using grade domaining in Mineral Resource estimation on a porphyry copper deposit namely:

(i) dependency between grade domains

(ii) uncertainty in the domain boundaries,

(iii) artefacts in maps, histograms and scatterplots,

(iv) sensitivity to the cut-off definition,

(v) self-justification approach, and

(vi) bias in the kriging variance.

It was concluded that the above limitations can prove to be disastrous in a Mineral Resource estimate and produce a sub-standard estimate were grades can be overestimated or underestimated.

To overcome the above-mentioned limitations, Emery and Ortiz (2005) suggest a five-step methodology using grade domains. This involves stochastic modelling methods and the estimation of the grades using co-kriging. Although this five-step approach has its drawbacks, there was some improvement compared to traditional grade domaining with the results being comparable to kriging without considering domains.

Escondida Mine, Chile

The case study in Rossi and Deutsch (2014) describes the process followed to define the estimation domain for a copper deposit at Escondida Mine in Chile. The approach to defining estimation domains was grounded on geological characteristics and statistical analyses of grade. The geological variables considered in determining the domains were mineralisation type, alteration, lithology and structural domains resulting in the identification of 14 estimation domains.

The issue surrounding boundary uncertainty is also raised in this case study. The authors give reference to Larrondo and Deutsch (2005) and Emery and Ortiz (2006) on statistical contact analysis which assists in dealing with data along the contacts of domains. This methodology consists of using swath plots of grades in the deposit to determine whether hard or soft boundaries are appropriate for estimation purposes.

Minimum, good and best practices are summarised by Rossi and Deutsch (2014); as a minimum, the methodology employed to determine domains in the deposits should account for obvious mineralisation controls which can be identified through mapping of the geology and the genesis of the orebody. This should be supplemented by methods identifying some relationship between the geological attribute and the grade.

Good practice is when all the available geological information, the relationship of the grades and each geological variable are taken into consideration. Best practice is when the definition of the estimation domains is supported by some form of uncertainty best determined by simulation methods.

Rooikoppies, Marikana, Western Bushveld Complex, South Africa

Davey (1992) did a study after completion of an exploration project on the farm Rooikoppies which is 20km east of the town of Rustenburg and observed lateral variations in the units of the Critical Zone of the BC. The information acquired in the exploration project included drill hole sampling and assaying, surface mapping, trenching and rock exposure from development underground excavations.

This information enabled the demarcation of different zones of the UG2 orebody. Two zones (R.P.M and Western Plat facies) were inferred based on the thickness of the orebody (See Figure 12).

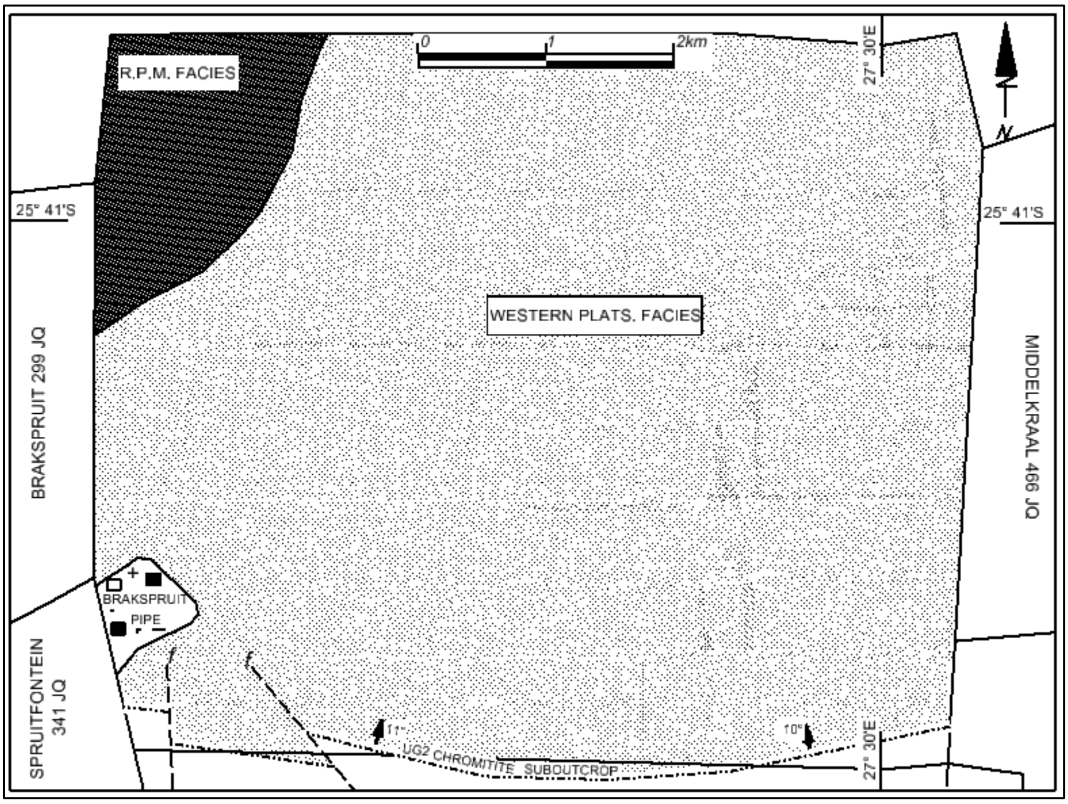

Figure 12: Geozones plan of the different facies of the UG2 identified from exploration data. Source: Davey (1992).

The leaders of the UG2 show variations and are in one zone close to the main band of the UG2 and in the other zone much further from the UG2 main band Figure 13. A different grade profile is associated with the variations in the position of the leader in relation to the main band of the UG2.

Where the pyroxenite separating the UG2 main band is wider, the grades are less, with grades appearing on the leaders themselves and the main band.

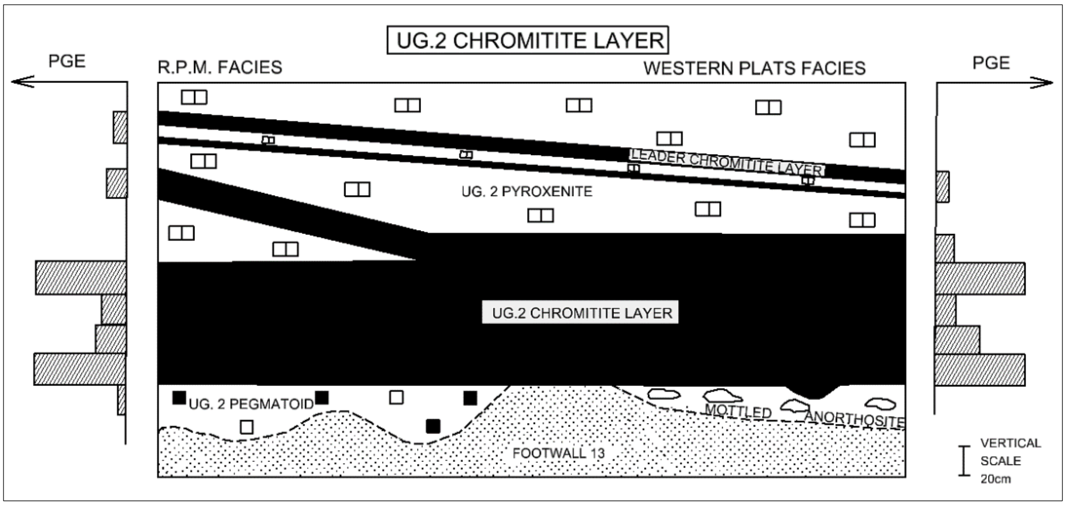

Figure 13: PGE grade profile of two UG2 facies at Rooikoppies. Source: Davey (1992).

2.10 Conclusion

The literature review conducted confirmed the benefits of attempting to delineate geozones in the deposit as well as highlighting some of the pitfalls that need to be addressed in determining the zones. Reliance on the application of statistics in Mineral Resource estimation was proven by the detailed literature review. The need to use geostatistics in estimation has been highlighted, the benefit of which is that the spatial arrangement of collected sample values can be used to the advantage of the estimation which is something that statistics alone cannot accomplish. The case study provided by (Davey, 1992) confirm that the UG2 orebody can and has been domained in the Western Limb of the BC based on the thickness and the grade profile of the reef.

3 RESEARCH METHODOLOGY

3.1 Introduction

The research methodology was guided by the assumptions and methods detailed in the literature review. To achieve the objectives of the study a methodology was followed which is typically the process followed when conducting a Mineral Resource Estimate in industry. This chapter outlines the specifics of how the data was treated at various steps followed from the data assembly through to the Exploratory Data Analysis (EDA), the variography, the estimation and the results comparison.

3.2 Data Assembly

A Microsoft (MS) Excel file containing the X, Y, Z coordinates of the borehole and channel sample data together with a number of measured variables and geology was acquired which is the same file that was used in the 2018 annual Amandelbult Resource estimation update process. The file was then imported into Datamine™ software. The grade data acquired from boreholes and channels consisted of the sample assays, these were analysed at an offsite laboratory and are stored in an electronic database which can be exported to an Excel format for data processing.

3.3 Global Data Analysis and Classed Data Posting

In order to conduct data analysis on the dataset, the Excel file was imported into Datamine ™ software. Summary statistics were calculated to obtain an understanding of the statistical characteristics of the data. Furthermore, histograms and cumulative frequency were plotted. A global visual summary of the spatial distribution of the data was obtained through classed data posts of the orebody thickness, density and platinum within Datamine software using appropriate data ranges.

> *"Posting the values coloured differently for values above and below different grade thresholds provides an assessment as to the continuity of high and low-grade trends"* (Rossi & Deutsch, 2014).

Unlike statistical summaries or graphical statistics, plotting values with different colours shows indications of highs and lows of data in space. Colour coded maps are very useful in showing this with application used in many field for example in GIS AvRuskin *et al*. (2004), in mining Krige and Ueckermann (1963), environmental studies Zapata-Rios *et al*. (2012) and pollution studies Goovaerts (1997).

The output results from data posting were then used to guide the preliminary domains. Variables that show areas of highs-lows or of identical characteristics were determined visually and the data was then grouped using this criterion as a guide. The main aim of the process is to identify homogenous area and group the data as such.

3.4 Exploratory Data Analysis

In order to get more detail from the data set, an exploratory data analysis (EDA) was carried out on the individual variables. The EDA was done firstly on the whole data set and then on each domain identified in the data post study. Graphical statistics were then used to compare the various data populations in the identified zones using histograms, cumulative frequency plots, Q-Q plots and box plots.

Rossi & Deutsch (2014) and Mosobalaje *et al*. (2019) highlight the importance of these graphical tools in assisting in separating different statistical populations. The separation of populations is also important for the variography analysis process.

3.5 Geological Study

Most ore deposits are associated with some structures for example, gold mineralisation maybe associated with quartz veins or shear zones. To check if there is any correlation with geology and the data set, a super-embossed plan of geology structures at Amandelbult where overlain together with the data. McArthur (1988) highlights the importance of consideration of geology in geostatistical studies and how geology can be used to design an estimation technique in a massive sulphide deposit. The study by Davey (1992) also emphasises the consideration of geology when domaining a deposit as geology is highly related to grade distribution.

3.6 Variography

Spatial data analysis for the whole domain as well for each domain identified in Step 3 was done using Datamine ™ software. Journel and Huijbregts (1991) emphasise the fact that the process of characterisation of the spatial behaviour of a variable is the initial and most important step taken when conducting geostatistical studies.

3.7 Kriging Neighbourhood Study

A kriging neighbourhood analysis (KNA) study was conducted using the variograms identified in the various zones. The KNA was done to check if the current block size used at Amandelbult were appropriate for the new variograms in the different zones. This exercise was done for completeness as the current block size is entrenched on the mine,

Incorrect neighbourhood parameter selections can lead to reduced estimation accuracy and conditional bias in the estimates, more so if the search is too restrictive (Vann *et al*., 2003; Khakestar *et al*., 2013).

3.8 Estimation and Results Comparison

To solve ordinary kriging solution for estimating blocks, the variogram model parameters in the variography step were used. The first estimation was done using the variograms produced without domaining the orebody. The follow-up estimations were then done using the variograms produced from each identified geozone. The block estimates were done using Datamine™ software using the search parameters currently in place at Amandelbult.

Block estimates need to be checked for quality to make sure that they are realistic and represent as close as possible to the data that was used to produce the estimates. This is to guarantee that the model is appropriate for its intended use (Deutsch *et al*., 2014). The quality of estimates of the non-domained and domained zones were compared by using the correlation coefficient of the true and estimated values as well as their scatter plots. Comparison of estimates using these methods is covered by Isaaks & Srivastava (1989). Additionally Asli & Marcotte (1995) show a case where the mean absolute error and the mean square error can also be used for this purpose.

3.9 Conclusion

The research methodology chosen to achieve the objectives of this study is based considerable evidence obtained from the literature review. The application of statistics is widely used in a number of industries including data analysis for resources estimation processes and justified for example by application by Mosobalaje *et al.* (2019). The impact of geological controls on the orebody and the need for its consideration when conducting Resource Estimates has been illustrated by McArthur (1988). Taking into consideration the literature review, the methodology used for this research is concluded to be able to meet the objectives set out in the first chapter. The chapter to follow describes the data set used for the study.

4 DATA DESCRIPTION

4.1 Introduction

Storage of data in a suitable database is good practice as this ensures that data is stored an organised manner. This allows for consistency in data capturing, easy access to the data, data validations and exportation to several file formats to allow usability in various software. Data collection for Mineral Resource estimation usually involves capturing of lithological log, structural information and assay results for sampled units mainly from drilling or chip sampling. If the data is not stored in an organised manner, this may result in possible data loss and difficulty in its tracing. Validation of the recorded data is also crucial. This is because data is collected by various people and consistency may be an issue. If the data is not validated, errors will be detected during the process of estimation which can be a draw back as the data may require to be rectified before proceeding with other steps. Sampling also introduces errors which need to be reduced as far as possible or avoided. The process of Quality Assurance/Quality Control (QA/QC) is an important process which also ensure that data errors and detected and dealt with before the mature stages data usage for Mineral Resource estimation.

4.2 Data Acquisition and Sources

The dataset consists of a total of 8256 boreholes and underground channel sample of the UG2 reef composites contained in an MS Excel spread sheet. A spatial plot of the dataset is shown in Figure 14. The dataset displays a pseudo grid with a high concentration of data in the mined-out or currently mining areas as underground sample collection is conducted along excavations. The sparse data down dip are surface boreholes.

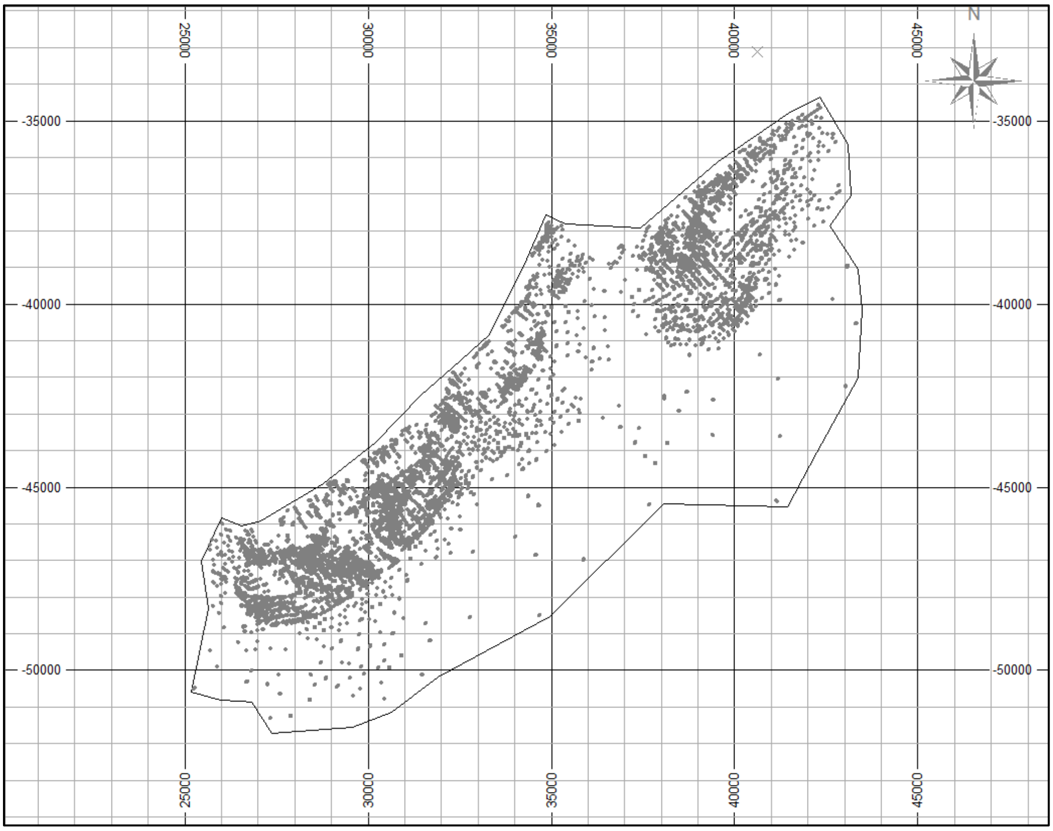

Figure 14: Spatial plot of the dataset.

4.2.1 Channel samples

The channel samples used in this analysis were cut underground in raises and in the panel advance strike gully (ASG) faces. Primarily for safety reasons no routine sampling of the panel face is done as the panel excavation size is limited and the space is confined it causes difficulties in machinery operation. The samples are cut along to the orebody on a grid spacing of ca. 34m apart using a diamond saw blade which cuts samples of dimensions 4cm x 4cm x 10cm-20cm along the hanging wall lithology, reef and footwall lithology (Langwieder, 2018). The samples are bagged in plastic bags and barcoded to create a unique sample ID number and captured electronically in a computer software package. A total of 4188 reef composite samples were available for utilisation in this research study.

4.2.2 Borehole Information

A total of 4068 diamond core borehole intersections were used in this study. The boreholes were drilled from surface and underground at various angles of between -45^0 and 45^0 across all directions from the strike of the orebody. The core is logged and sampled by the site geologists and captured electronically into a borehole database software. The individual samples are taken at intervals of 15-25cm along the hanging wall, reef and footwall. Since the boreholes are drilled at various angles, the orebody dip and strike were taken into consideration and the boreholes intersection widths were corrected for true thickness in Datamine™ software. After correcting for dip and strike, reef composites are created in Datamine, this process combines the individual samples into one unit.

4.2.3 Assay and Density Determination Techniques

The most prominent method of analysing PGEs is fire assay which uses various collectors for example Pb or NiS which concentrates and confines the PGEs (Noble, 2011; Lomberg, 2014). The fire assay technique involves pulverizing the rock sample and mixing it with a fluxing agent with Pb or NiS added as a collector. This mixture is then heated at approximately 1000^0C for about 20 minutes after which fusing would occur with the precious metals and Pb separated from silicates. Cupellation is then used to extract the

PGEs which are then analysed using flamed atomic absorption, optical emission spectrometry, mass spectrometry or instrumental neutron activation analysis (SGS, 2019). Base metals, although very minimal are analysed using one of the following methods; Pressed pelleted and X-Ray fluorescence, aqua regia leach, four-acid digestion, sodium peroxide fusion and titrimetric and gravimetric techniques (Lomberg, 2014). The density of the rock samples was determined using a pycnometer, but some of the historic densities were determined by the Alchemy Method.

4.3 Data Validation

4.3.1 Channel and borehole validation

A series of validations were done on the data to ensure that it is suitable for the use of the research. Working with un-validated data always leaves room for questioning of the integrity of the data (Dohm, 2018b). A customized Datamine™ script written by Stevenson (2010) was used to aid in the validation and checks on the data which follows three steps, a stratigraphic sequence validation, a general validation and a prill validation (Stevenson, 2010). The output of the script is an excel sheet containing all the flagged boreholes and channel samples for investigation. Below is a description of the checks done at each of the steps:

1. Lithology Validation:
    - Lithology out of sequence; and
    - Unknown lithology report.

2. General Validation:

    - Start of hole missing,
    - Overlap between entries,
    - Gap between entries,
    - Missing PGE grades entries,
    - Zero width entries,
    - Repeat PGE and width within sections,
    - Repeat PGE and width in different sections,
    - Sample reef PGE outside range,
    - Collars within range,
    - Samples width outside permissible range,
    - Missing hanging/footwall information,
    - Composite reef width anomalies,
    - Bimodal PGE distribution problem,
    - Density out of range and
    - Borehole dip angles out of range.

3. Prill validation:

    - PT out of range,
    - Pd out of range,
    - Rh out of range,
    - Au out of range,
    - Prill sum <> PGE,
    - Pt : Pd ratio out of range,
    - Pt=Pd and
    - Au>Rh.

The data prior to the period 2018 has previously been validated and subsequently used in the 2018 UG2 Resource Model (Colquhoun 2018).

4.3.2 QA/QC

The act of sampling is associated with and introduces a number of errors. These errors may be encountered during the actual sampling stage, preparation of the sample or during the analysis stage. Gy (2004), discusses 10 errors which are associated with sampling. Since mining relies on sampling of the ore deposits for decision making, it is clear that an understanding of these errors and how they can be overcome is paramount to ensure the data that will ultimately be used to predict resources and reserves is of the highest quality achievable.

A QA/QC program is thus implemented to detect the errors that are introduced in the various stages of the sampling, preparation and analysis and is used to as a tool to rectify any short comings in the shortest time possible (Rossi & Deutsch, 2014).

The assay data to be used in the research was obtained from a certified laboratory. A process of QA/QC validation was conducted in January 2018 van der Neut (2018) on the assay data and the validation deemed the data to be acceptable and suitable for the purpose of this research. This validation included intra-laboratory checks, certified reference material, duplicates and blanks to check for precision, bias and accuracy of the assay results.

4.4 Conclusion

The data set used in this study consist of many borehole intersections and channel samples. The data was checked that it plots correctly and is located within the limits of the study area. The assay method used is standard for PGE deposits. Data validation was conducted and any errors dealt with before the data was used in this research report. The QA/QC on the assay data also confirmed that the data is acceptable to be used for the purpose of Mineral Resource estimation processes and for the purpose of the analysis of this research study.

5 ANALYSIS OF THE DATA SET

5.1 Introduction

Handling and analysing large amounts of data can be a challenging task especially if the data is in the form of thousands of assay values or measurements of the thickness of a layer at multiple location for instance. As such statistical analysis is deployed to organize the data in some form of summary in order provide some organised form of information from the raw data. Application of statistics is deployed in a number of fields for instance mining (Mosobalaje *et al*., 2019), medicine (Kestin, 2015) or climatology (Kumari *et al*., 2017).

One of the common statistical calculations for measuring the central tendency of a set of discrete numbers is the mean of the data (Caldwell, 2012). For example for several measurements taken of some numerical value, the mean can be calculated as:

$$mean = \mu = \bar{z} = \frac{1}{n}\sum_{i=1}^{n} z_i \qquad \text{Eq 9}$$

where n is the number of values and Z_i the individual values. The summing of the values Z_i and then dividing by the number of the available values n thus reduces the data to one value from which an approximation of where the values falls approximately. Of course, in most instances some of the values will be large and some small and the variance of the data in the form:

$$variance = \sigma^2 = \frac{1}{n-1}\sum_{i=1}^{n}(z_i - \mu)^2 \quad \text{Eq 10}$$

provides a measure of how the data values differ or vary from the mean were (n) is the number of values available, (z_i) are the individual values and (μ) is the mean of the data. When subtracting the values from the mean, some of the values will give a negative outcome, thus squaring thus assists in dealing with such instances.

According to Caldwell (2012) the process of squaring in the variance calculation increases the magnitude of the numbers thus reducing the variance to the standard deviation (SD) (σ) , which is the square root of the variance brings back the value to normality. A large SD means that the values are highly variable, and a small SD means little variation in the data.

$$Standard\ deviation = \sigma = \sqrt{\sigma^2} = \sqrt{\frac{\sum_{i=1}^{N}(zi-\bar{z})^2}{N-1}} \quad \text{Eq 11}$$

Another way of presenting data is in the form of graphics. Graphical representation of the data also provides quick visual insight of the data. The most common is the histogram (Scott, 2008) which bins the data in several limits and can indicate whether the data is distributed normally, skewed (positively or negatively) or whether the data has multiple populations (Figure 15).

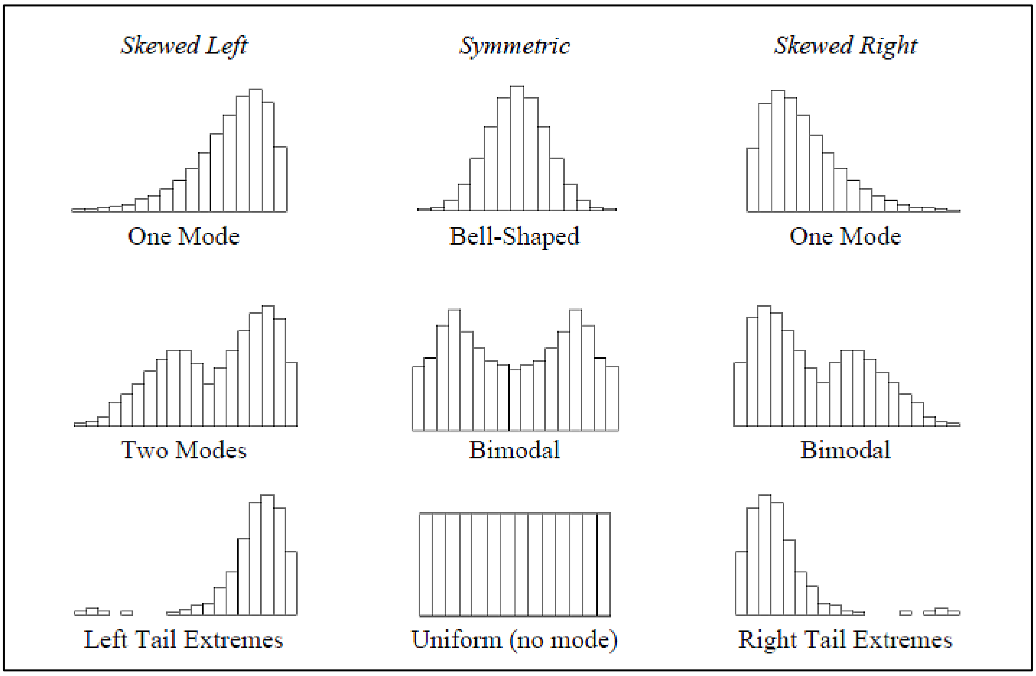

Figure 15: Examples of histograms. Source: Doane and Seward (2011).

The skewness of the histogram is determined by the following formula:

$$Skewness = \sqrt{\beta_1} = \frac{\frac{1}{n}\sum_{i=1}^{n}(z_i - \bar{z})^3}{\sigma^3} \qquad \text{Eq 12}$$

A skewness of less than -1 and greater than +1 indicate a distribution that is highly skewed whilst a skewness of between -1 and -1/2 or between +1 and +1/2 indicates a distribution that is moderately skewed. If the skewness is between -1/2 and +1/2 then the distribution is approximately symmetrical/normal (Dohm, 2018b).

Other graphical tools for example a cumulative plot also provides some insight into the data indicating how much percentage of the data values falls into. All these tools assist in data analysing where large amounts of data are available to make some form of decision.

For describing data that is distributed in space, colouring of the values within some sort of limits provides a visual assessment of data. The use of coloured codes maps for data visualization and interpretation is used in many applications including Geographic Information Systems (AvRuskin *et al.*, 2004), mining (Krige & Ueckermann, 1963) and environmental studies (Zapata-Rios *et al*., 2012). Colour coded maps provide a rapid analysis of trends in data values within regions and can indicate area where certain values are high and areas where values are low as shown on Figure 16 and Figure 17.

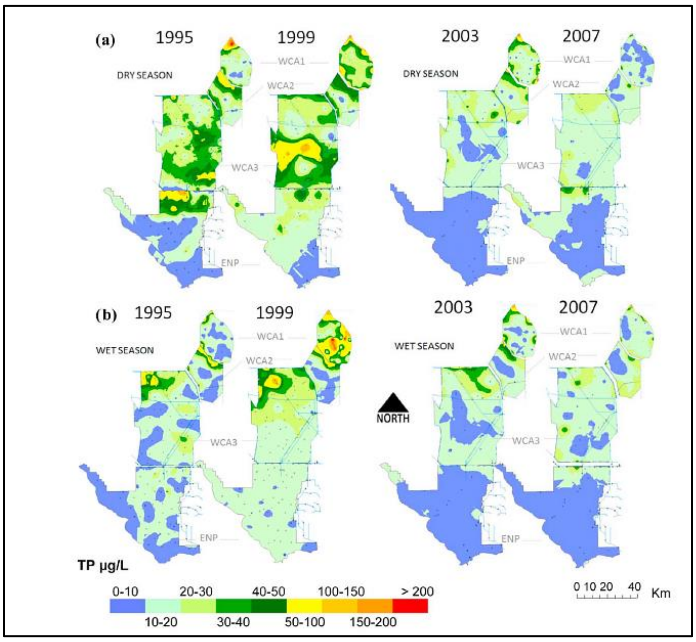

Figure 16: An examples of a colour coded map to illustrate levels of phosphorus levels for a season and year. Source : Zapata-Rios *et al*. (2012).

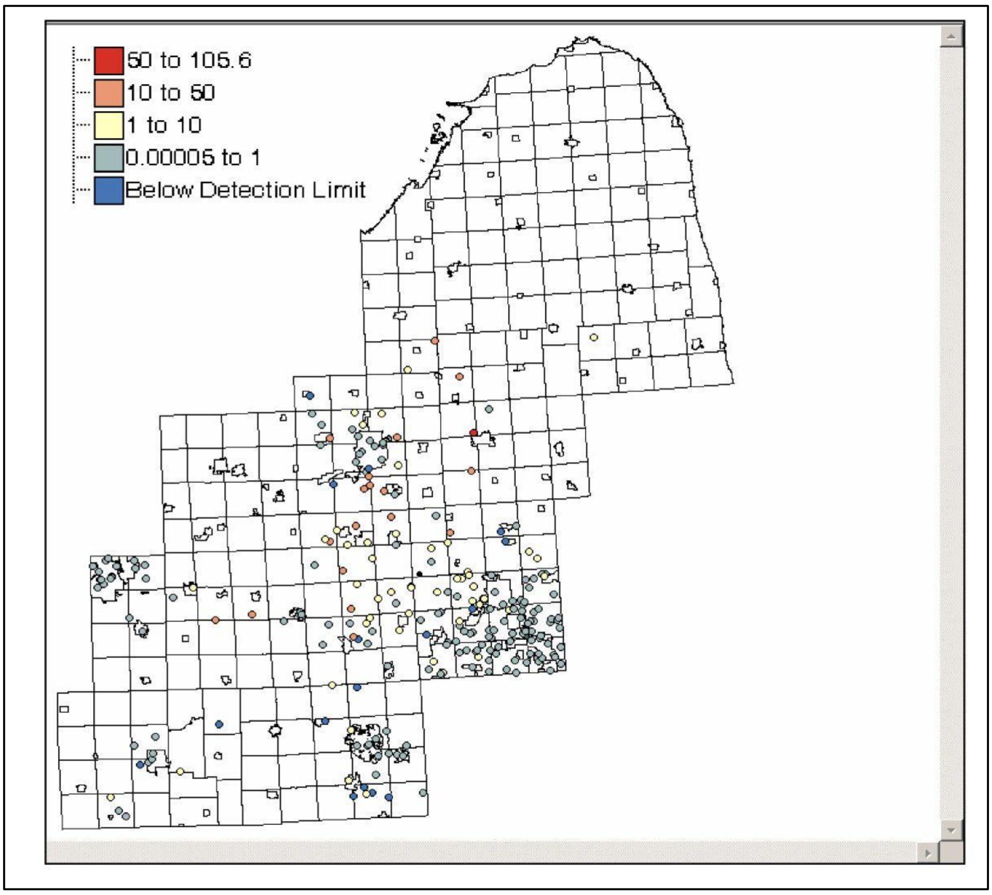

Figure 17: Colour coded map showing levels of arsenic in drinking water in eastern Michigan. Source AvRuskin *et al*. (2004).

5.2 Orebody Thickness

The thickness of the orebody is one important variable to be considered in mining as it informs decisions on the mining method, type of equipment to be used during orebody extraction and is directly linked to the tonnages that are envisaged to be mined at some stage of extraction.

5.2.1 Thickness (cm) analysis

The data for the orebody thickness consist of 8256 intersections. A histogram of the thickness data set is shown in Figure 18 and it reflects a shape close to a normal distribution. The statistics suggest that the thickness ranges between a minimum of 0.614m and a maximum of 2.714m and has a mean of 1.382m.

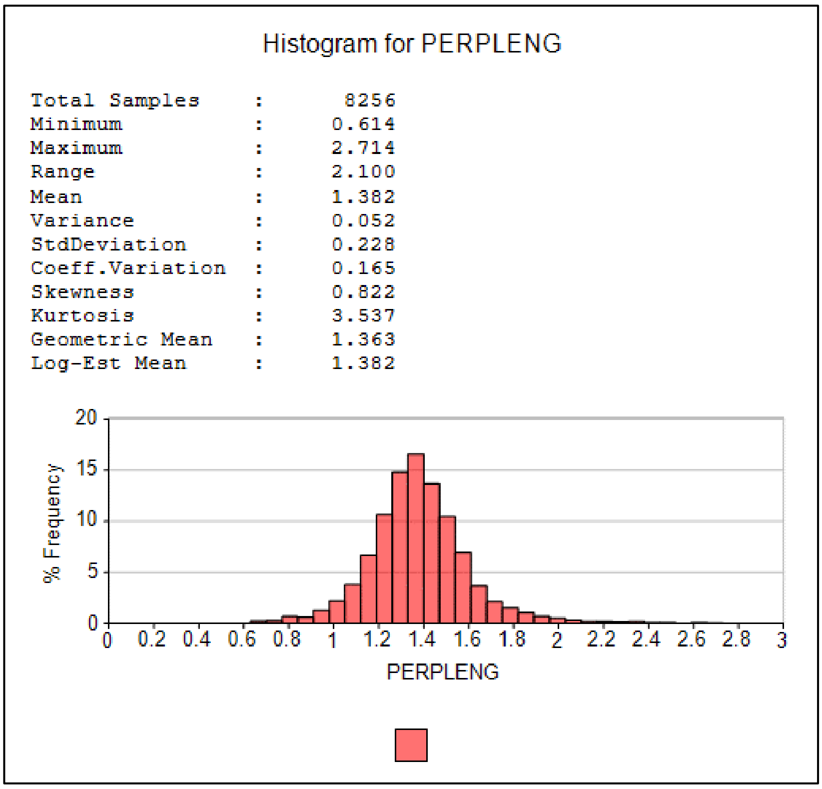

Figure 18: Histogram and summary statistics of the orebody thickness.

To investigate if the thickness data has multiple populations, a cumulative plot was generated and shown in Figure 19. The cumulative plot suggest that approximately 60% of the thickness values fall between 1.2m and 1.4m and the different slopes of the straight lines suggests three populations of thickness less than 1.2m, thickness of 1.2m to 1.4m and thickness greater than 1.4m.

To assist in analysing the data spatially, classed post mapped of the thickness were generated in Datamine ™ software. A classed data post map is map which display XY location of grouped data using either symbols and/or different colours depending on bin threshold selected (Surfer, 2016).

Rossi and Deutsch (2014) indicate that posting of data values using different colours within specific threshold provides a visual assessment of the continuity of trends in the data i.e. high and low values.

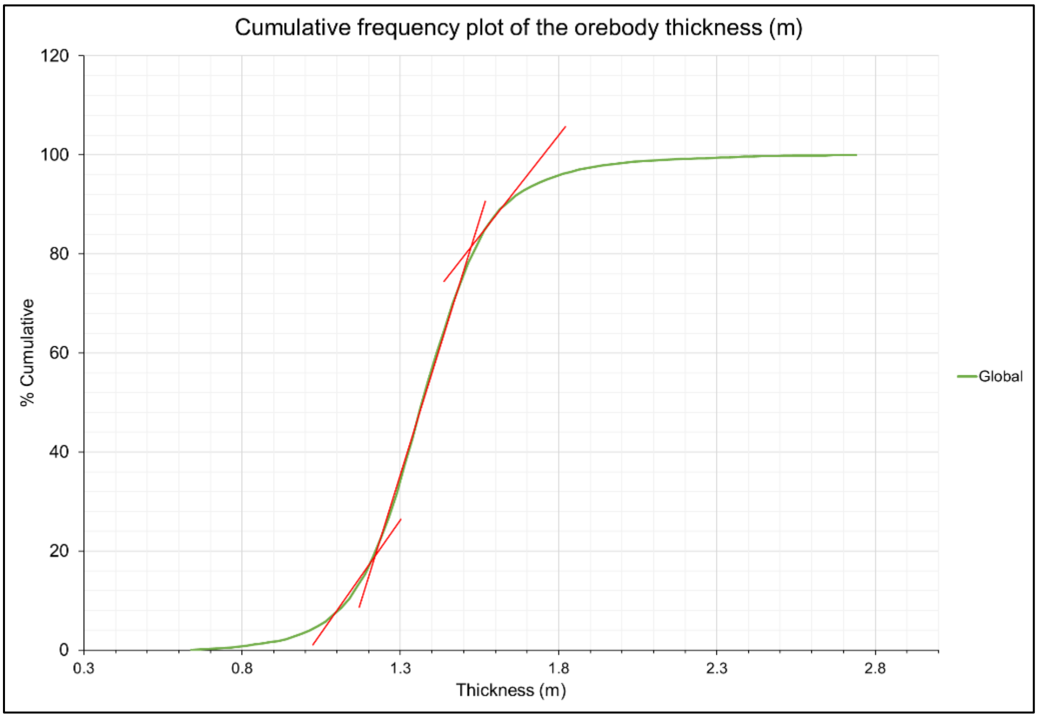

Figure 19: Cumulative plot of the orebody thickness.

For the orebody thickness, a number of colour schemes were attempted and are shown in the appendix with the post map showing clearer detail shown in Figure 20. From the data post, zones where grouped by looking for similarities in colours and boundaries where guided by changes in colour from area to area. Unlike the histogram and cumulative plot, the data post can clearly indicate different classes of values spatially across the study area. From the data posting (Figure 20) the following observations can be made: Thickness Zone 1 (T-Zone 1) indicates that the reef width is predominantly below 1.3m thick and the narrowest of all the zones.

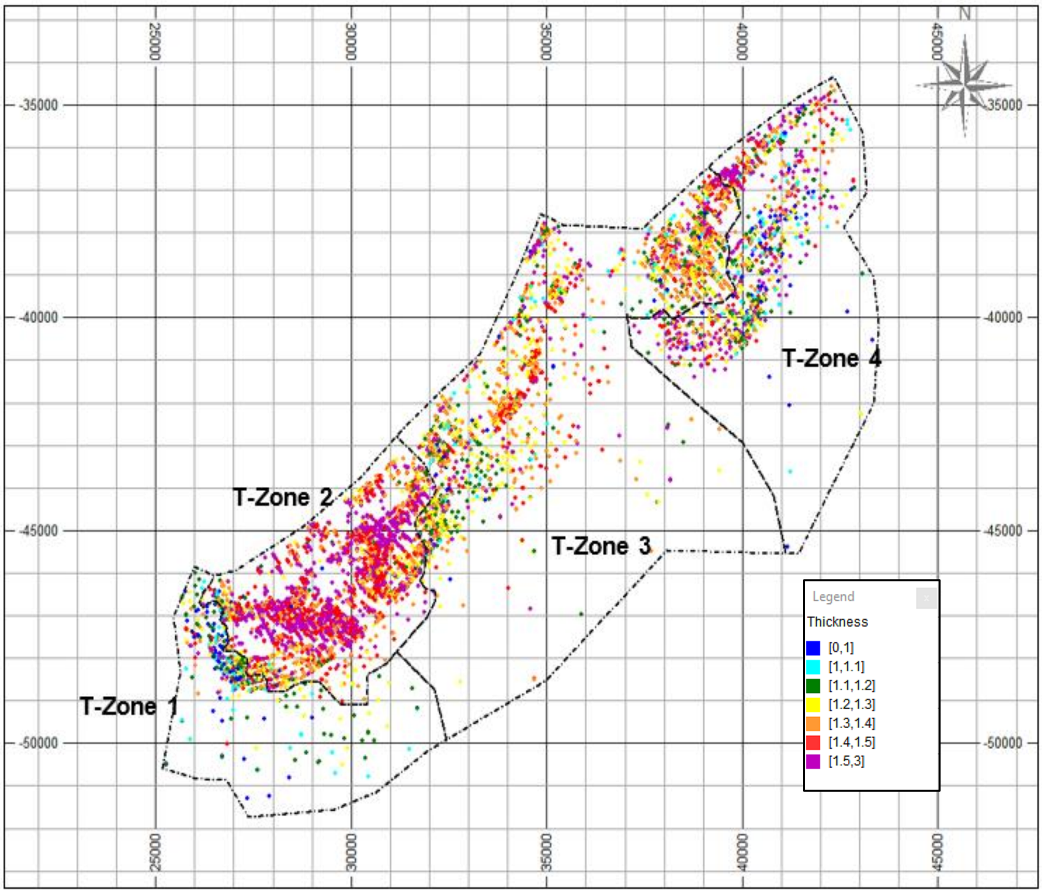

Figure 20: Thickness (m) classed post map.

Thickness Zone 2 (T-Zone 2) where reef thickness is greater than 1.3m is notable on the east from T-Zone 1. Thickness Zone 3 (T-Zone 3) represents a reef thickness predominantly ranging from 1.1m to 1.4m. A mixture of colours stand out in Thickness Zone 4 (T-Zone 4), indicating that the reef thickness is highly variable in the area.

5.2.2 Thickness statistics

The statistics of the orebody thicknesses in the various zones as identified on Figure 20 are shown in Table 1. Of all the zones, T-Zone 1 the narrowest has an average of 1.184m, T-Zone 2 has the highest average with a thickness of 1.461m. T-Zones 3 and 4 averages are almost identical with averages of 1.331m and 1.387m respectively. In all cases the results reflect the thickness post map shown in Figure 20.

The highest variance of 0.108m^2 and a coefficient of variation of 0.237 compared to the other zone is observed for T-Zone 4 which is aligned to the erratic behaviour observed in Figure 20.

Table 1: Summary statistics of the orebody thickness for the various thickness zones.

	Global	**T-Zone 1**	**T-Zone 2**	**T-Zone 3**	**T-Zone 4**
No. of data points	8256	621	3322	2966	1347
Min (m)	0.614	0.648	0.705	0.614	0.644
Max (m)	2.714	2.250	2.592	2.648	2.714
Range (m)	2.100	1.602	1.887	2.034	2.070
Mean (m)	1.382	1.184	1.461	1.331	1.387
Mode (m)	1.400	1.282	1.400	1.310	1.190
Median (m)	1.370	1.179	1.455	1.320	1.335
Variance (m^2)	0.052	0.044	0.030	0.035	0.108
Standard deviation (m)	0.228	0.209	0.173	0.187	0.329
Coefficient of variation	0.165	0.176	0.118	0.140	0.237
Skewness	0.822	0.709	0.677	1.458	0.944

The cumulative plots of the orebody thickness for the various zones are shown in Figure 21. T-Zone 1 which is the first distribution on the left has a thinner thickness and T-Zone 2 which has a distribution to the right has the thickest reef in the orebody.

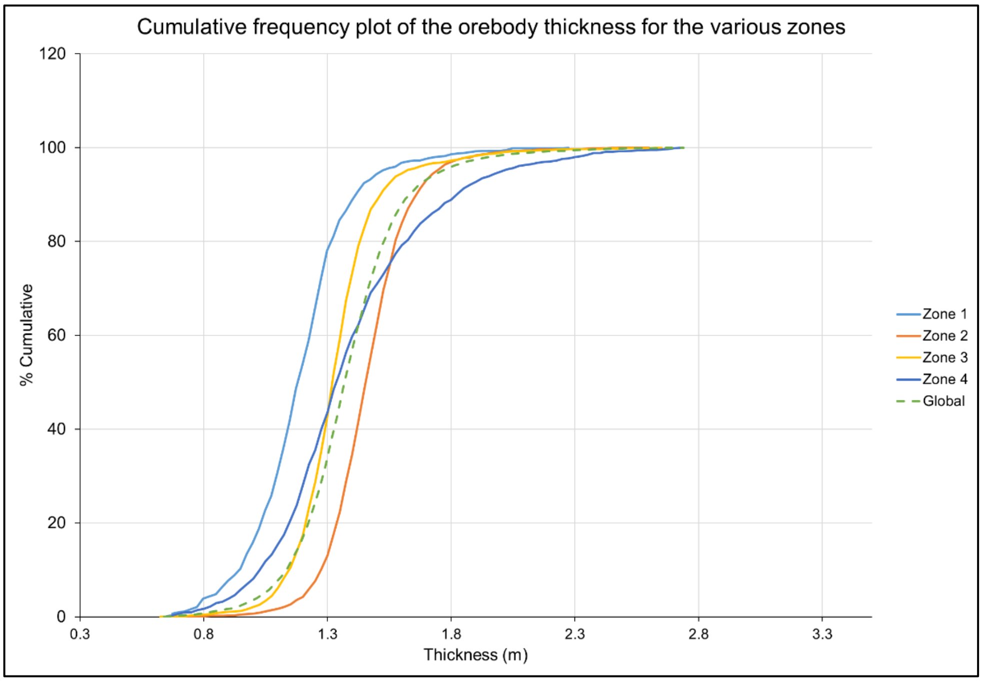

Figure 21: Stacked cumulative plot of the orebody thickness of the various zones.

The histograms of the zones under study are represented in (Figure 22). Visually all the histogram plots appears to reflect a normal distribution, however when looking at the skewness results from the different zones (Table 1), Global (0.822), T-Zone 1 (0.611) and T-Zone 2 (0.780), values suggest that the individual distributions are moderately skewed. T-Zone 3 and T-Zone 4 have skewness values of 1.117 and 1.247 which suggest a distribution that is highly positively skewed.

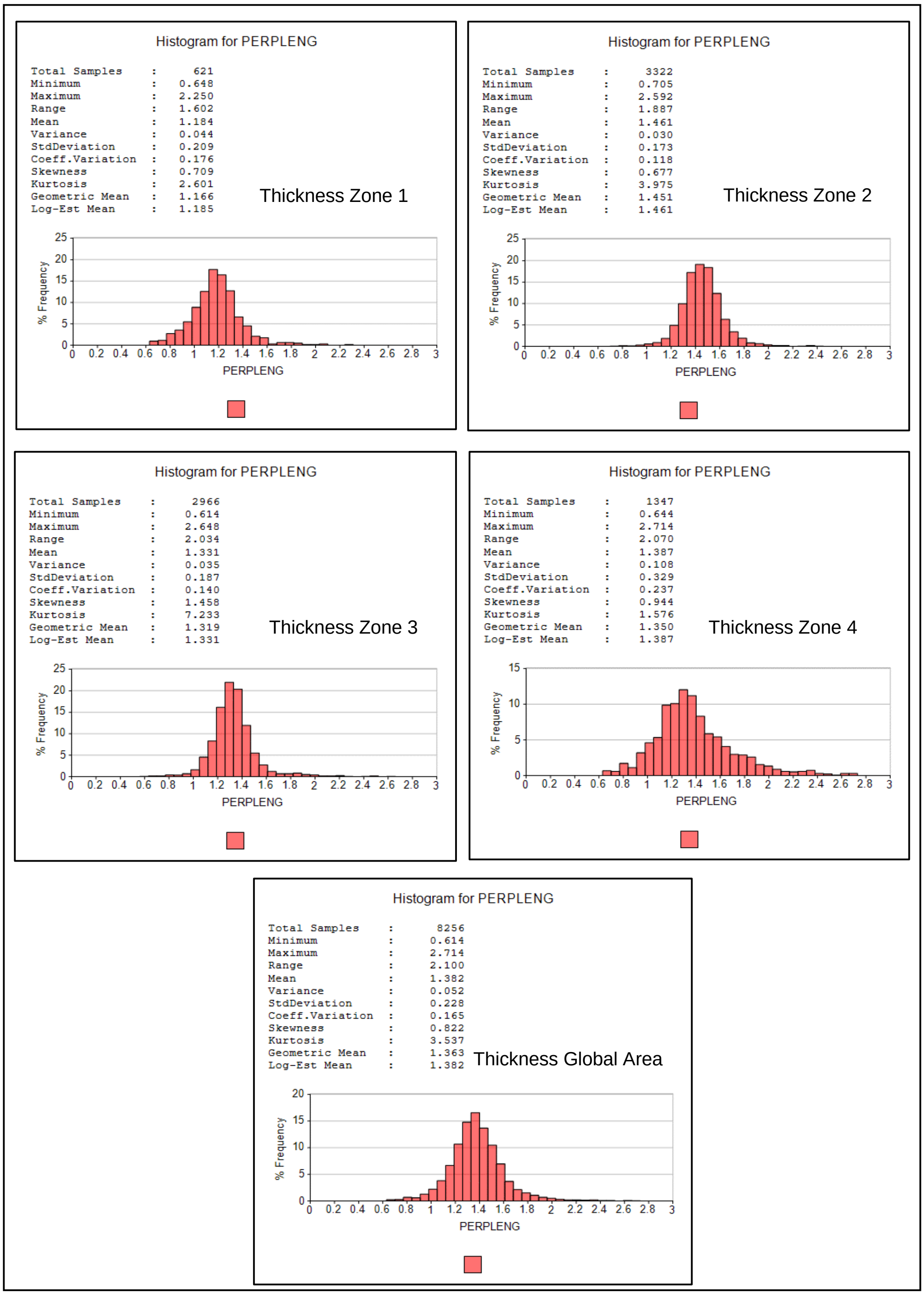

Figure 22: Histogram of the various zones and global zone.

The thickness zone box plot (Figure 23) confirms the lower mean thickness in T-Zone 1 and higher mean in T-Zone 2. T-Zone 4 box plot is the widest and illustrate a wider range and higher variability of data values compared to the other zones. The higher variance observed earlier in the summary statistics is also in support of this fact.

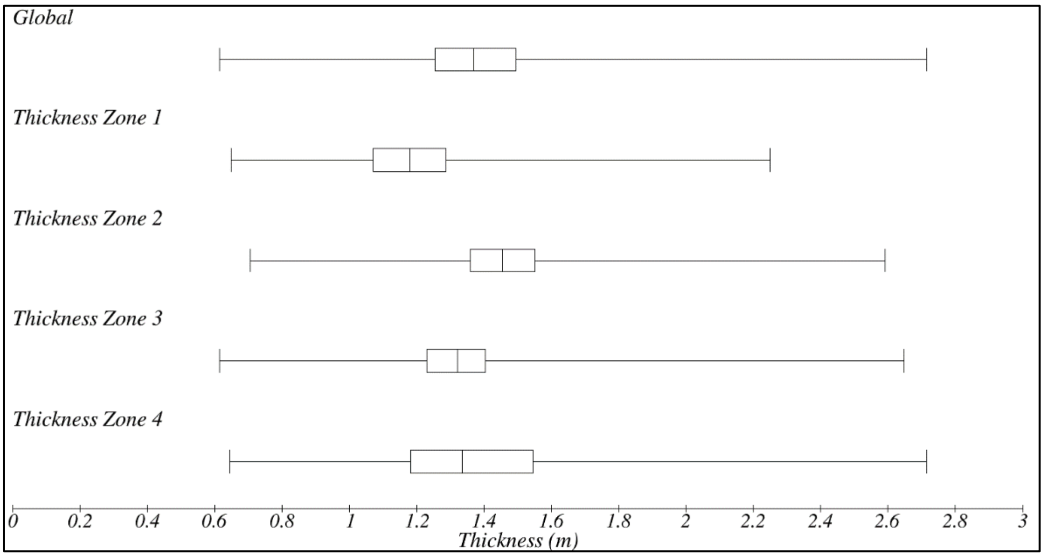

Figure 23: Box plot of the thickness of the orebody of the various zones.

For further graphical analysis of the thickness data set, Q-Q plots of the Zones were constructed (Figure 24). If two data sets have similar distribution then the solid line (which represents the quartiles of the data set) shown in the Q-Q plot should plot on the straight line which is 45^0 from the horizontal meaning $x = y$. From the six Q-Q plots it is evident that neither plot on the 45^0 line.

In the first 3 plots the points plot above the 45^0 line which illustrates that T-Zone 2, 3 and 4 have higher thicknesses compared to T-Zone 1. In Plot 4, the points plot below the 45^0-line illustrating that T-Zone 2 is thicker than T-Zone 3. Plot 5 shows that T-Zone 4 is thinner than T-Zone 2 for thicknesses below approximately 1.5m and thicker than T-Zone 2 for thicknesses thicker than 1.5m. Examination of Plot 6 show that T-Zone 4 has a thinner reef for thickness below approximately 1.3m and has thicker thickness for thickness above approximately 1.3m.

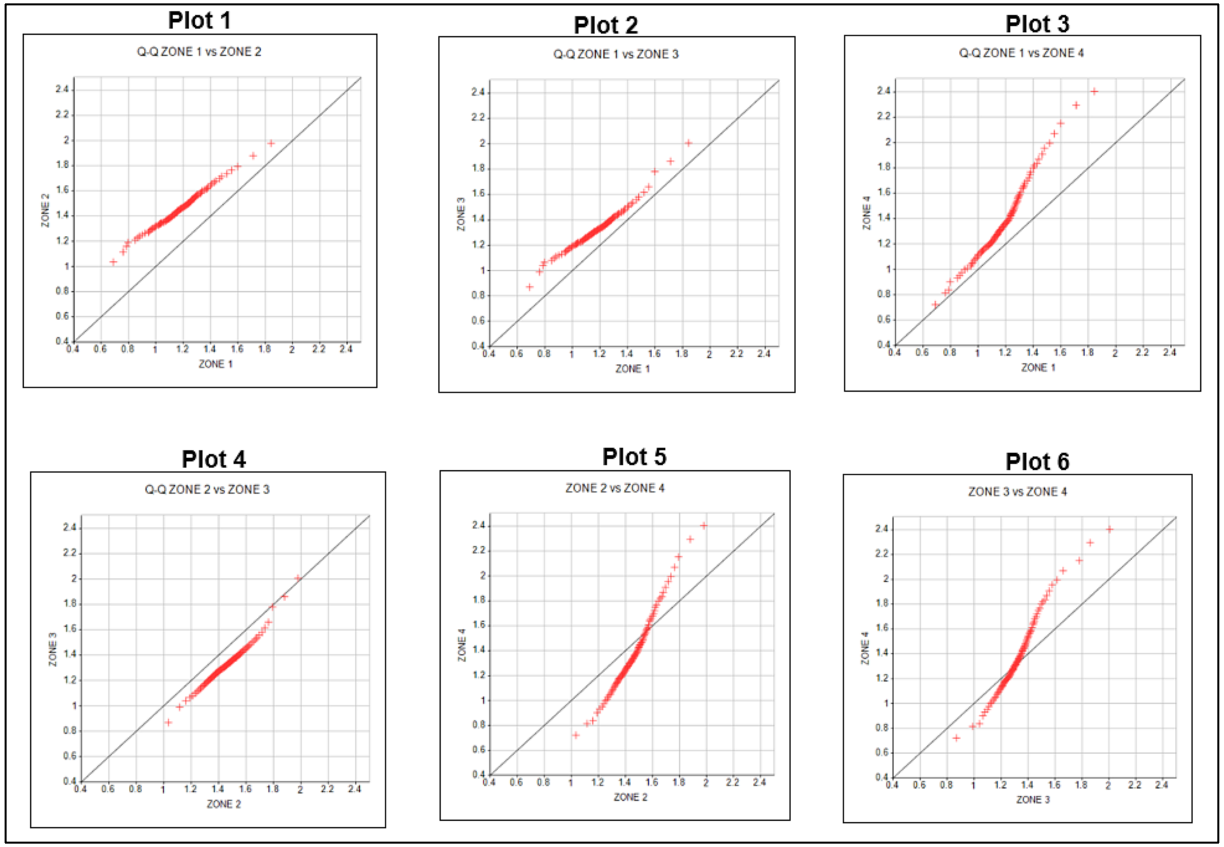

Figure 24: Q-Q plots of the orebody thickness of the various zones.

5.2.3 Influence of geology on the thickness of the orebody

In order to check if there is an influence of geological structures across the study area in comparison to the identified thickness zones, the main geological structures, namely faults, dykes, potholes, slumps and internal waste were overlain on the boundaries of the zones identified earlier (Figure 25). Linear structures i.e. the faults and dyke shown no correlation or relationship with the orebody thickness. This is expected as the orebody is of igneous origin and the linear structures are younger than the orebody hence any influence in the orebody itself will only been seen in the displacement of the lithologies in the case of faults and intrusion in the case of dykes.

Most potholes and slumps are mapped during mining of the reef and are difficult to detect from drilling in the case of the UG2, as a result the slumps and potholes shown in Figure 25 are concentrated in the mined out areas with very few of these structures identified in the mining area ahead of current mining. A relationship between the thickness zones and the occurrence of slumps and potholes is not indicated at this stage as these structures seem to be randomly distributed across the area and show no obvious correlation with the thickness of the orebody on a large scale.

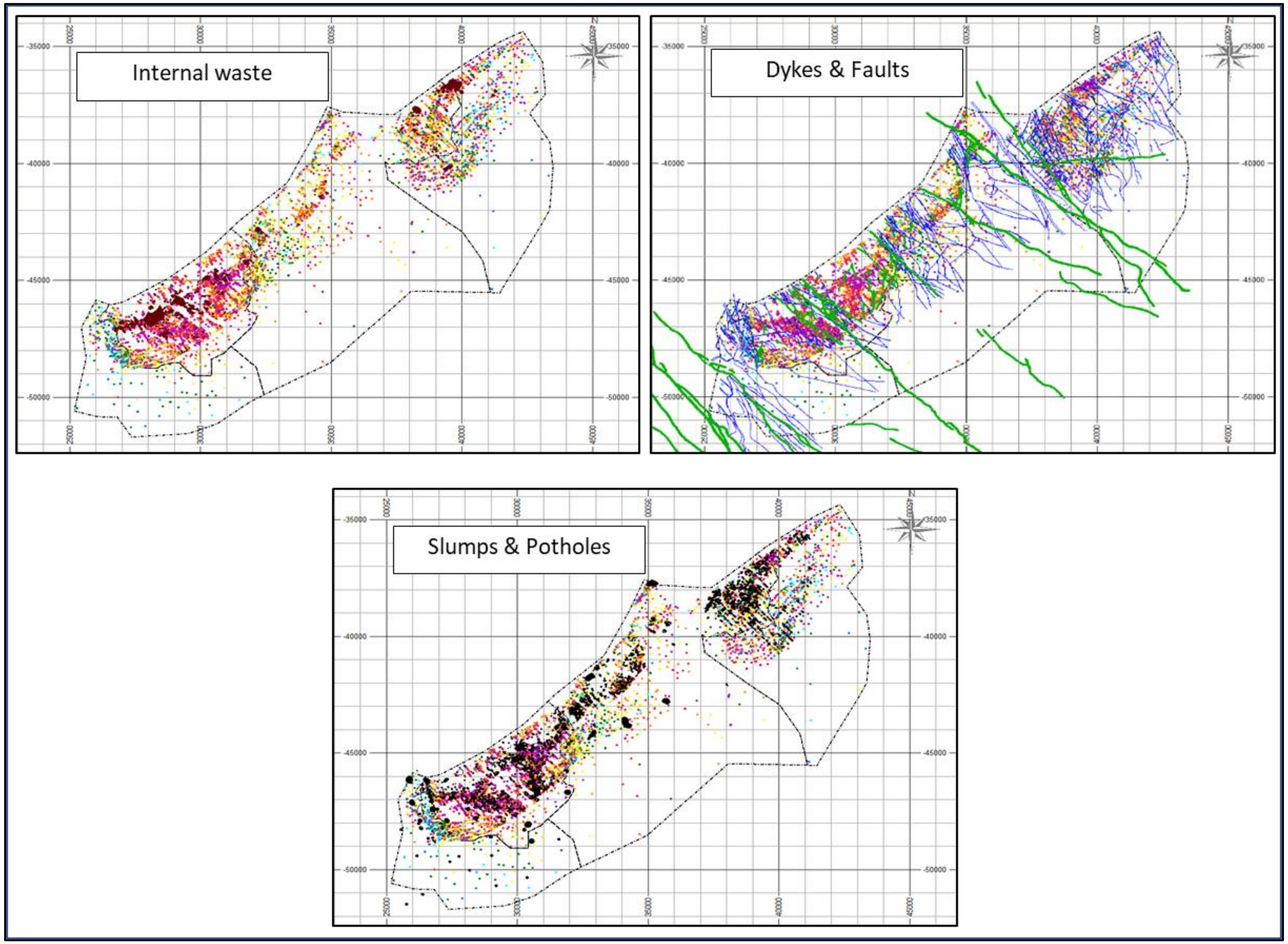

Figure 25: Thickness zones and data superimposed onto geological structures.

There is however an indication that there are more intersections with internal waste in T-Zone 2 in comparison to the other zones. Internal waste is within the reef and thus causes an increase in orebody width hence the thicker reef observed in T-Zone 2 which is also indicated in the summary statistics. An illustration of the impact internal waste on the reef is shown in Figure 26.

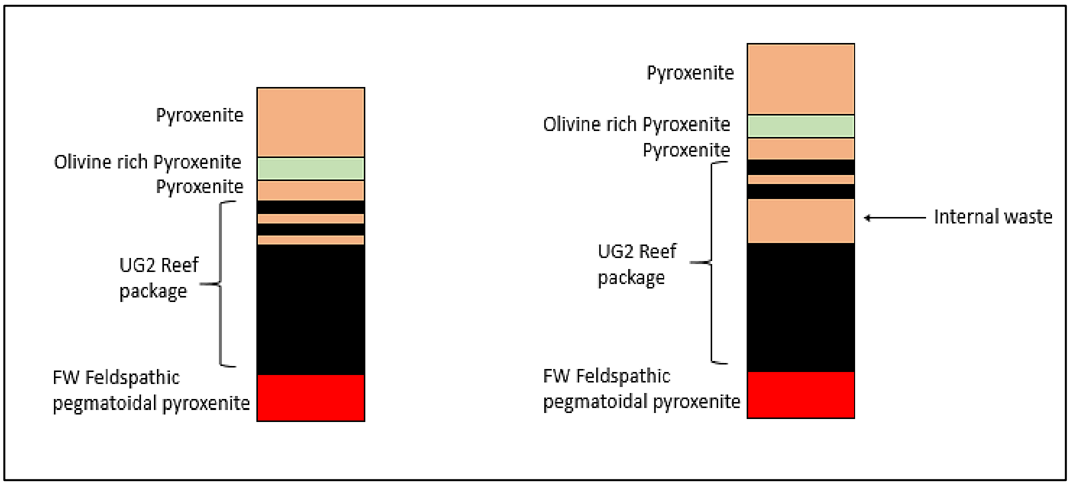

Figure 26: Illustration of the influence of increased internal waste within the reef on orebody thickness.

5.2.4 Thickness variography

Kriging estimation methods such as Ordinary Kriging (OK), Simple Kriging (SK) or Indicator Kriging (IK) require a variogram in order to give weight to samples that are used either to estimate a point location or a square or rectangular block/s of certain size. The main use of a variogram is to define the spatial correlation of regionalised variables. The notion is that samples that are close to each other are more likely to be similar than samples that are further from each other (Isaaks & Srivastava, 1989). Guibal (2001) states that a variogram can also be used for data validation, different data type comparisons, sampling density optimization and aiding in determining domaining for resource evaluation.

The first step in variography is to calculate the experimental semi-variogram using Eq. 13, and secondly to fit a suitable semi-variogram model to be used in the solving of the kriging solution. According to Journel and Huijbregts (1991), every geostatistical study starts with the creation of a model that describes the spatial structure of the variable under study. Variography involves choosing a lag distance h which is the distance at which samples are paired together to calculate the half-squared difference of the pairs using the formula:

$$\gamma^*(h) = \frac{1}{2N_h} \sum_{i=1}^{N_h} \left[Z(x_i) - Z\left(x_{(i+h)}\right)\right]^2 \qquad \text{Eq 13}$$

For instance if a lag of 100m is used, all samples that are 100m apart are paired and their grade value half squared differences are summed and divided by the number of pairs at 100m apart to determine the experimental variogram value for h = 100m.. This is done for 200m, 300m, 400m, 500m and so on depending on the extend of the data. Isaaks and Srivastava (1989) highlights the fact that it is nearly impossible in practice to have samples that are taken at exactly the specific lag, and thus a certain tolerance is used in order to increase the number of paired samples.

Despite distance, direction can be used to an advantage when paring the samples. If mineralisation is more continuous in a certain direction then samples can be paired within specified limits Figure 27.

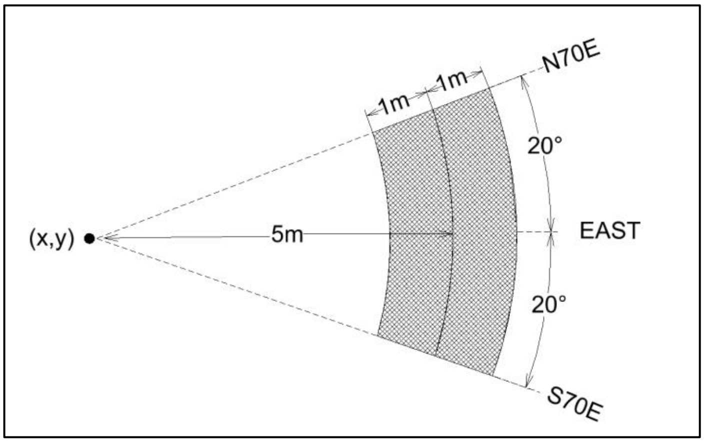

Figure 27: An example of how lag tolerance and direction tolerance is applied to select samples to pair with the point at (x, y) in practice. A sample falling within the shaded area will be paired with the sample at (x, y). Source: Isaaks and Srivastava (1989).

Upon calculation of the various lag, the half squared distance differences (experimental variogram) are plotted on a graph with the y-axis representing the squared differences value and the x-axis representing the different lag distances (Figure 28).

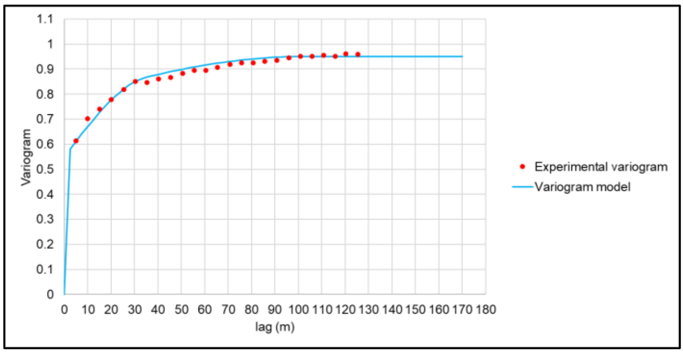

Figure 28: Example of a variogram with experimental points and model fitted. Source: Course exercise for Dohm (2018a) .

The main features of a variogram model (Figure 29) are the nugget, range and sill. The nugget effect is the discontinuity at the origin of the variogram and accounts for but not limited to the sampling error, location error and short scale structures (Guibal, 2001).

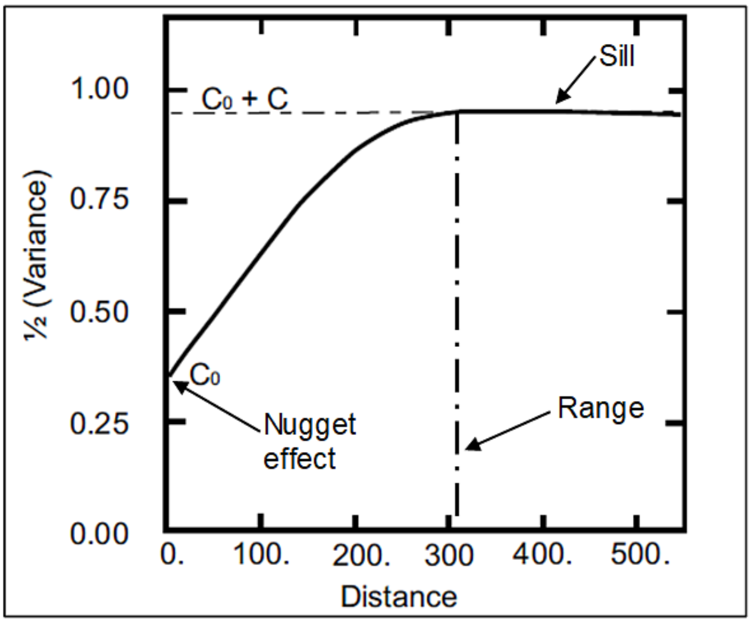

Figure 29: An example of a variogram and its features. Modified from Guibal (2001).

The influence of the nugget effect on kriging performance measures is shown in Figure 30 and illustrate that a higher nugget effect has negative implications on the performance measures.

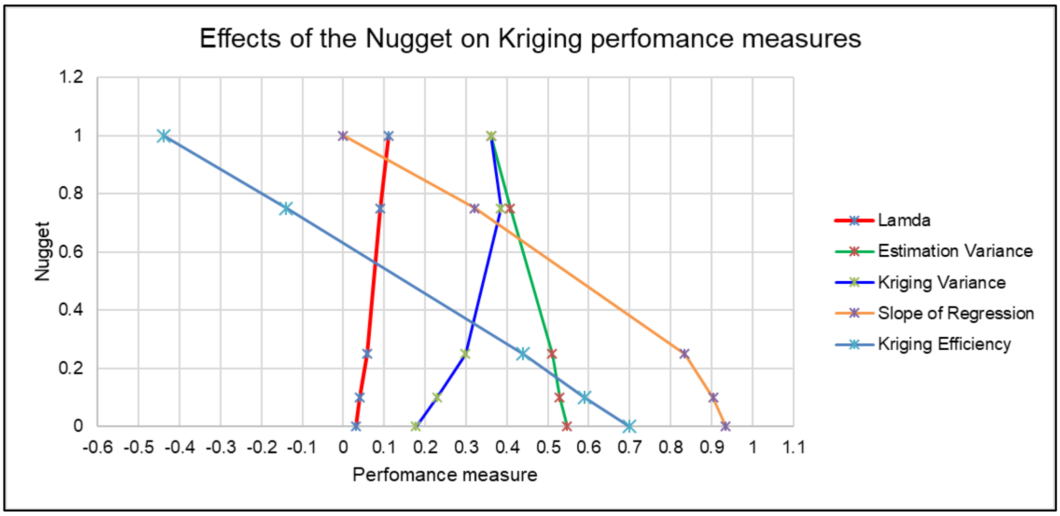

Figure 30: Influence of the nugget effect on the various kriging performance measures. Source: assignment for Dohm (2018a).

As the squared differences are calculated with an increasing lag distance, the resulting values eventually reaches a plateau. The distance at which this plateau is reached is termed the range of a variogram. Beyond the point where the plateau is reached, there is no longer spatial correlation between the sampled points (Glass, 2003). The sill of a variogram is the plateau that is reached at the range (Isaaks & Srivastava, 1989).

As discussed earlier, once the squared differences have been plotted, a model needs to be fitted to the points. Journel and Huijbregts (1991) distinguishes between two types of theoretical models of regionalization, namely models with a sill (also called transitional models) and models without a sill. Models with sills include spherical models, exponential models and Gaussian models where models lacking a sill include linear models and logarithmic models (Figure 31).

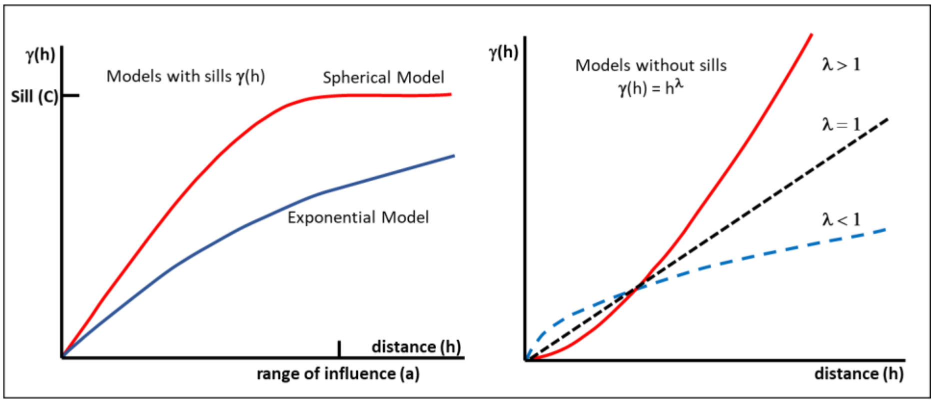

Figure 31: Types of variogram models, modified after (Clark, 1979).

The experimental semi-variograms of the orebody thickness are represented in Figure 32. The variography was done using Datamine™ software. Since variography is sensitive to outliers a filter of 0.7m to 1.4m was introduced for T-Zone 1 variogram to make the structures of the variograms less noisy meaning that all values below 0.7m and above 1.4m were excluded for the semi-variogram calculation in this zone. T-Zone 3 data values were also filtered at between 1m and 1.6m to improve the semi-variogram. All the other zones (T-Zones 2, 4 and the Global) semi-variogram were calculated without a filter as the variograms were well behaved. The input values of calculating the semi-variograms are shown in Table 2.

Table 2: Values used in experimental variogram calculation.

Zone	Lag (m)	Filter minimum (m)	Filter maximum (m)	No. of excluded samples	% excluded
1	40	0.7	1.4	76	12
2	220	-	-	-	-
3	130	1	1.6	224	8
4	205	-	-	-	-
Global	155	-	-	-	-

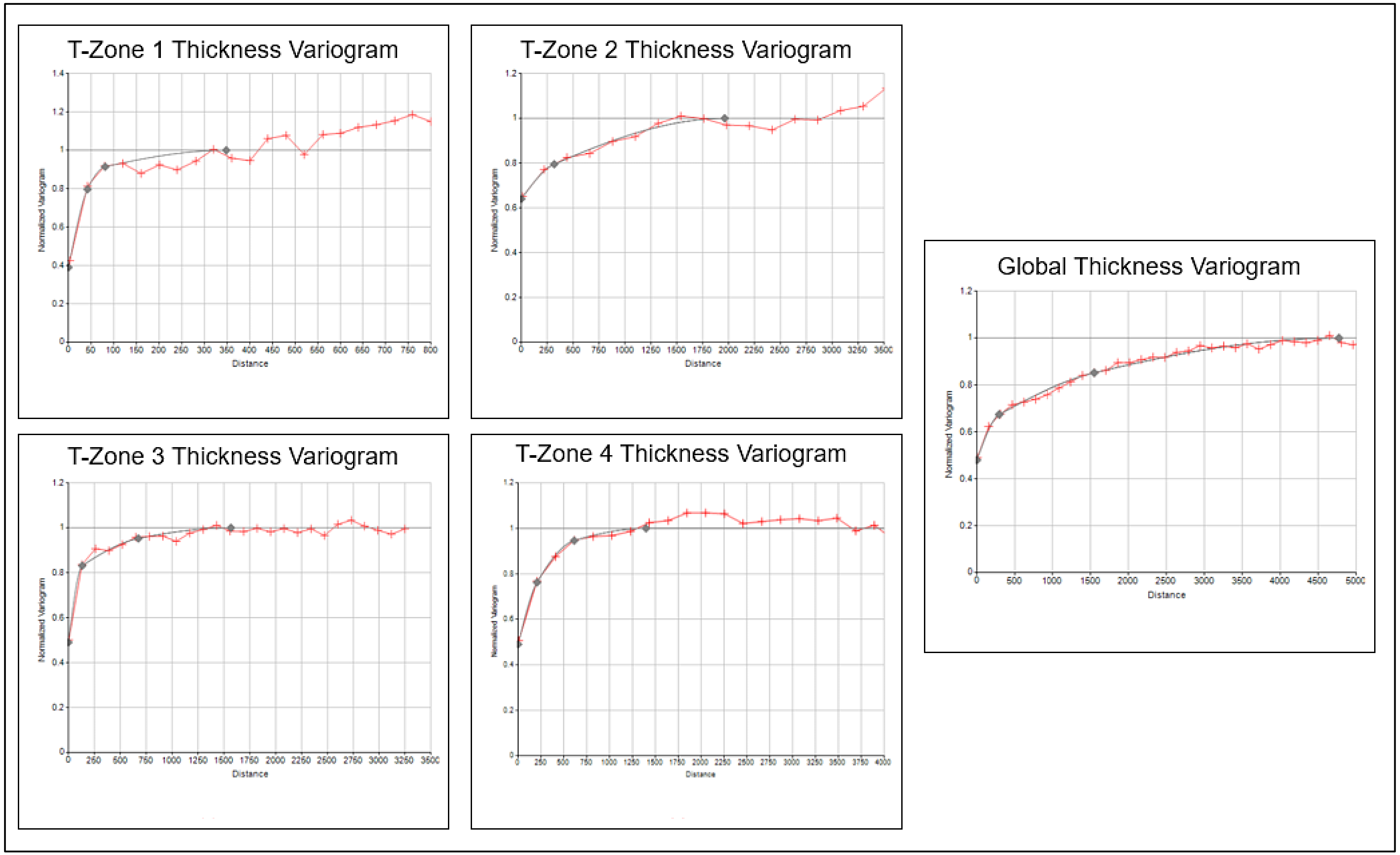

Figure 32: Experimental variograms of the orebody thickness with fitted models.

Analysis of the data posting did not reveal any obvious preferred direction of continuity thus isotropic variograms were constructed. Clear structures as shown in Figure 32 were obtained from the semi-variogram analysis and spherical models were fitted with the model parameters shown in Table 3.

For a comparison of the thickness variograms, a plot of the all the variograms is shown on Figure 33. T-Zone 2 variogram has a relatively higher nugget than the other zones which have nuggets of below 50%. The global zone has the longest range in excess of 4.5kms whilst the individual zones have ranges of less than 2kms. This is because of the longer distance of the global area as compared to the individual zones which have smaller limits. T-Zone 1 variogram has a relatively short range of approximately 340m which is expected as this zone is the smallest and contains the least amount of data in comparison to the other three zones.

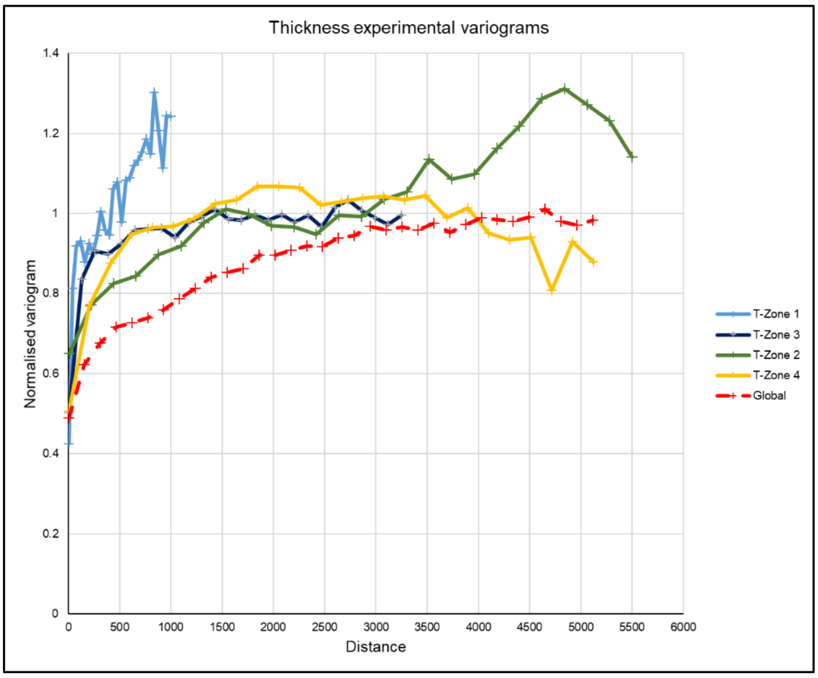

Figure 33: Theoretical variograms of the thickness zones.

Table 3: Thickness variogram model parameters for the various zones.

		Structure 1		Structure 2		Structure 3	
Zone	**Nugget**	**Range**	**Variance**	**Range**	**Variance**	**Range**	**Variance**
1	0.39	42	0.15	81	0.33	348	0.13
2	0.64	318	0.09	1962	0.27	-	-
3	0.49	133	0.30	675	0.09	1568	0.12
4	0.49	207	0.12	614	0.25	1398	0.14
Global	0.48	295	0.14	1551	0.10	4773	0.28

5.3 Density

According to Appleyard (2001), density forms one of the three parameters of a resource estimate together with the volume and grade and consequently in resource estimation. As such good practice requires a good enough quantity database of the density. Out of a total of 8256 boreholes and channel samples, 7027 have density measurements. This represents about 85% of the total database.

5.3.1 Density (t/m^3) analysis

The density data values are 7027 in total with the histogram of the data values shown on Figure 34. The density data has a minimum value of 3.357 t/m^3 and a maximum of 4.809 t/m^3. The shape of the histogram indicates that the density is normally distributed with a mean of 4.090 t/m^3. The cumulative plot on Figure 35 indicates that most of the data falls between 4.0 t/m^3 and 4.2 t/m^3 and similarly with the thickness cumulative plot no obvious mixed population are revealed by the histogram and cumulative plot.

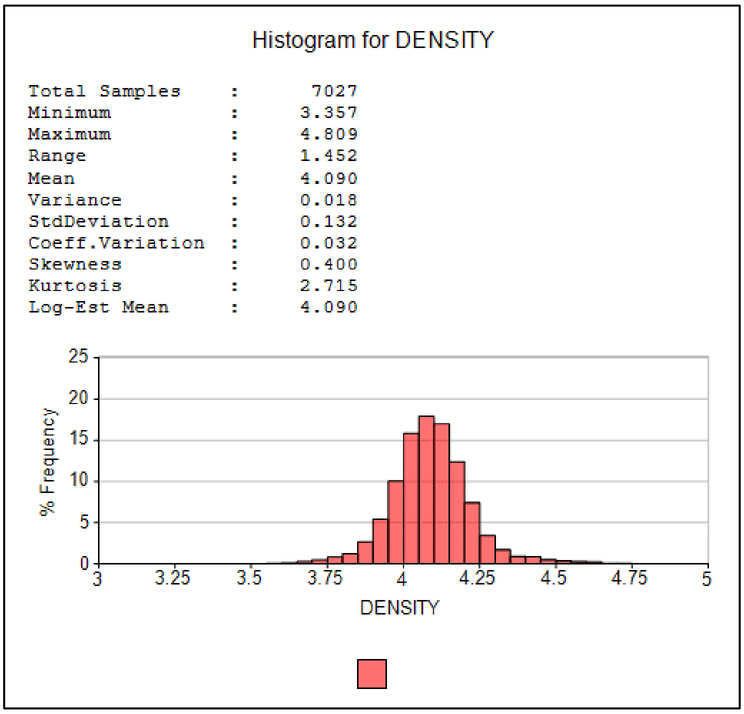

Figure 34: Histogram of the density data (t/m3).

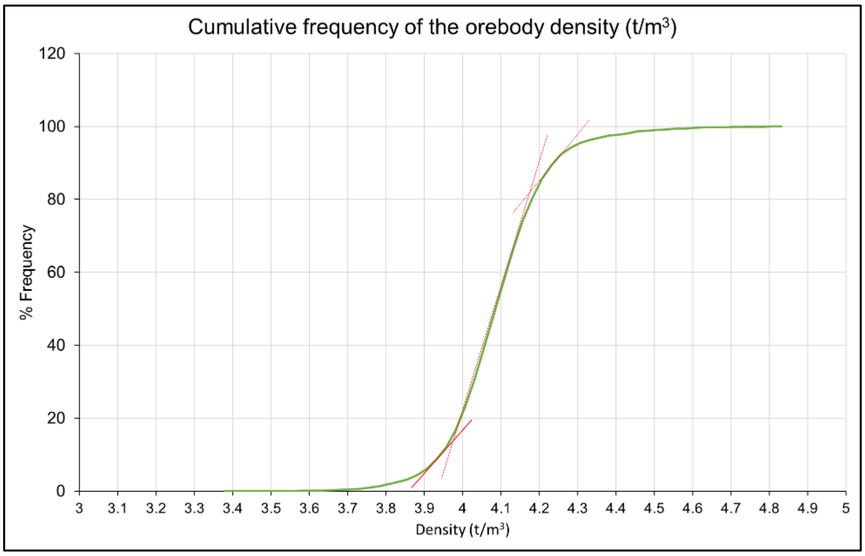

Figure 35: Cumulative frequency plot of the orebody density.

To spatially analyse the data, the density values were plotted on a data post with the data subdivided by 0.1t/m^3 intervals. Figure 36 represents a classed data posting of the 7027 density data points across Amandelbult Complex. As with the thickness, several post maps for the density were tested and are shown in the appendix. From the data posting selected for the data analysis, three zone are identifiable.

Density Zone 3 (D-Zone 3) indicates that the data in the area has the lowest density whilst Density Zone 2 (D-Zone 2) indicates that it has a higher density due an obviously prevalence of warmer colours. Density Zone 1 (D-Zone 1) also indicates an area of lower density but this density in higher than that observed in D-Zone 3. The data ranges for D-Zone 1 are predominantly in the ranges of between 4.0 t/m^3 and 4.1t/m^3. D-Zone 2 data ranges between mostly 3.9 t/m^3 and 4.1 t/m^3 with a notably greater variety of colours ranges compared to D-Zone 1 and D-Zone 2. D-Zone 2 values fall predominantly in the higher range between of 4.1 t/m^3 and 4.81 t/m^3.

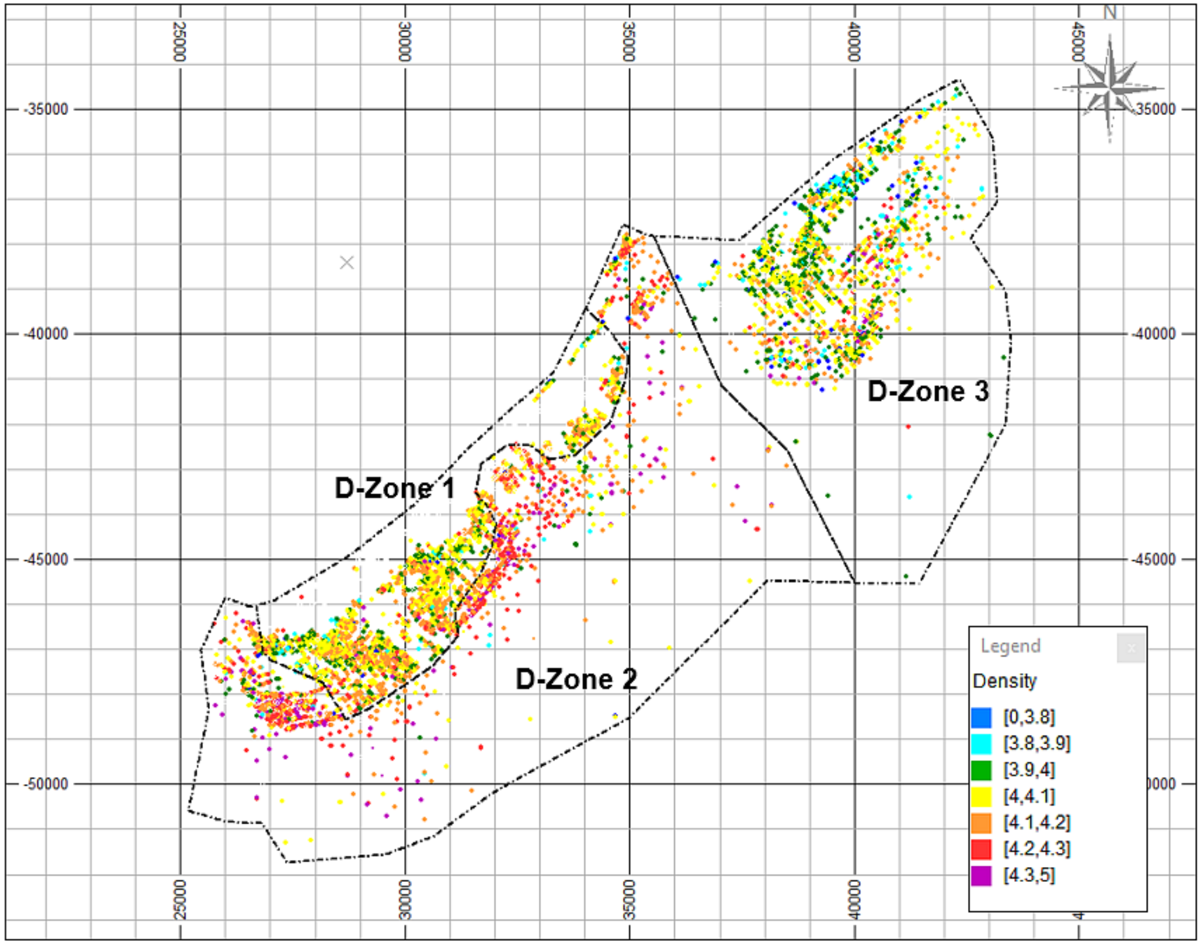

Figure 36: Classed data post of the orebody density (t/m³).

5.3.2 Density statistics

The summary statistics of the orebody density (t/m^3) for the three zones and the global area are shown in Table 4. A mean of 4.176t/m^3 for D-Zone 2 confirms that this zone has a slightly higher density in comparison to the other zones as also observed from the data post. Also a low mean for D-Zone 3 of 4.030t/m^3 supports the fact that the orebody density is the lowest of all the other three zones. D-Zone 1 also has a lower mean of 4.068t/m3 which coincides with the data post examination findings.

Table 4: Summary statistics density (t/m^3) for the various zones.

	Global	D-Zone 1	D-Zone 2	D-Zone 3
No. of data points	7027	2625	2197	2205
Min (t/m^3)	3.357	3.554	3.357	3.483
Max (t/m^3)	4.809	4.541	4.809	4.599
Range (t/m^3)	1.452	0.987	1.452	1.116
Mean (t/m^3)	4.090	4.068	4.176	4.030
Mode	4.068	4.068	4.215	4.004
Median	4.086	4.071	4.173	4.034
Variance (t/m^3)^2	0.175	0.008	0.020	0.015
Standard deviation (t/m^3)	0.132	0.088	0.142	0.123
Coefficient of variation	0.032	0.022	0.034	0.030
Skewness	0.400	-0.416	0.354	0.122

The high variability observed in the data post in D-Zone 3 is confirmed by the summary statistics. The variance in D-Zone 3 is 0.151(t/m^3)^2. This zone and D-Zone 2 have higher variances than D-Zone 1. In fact by differentiating and portioning the area into the zones, the variance between D-Zone 1 and D-Zone 2 differs by 60% and between D-Zone 1 and D-Zone 3 it differs by 47%.

The histograms of the density zones are represented below in Figure 37. The shapes of the histograms indicate normal distributions with the shape of the global area better pronounced of a normal distribution. The skewness of all the D-Zones is between -1/2 and +1/2 which indicates that the shapes of the distributions are approximately symmetrical

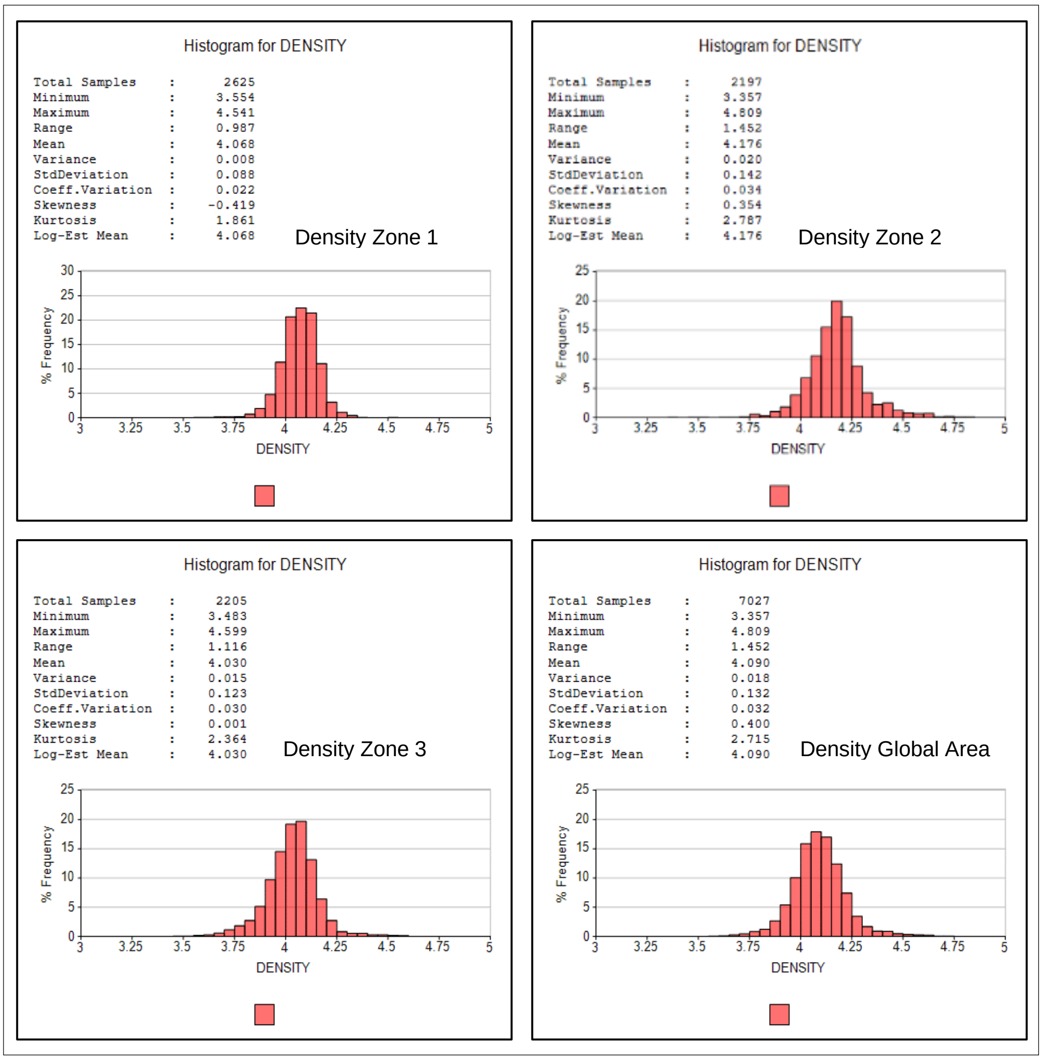

Figure 37: Density histograms (UG2).

Both D-Zone 2 and D-Zone 3 have longer tails to the right and the left which is also supported by the high variance. D-Zone 1 has shorter tails indicating a low standard deviation. Figure 38 represents a combined cumulative plot of the density for the four zones and the global area. D-Zone 2 cumulative plot is more to the right which is an indication of that it has higher values in comparison to the other zones. D-Zone 3 however plots the farthest to the left which is an indication of lower values in the zones which is evident in the data post as well.

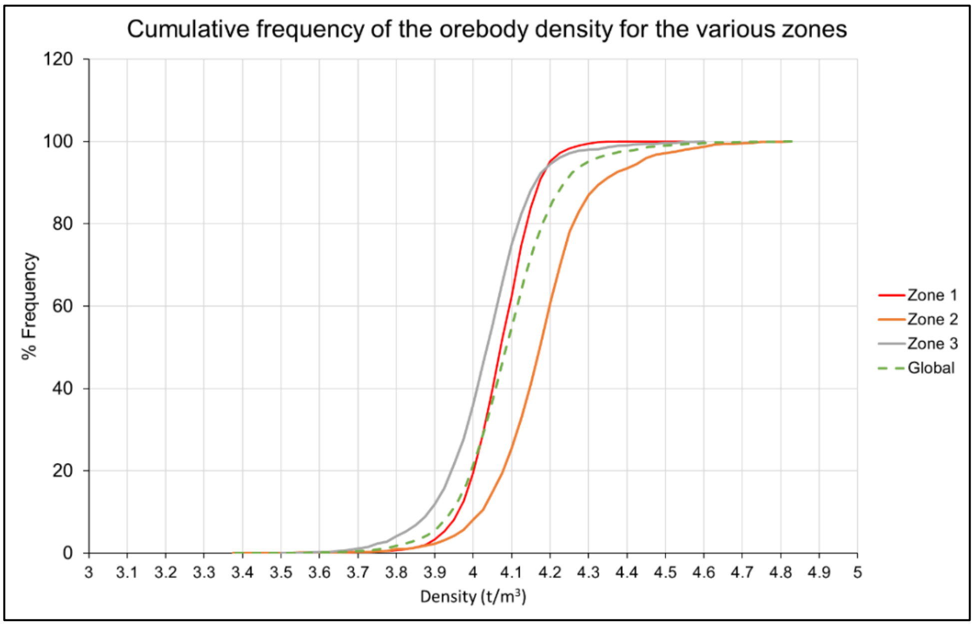

Figure 38: Cumulative frequency plot of the density.

An analysis of the box plots for the density is supported by the graphical representation on Figure 39 and indicates overall high values for zone two and lower values for D-Zone 3.

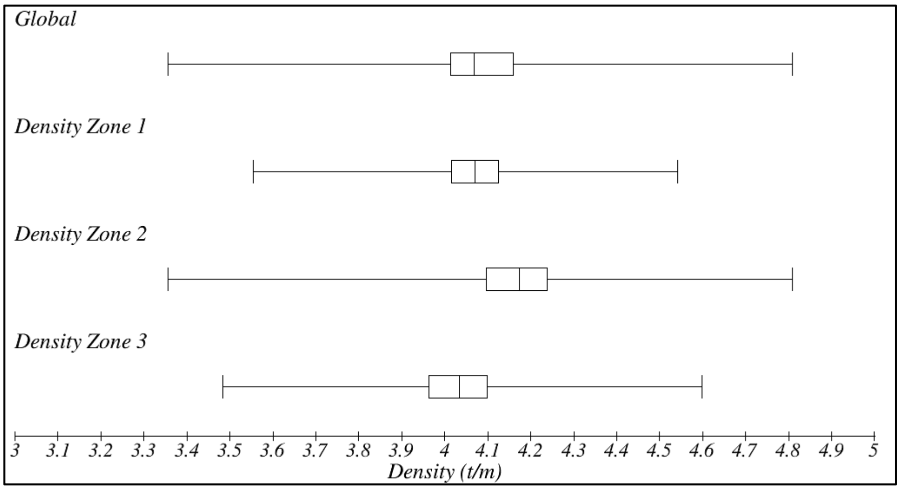

Figure 39: Density box plots.

To further compare the density zones Q-Q plots were constructed to aid in the analysis (see Figure 40). Deviation from the 45^0 line highlights a difference in the density distribution between the zones.

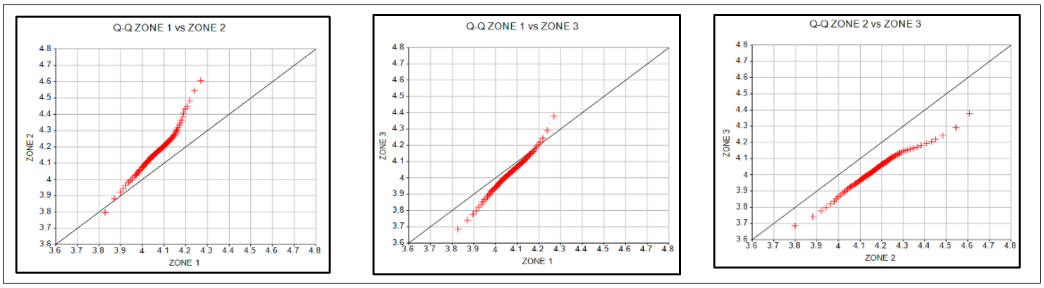

Figure 40: Q-Q plot of the density for the various zones.

An examination of the Q-Q plots shows that for the three zones the quartiles in comparison with each other do not plot on the 45^0 line. D-Zone 1 and D-Zone 2 Q-Q plot indicates a higher density in D-Zone 2, D-Zone 1 and D-Zone 3 indicate lower density for D-Zone 3. The Q-Q plot of D-Zone 2 and 3 shows a lower density for D-Zone 3 compared to D-Zone 2.

5.3.3 Influence of geology on the density

The density zones with the various known geological structures are shown in Figure 41. D-Zone 1 which was identified during the statistical analysis as having a lower density shows a correlation with the presence of internal waste areas. The zone with the most internal waste occurrence falls predominantly in D-Zone 1. Since the internal waste is a pyroxenite which has a lesser density than chrome, this is expected as shown by the density profile on Figure 42.

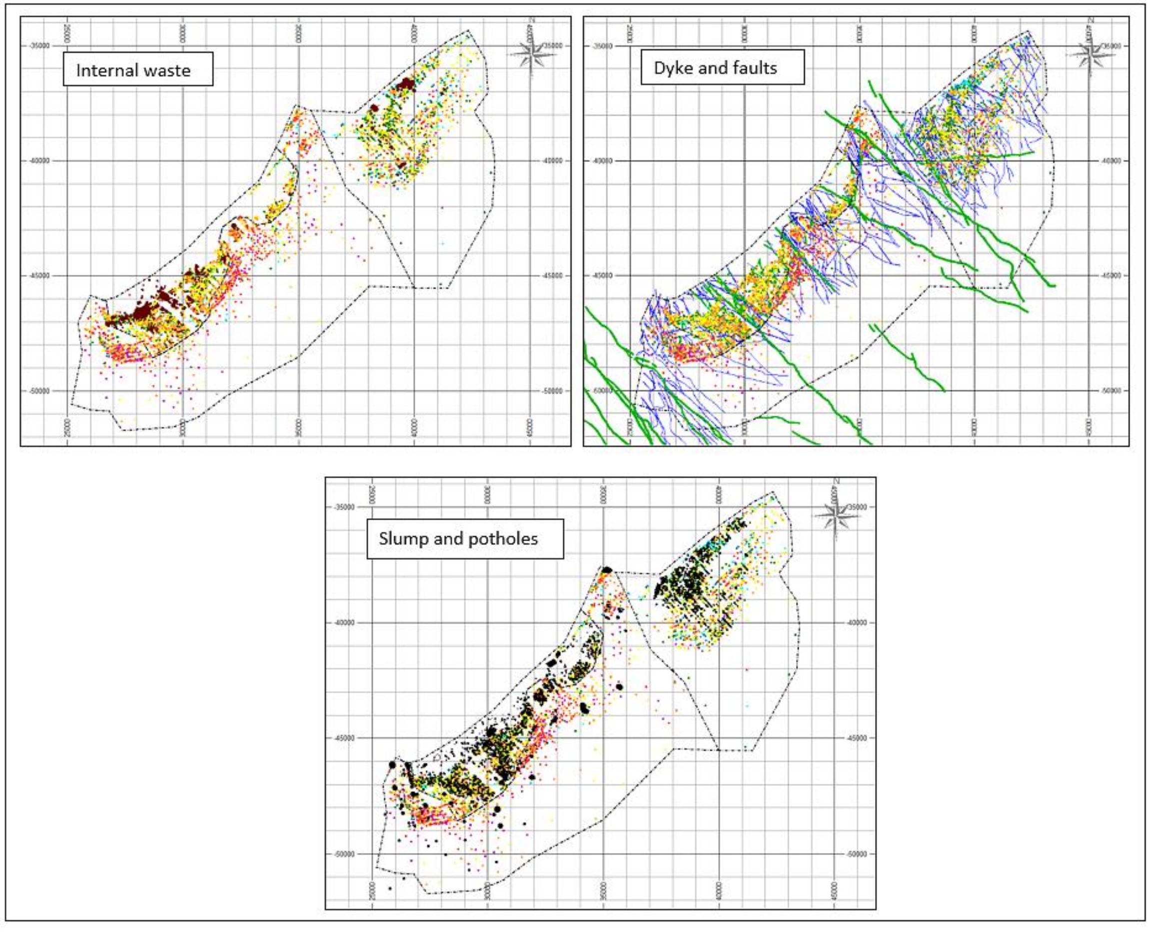

Figure 41: Geology superimposed onto the density zones

The slumps and potholes however shown no relation with the density zones and the faults and the dyke structures.

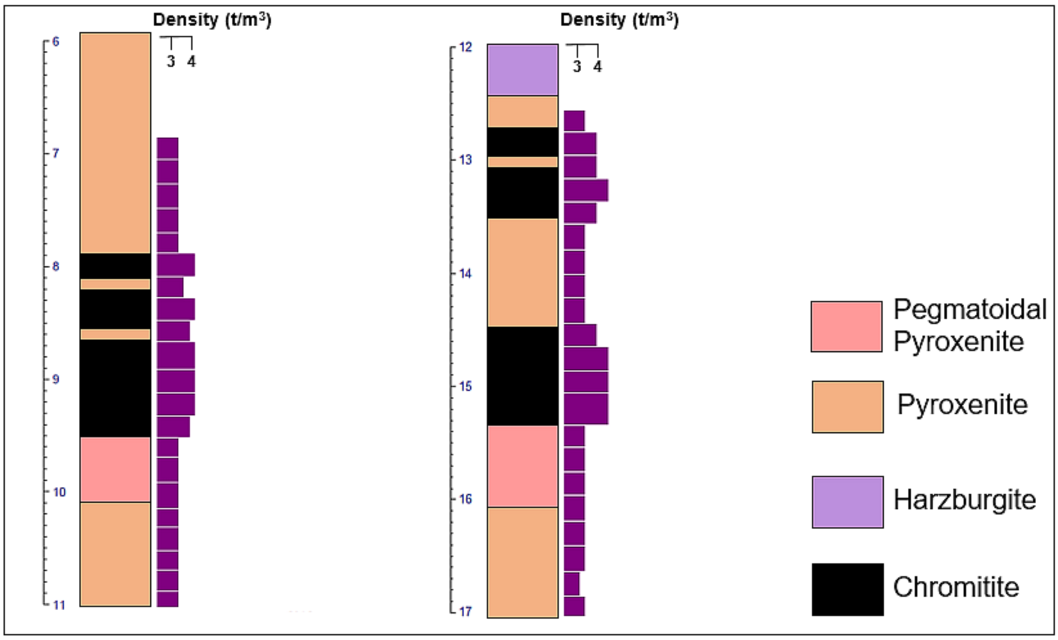

Figure 42: Comparison of two borehole density profiles where the internal waste is minimal and where it is excessive.

5.3.4 Density variography

The orebody density experimental variogram and subsequent models are shown on Figure 43. The structures for D-Zone 1 and D-Zone 2 are clear, however for D-Zone 3 the semi-variogram shows a rise till the 480m lag, then drops and then starts to rise again from the 1150m lag which indicative of a trend in the data. An attempt to improve the variography for D-Zone-3 is out lined in the next sub-section. The input for the variography calculations is shown in Table 5 and resulting model parameters are shown in Table 6.

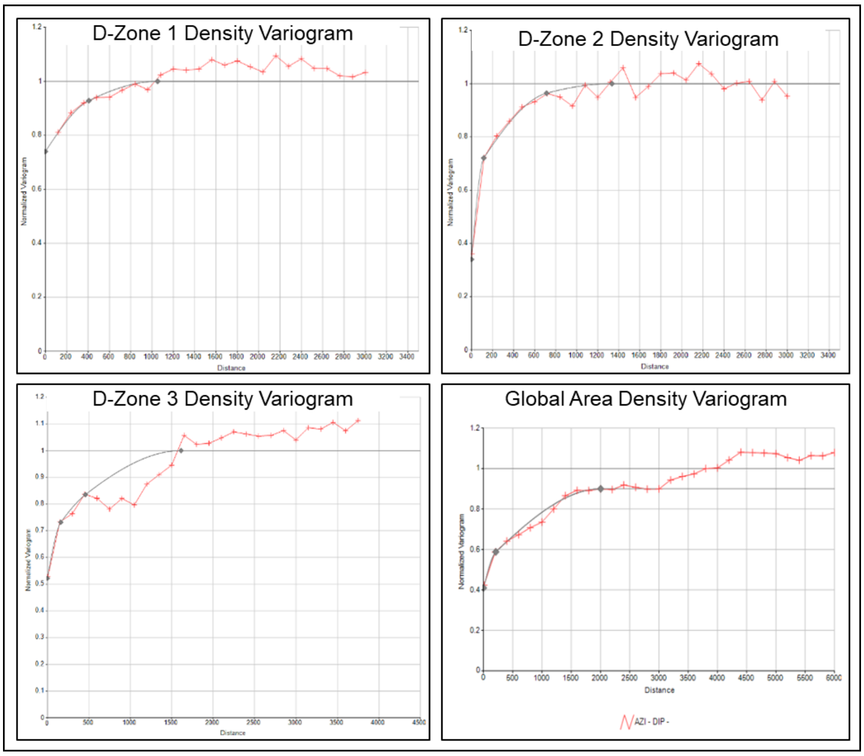

Figure 43: Experimental variogram of the orebody density of the various zones.

Table 5: Experimental variogram calculation values for the density.

Density Zone	Lag (m)	Filter minimum (t/m^3)	Filter maximum (t/m^3)	No. of excluded samples	% excluded
1	120	3.75	4.50	12	0.5
2	120	3.80	4.625	38	2
3	150	-	-	-	-
Global	200	-	-	-	-

Table 6: Density variogram model parameters.

		Structure 1		Structure 2		Structure3	
Zone	**Nugget**	**Range**	**Variance**	**Range**	**Variance**	**Range**	**Variance**
1	0.74	408	0.1	1053	0.16	-	-
2	0.34	117	0.31	714	0.22	1335	0.13
3	0.52	163	0.14	460	0.06	1614	0.28
Global	0.41	212	0.12	2004	0.37	-	-
Global*	0.46	212	0.13	2004	0.41	-	-

*The sample variance and variogram sill are not equal. The variogram parameters have been standardised to sum to one for the kriging exercise.

5.3.5 Re-assessment of D-Zone 3

After noticing a trend in D-Zone 3, a decision was taken to try to further split this zone. A second post map was plotted (Figure 44) using only the data in D-Zone 3. After re-examination of D-Zone 3, two zone are notable from the classed post map.

Zone 3 data posting

With a re-run of the classed post map of the D-Zone 3 values, two further zones were identified, Density Zone 3-1 (D-Zone 3-1) and Density Zone 3-2 (D-Zone 3-2). From the visual examination of the data post D-Zone 3-1 data values indicate that they range mostly between 3.90t/m^3 and 4.10t/m^3 whilst D-Zone 3-2 data values range between 4.00 t/m^3 and 4.20t/m^3. D-Zone 3-2 also indicates that is has a few data values in the higher regions of greater than 4.20t/m3 which is not the case in D-Zone 3-1.

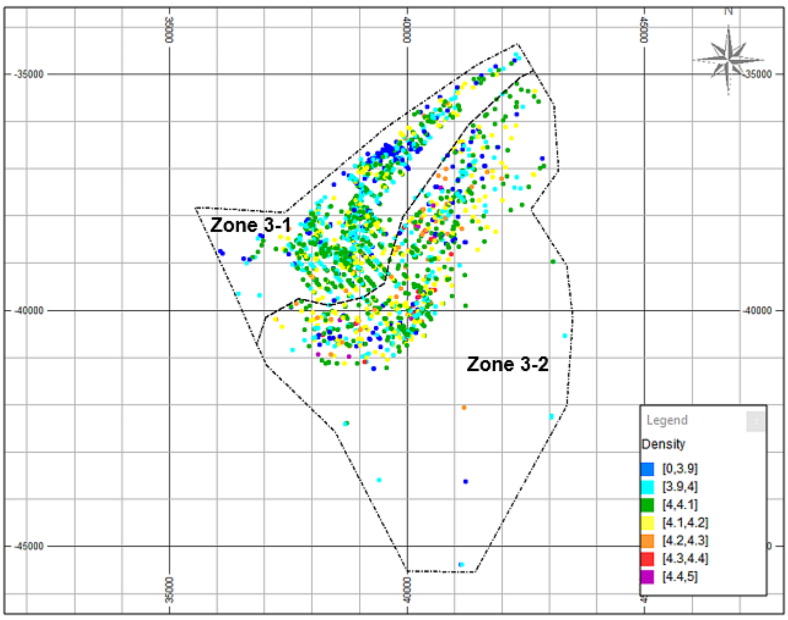

Figure 44: Data posting of D-Zone 3 with subsequent split into D-Zone 3-1 and D-Zone 3-2.

Zone 3 Statistics

A statistical comparison of the two zones (D-Zone 3-1 and 3-2) is represented in Table 7. The means of the two zones are not different from each other however their variances differ by 39% suggesting a larger spread of data values in D-Zone 3-2 which has a variance of 0.018$(t/m^3)^2$.

Table 7: Summary statistics of D-Zone 3 redefined.

	Global	D-Zone 3	D-Zone 3-1	D-Zone 3-2
No. of data points	7027	2205	1179	1026
Min (t/m^3)	3.357	3.483	3.519	3.483
Max (t/m^3)	4.809	4.599	4.263	4.599
Range (t/m^3)	1.452	1.116	0.733	1.116
Mean (t/m^3)	4.090	4.030	4.003	4.060
Mode	4.068	4.004	4.048	4.091
Median	4.086	4.034	4.013	4.065
Variance $(t/m^3)^2$	0.175	0.015	0.011	0.018
Standard deviation (t/m^3)	0.132	0.123	0.104	0.135
Coefficient of variation	0.032	0.030	0.026	0.033
Skewness	0.400	0.122	-0.854	0.158

The histograms of the two zones (D-Zone 3-1 and 3-2) are shown in Figure 45 together with D-Zone 3 and the global area. D-Zone 3-1 histogram is negatively skewed whilst zone D-Zone-2 looks approximately symmetrical. A skewness on -0.854 for D-Zone 3-1 confirms that the shape of the distribution is indeed moderately negatively skewed as observed from the histogram. D-Zone 3 also has a tail to the left whilst D-Zone 3-2 has longer tail to the right supporting that this zone has a few higher values in comparison to D-Zone 3-1. The trend observed in the variogram of D-Zone 3 could be caused by paring on higher values in D-Zone 3-2 and lower values in D-Zone 3-1. The combined cumulative frequency plot on Figure

46 highlight the lower density of D-Zone 3 and its further partitioned zones 3-1 and 3-2. The global cumulative plot is more to the right than for D-Zone 3, 3-1 and 3-2.

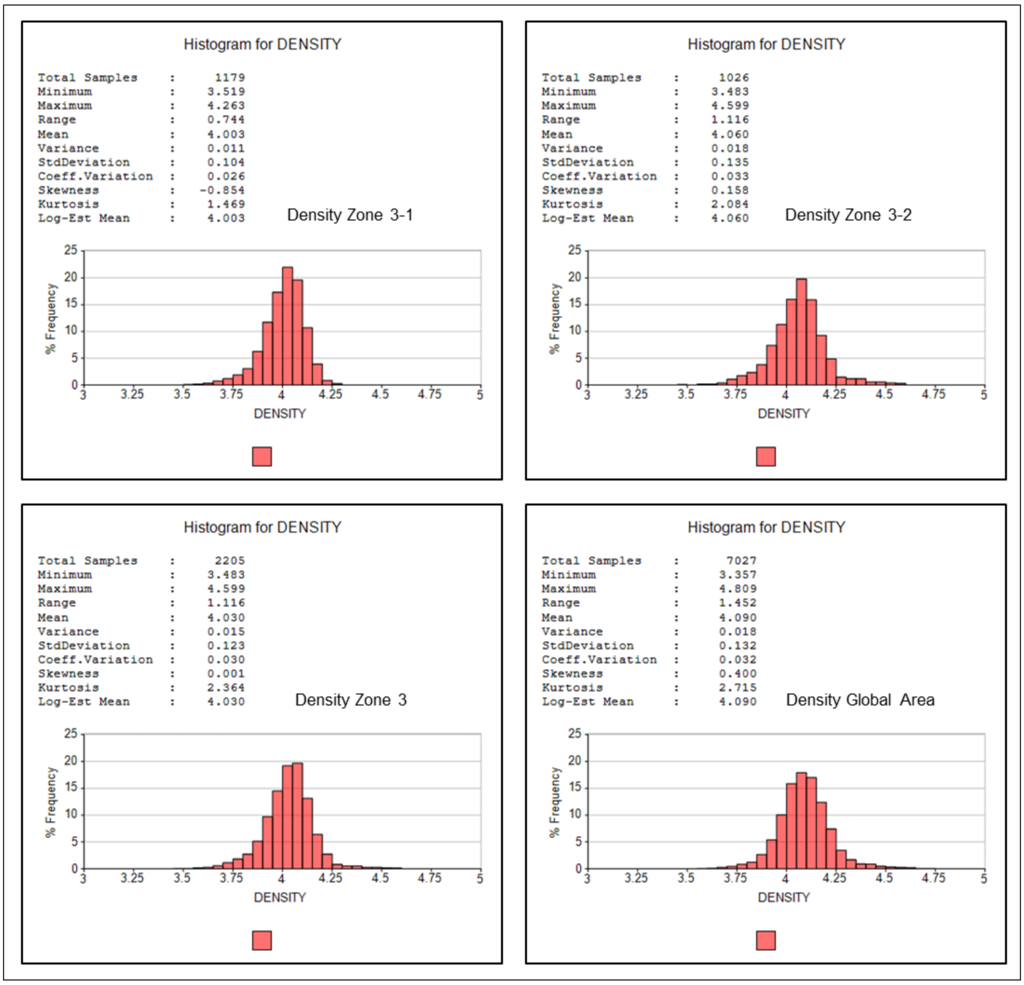

Figure 45: Histogram of the D-Zones 3-1, 3-2, 3 and the global area.

The box plot of D-Zone 3, 3-1 and 3-2 and the global area (see Figure 47) indeed show that D-Zone 3-2 has higher values than D-Zone 3-1. Also, the box plot shows that the lower values in D-Zone 1 also cause D-Zone 3 to show a lower average.

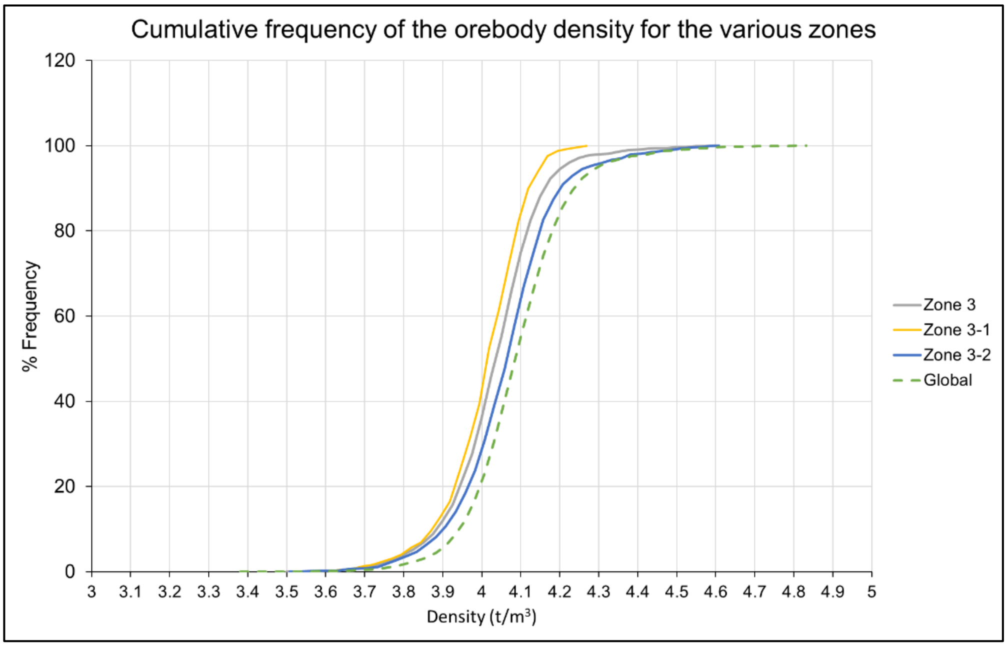

Figure 46: Combined cumulative frequency plot of the various zone.

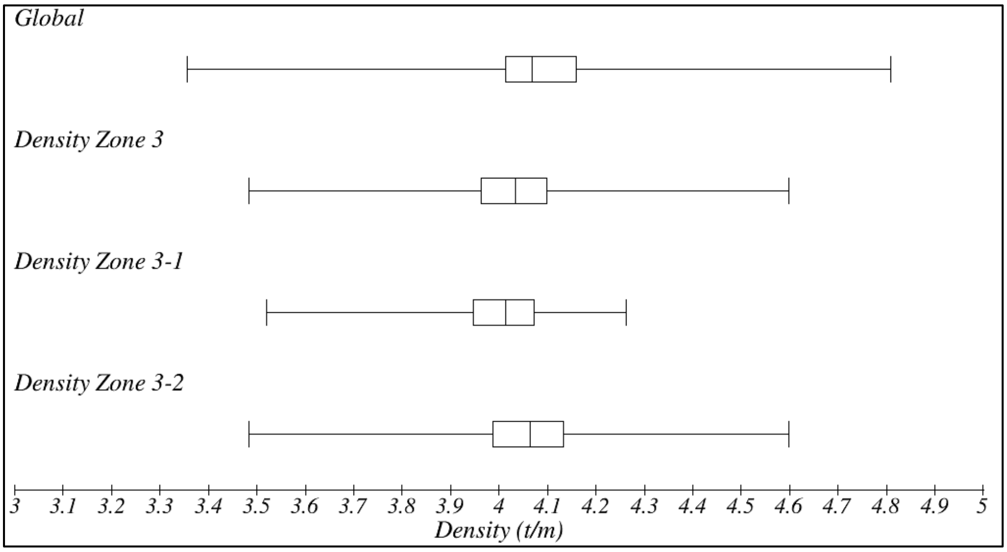

Figure 47: Box plot of the density of the various zones.

The Q-Q plot of D-Zone 3-1 and D-Zone 3-2 as shown in Figure 48 confirms that D-Zone 3-2 quartiles are higher than that of D-Zone 3-2. The points on the Q-Q plot slightly increase in a gentle angle starting from the 3.90t/m^3 of D-Zone 3-2 and then change steeply at the 4.20 t/m3 mark further showing the higher quartiles of D-Zone 3-2 in comparison to D-Zone 3-1.

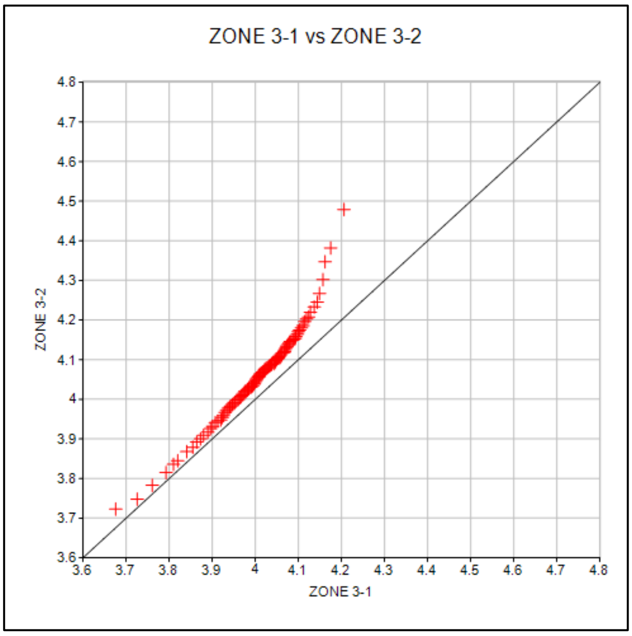

Figure 48: Q-Q plot of density zone 3-1 and 3-2.

Zone 3 variography

The variograms for D-Zone 3-1 and D-Zone 3-2 together with D-Zone 3 and the global zone are shown on Figure 49. The experimental variograms have improved as compared to prior to splitting of the D-Zone 3. D-Zone 3-1 reaches a plateau at 90% of the sample variance and has a higher nugget compared to D-Zone 3-2. A comparison of all the density theoretical variograms is represented in Figure 50. As with the thickness variograms, the global density as well shows a longer range as opposed to the variograms in the other four zones. Zone 3-1 has the highest nugget of 63% with the other zones having nuggets below 50% (excluding D-Zone 3). The values used for calculating the experimental variograms for the zones are shown on Table 8 and the model parameters are shown on Table 9

.

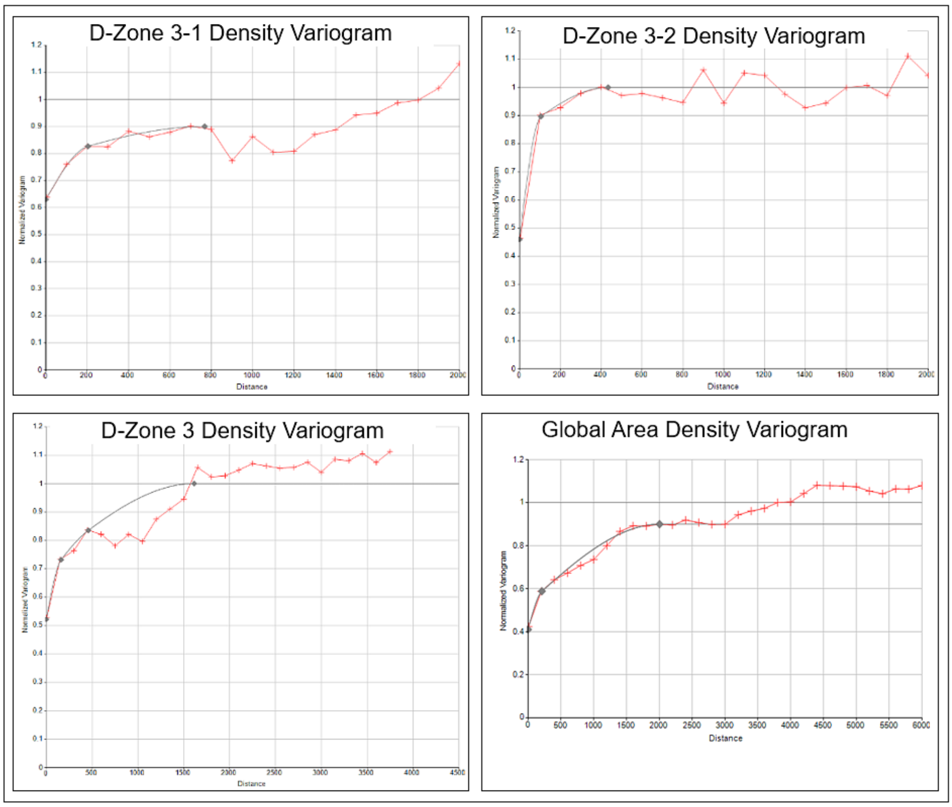

Figure 49: Experimental variogram of the orebody density of the various zones.

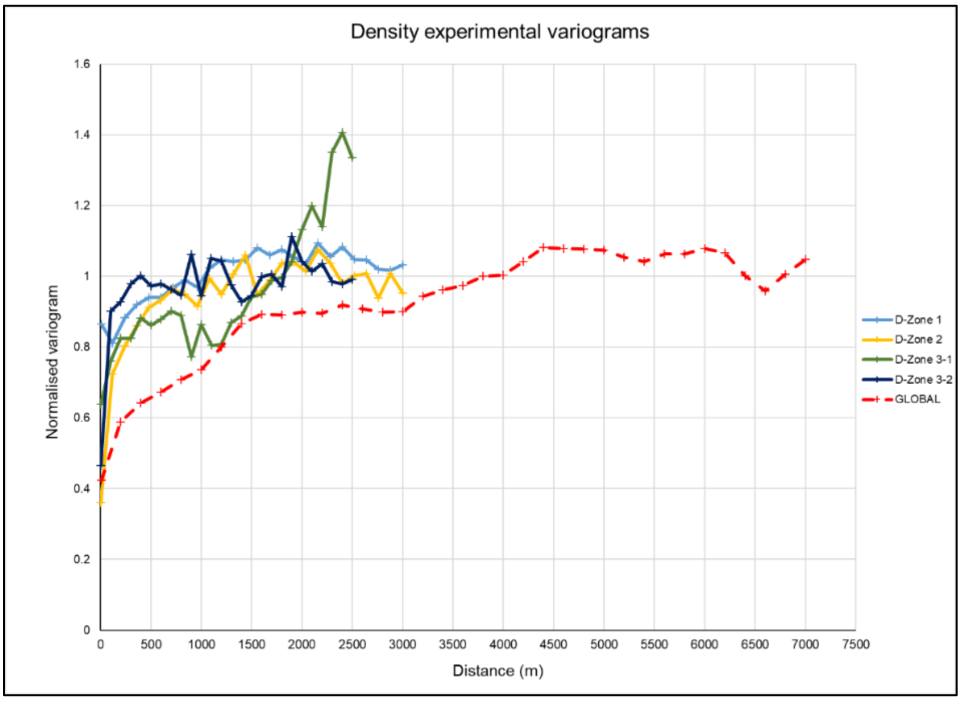

Figure 50: Theoretical variograms of the density.

Table 8: Values used for the calculation of the density experimental variogram.

Zone	Lag (m)	Filter minimum (t/m^3)	Filter maximu m (t/m^3)	No. of excluded samples	% excluded
3-1	100	-	-	-	-
3-2	100	-	-	-	-
3	150	-	-	-	-
Global	200	-	-	-	-

Table 9: Density variogram model parameter values.

		Structure 1		Structure 2		Structure 3	
Zone	Nugget	Range	Variance	Range	Variance	Range	Variance
3-1	0.63	204	0.15	768	0.12	-	-
3-1*	0.70	204	0.17	768	0.13		
3-2	0.46	105	0.38	434	0.16	-	-
3	0.52	163	0.14	460	0.06	1614	0.28
Global	0.41	212	0.12	2004	0.37	-	-
Global*	0.46	212	0.13	2004	0.41	-	-

*The sample variance and variogram sill are not equal. The variogram parameters have been adjusted to sum to one for the kriging exercise.

5.4 Platinum

Besides the Merensky Reef, the UG2 contains the highest concentration of platinum in comparison to the other ore bodies (UG1, LG's and MG's) mined within the BC. The 4E prill split of the UG2 at Amandelbult is 61% (platinum), 28% (palladium) 9% (rhodium) and 2% (gold) (Makgato & Laubscher, 2018). Only the platinum and not the combined 4E data analysis is undertaken in this research study as the rhodium has some missing assays. The missing rhodium values are because if the 4E sum is below 1.5g/t then rhodium is not assayed and also if the sample mass is not sufficient then rhodium will not be assayed as it is the last prill to be assayed (Colquhoun, 2018). These missing values are regressed prior to undertaking a Resource Model exercise to fill the absent values.

5.4.1 Platinum (g/t) analysis

The platinum data consist of 8256 intersections with a minimum of 0.743g/t and a maximum of 9.297g/t. The histogram of the platinum grade (Figure 51) is indicative of a normal distribution. The cumulative frequency (Figure 52) shows that 60% of the grade is in the region of ~2.5 to 3.5g/t.

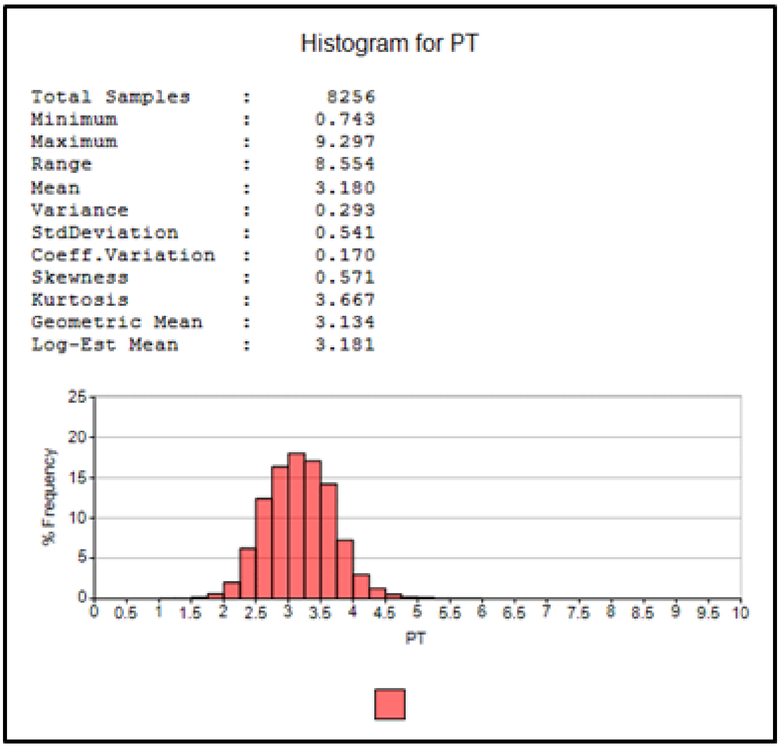

Figure 51: Histogram of the platinum grade.

A classed post map of the platinum grade at 0.25g/t intervals is shown on Figure 53 with three distinct zones evident as shown by the data posting. Additional post maps are included in the appendix which were tested to show the spatial trend of the platinum grade. Platinum Zone 1 (Pt-Zone 1) values ranges mostly between <2.75g/t and 3.00g/t.

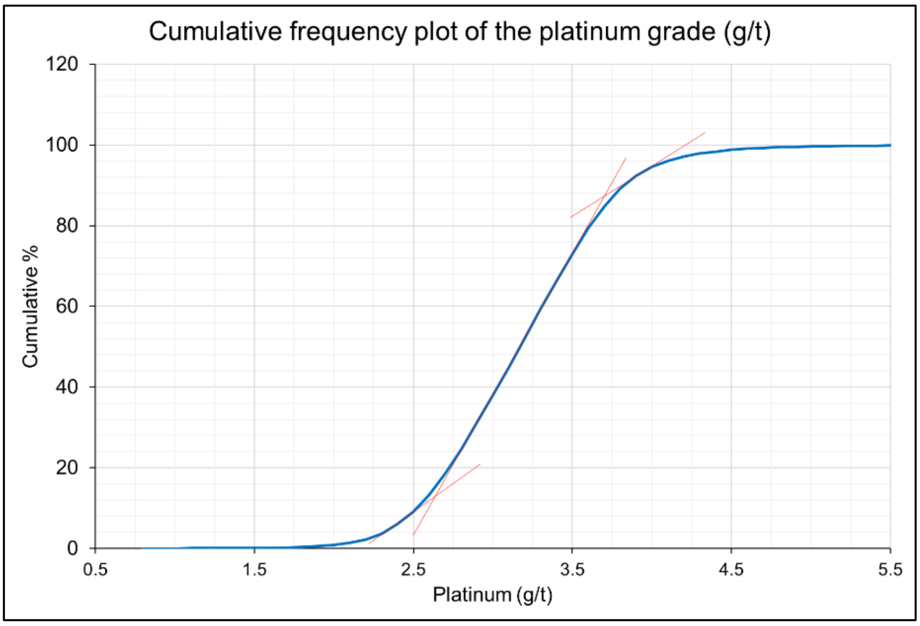

Figure 52: Cumulative frequency plot of the platinum grade (g/t).

The data post also reveals a low variability in Pt-Zone 1 in comparison to the rest of the area. Platinum Zone 2 (Pt-Zone 2) data post indicate a higher Pt value as indicated by the warmer colours with most of the data values higher than 3.50g/t. Platinum Zone 3 (Pt-Zone 3) has a larger range of values but values are predominantly in the less than 3.00g/t region as shown by the colder colours on the data post map.

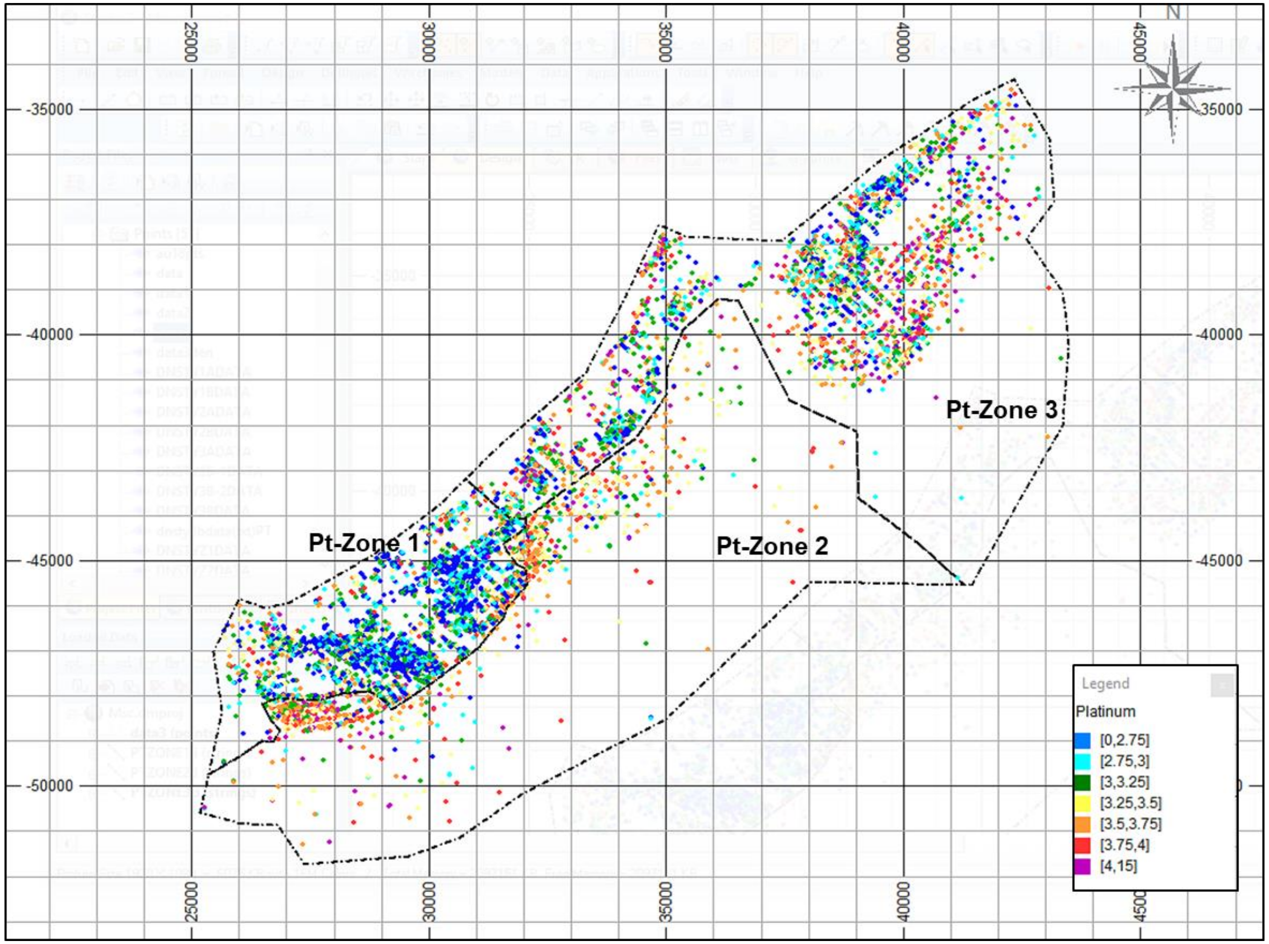

Figure 53: Classed post map of the Platinum grade g/t.

5.4.2 Platinum statistics

The Pt statistics (See Table 10) confirm a higher mean (3.320g/t) for Pt-Zone 2 than Pt-Zone 1 (2.957g/t) and Pt-Zone 3 (3.251 g/t). The high variance observed in the data post map in Pt-Zone 3 is confirmed by the summary statistics. Pt-Zone 3 has a high variance of 0.31g/t^2 compared to Pt-Zone 1 (0.237g/t^2) and Pt-Zone 3 (0.169 g/t^2).

Table 10: Summary statistics of the Platinum grade for the various zones.

	Global	**Pt-Zone 1**	**Pt-Zone 2**	**Pt-Zone 3**
No. of data points	8256	3175	1570	3511
Min (g/t)	0.743	1.088	1.481	0.743
Max (g/t)	9.297	9.297	5.592	6.729
Range (g/t)	8.554	8.209	4.111	5.986
Mean (g/t)	3.180	2.957	3.473	3.251
Mode	3.181	2.945	3.165	3.520
Median	3.174	2.917	3.489	3.229
Variance (g/t^2)	0.293	0.237	0.169	0.310
Standard deviation (g/t)	0.541	0.487	0.412	0.556
Coefficient of variation	0.170	0.165	0.118	0.171
Skewness	0.572	1.603	-0.396	0.391

The histogram of the platinum grade for the three zones and the global areas are shown in Figure 54. The shape of the distribution for Pt-Zone 2 is narrower than that of Pt-Zone 1 and Pt-Zone 2 and confirmed by the lower variance of 0.169 g/t^2. Pt-Zone 1 and Pt-Zone 3 histograms indicate a normal distribution, and this is also confirmed by a skewness of -0.396 and 0.391 for each zone respectively. Pt-Zone 1 has a skewness of 1.603 which indicates that the distribution is highly positively skewed and that the values are mostly in the lower region and lesser in the high region.

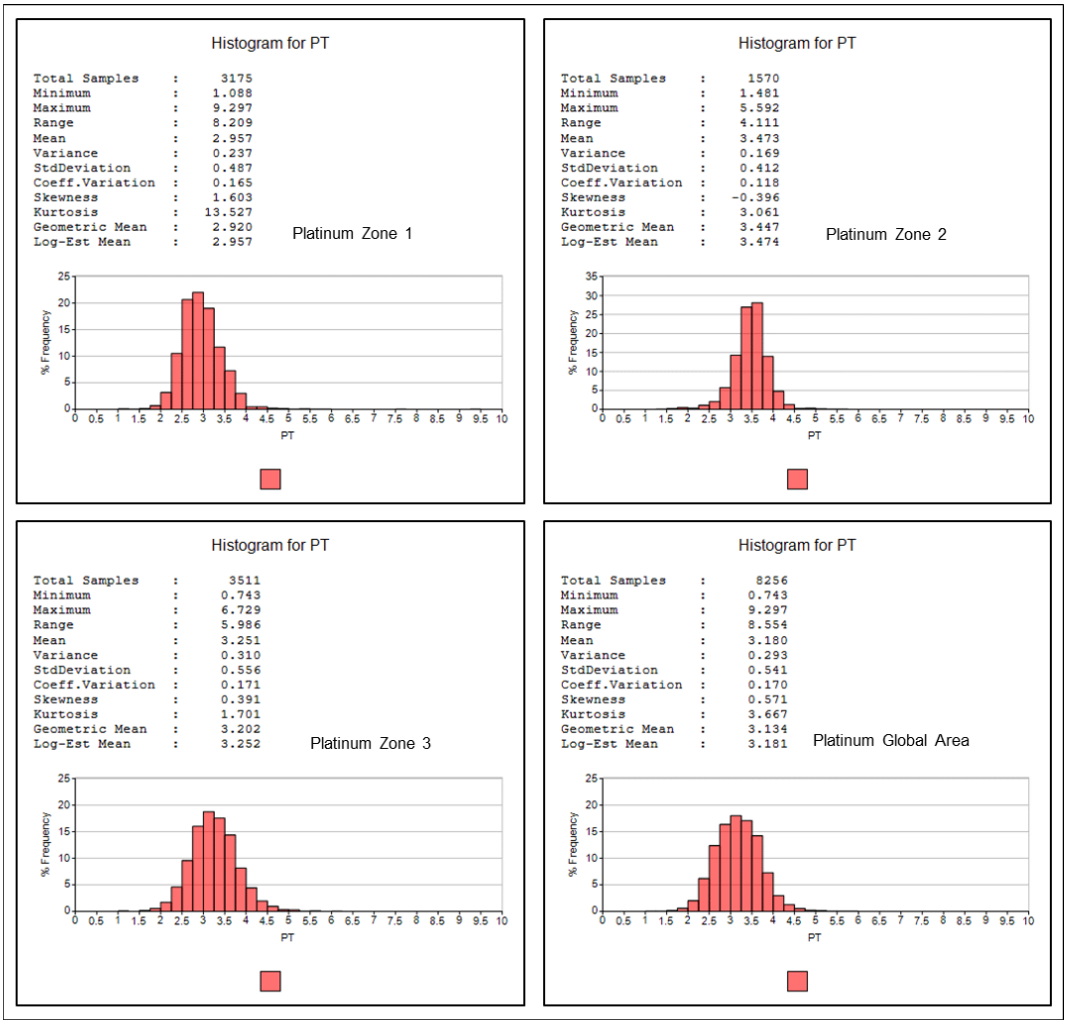

Figure 54: Platinum Histograms of the various zones.

The cumulative plot of the platinum grades in Figure 55 highlight the higher grade for Pt-Zone 2 as the plot is more to the right. The lower grade in Pt-Zone 1 is also illustrated in the plot as the cumulative line is more to the left in comparison to the other zones. Pt-Zone 3 plots very closely to the global plot. The global Zone is thus representative of Pt-Zone 3 than the other zone which plot on other side of it i.e. on the left for Pt-Zone 1 and to the right for Pt-Zone 2.

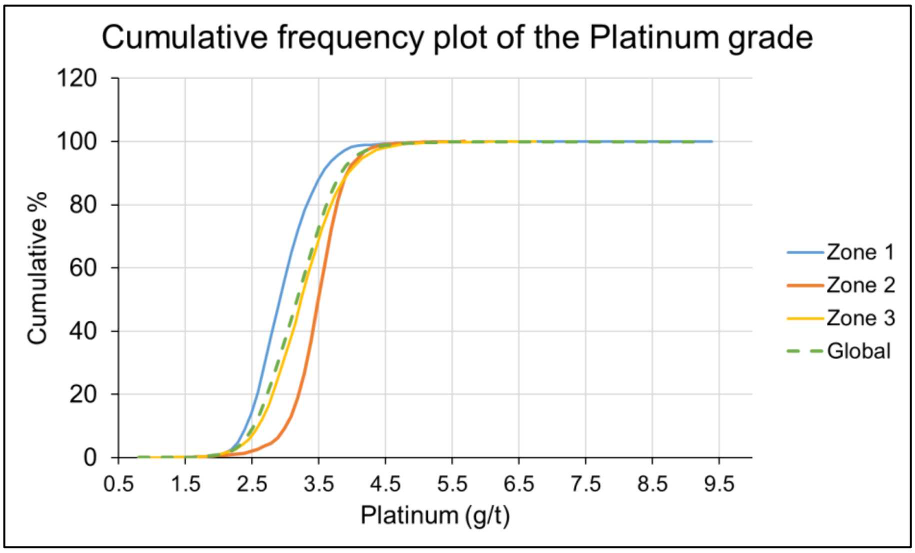

Figure 55: Cumulative frequency of the Platinum grade for the various zones.

The box plots as shown in Figure 56 demonstrate the higher platinum values for Pt-Zone 2 and a narrow distribution of these values. Also, the lower platinum values for Pt-Zone 1 are clear on the plot and indicate the majority of values below 3.00g/t. Pt-Zone 3 and the global zone have almost identical appearances on the box plot, this similarity is also noted in the cumulative plot shown earlier.

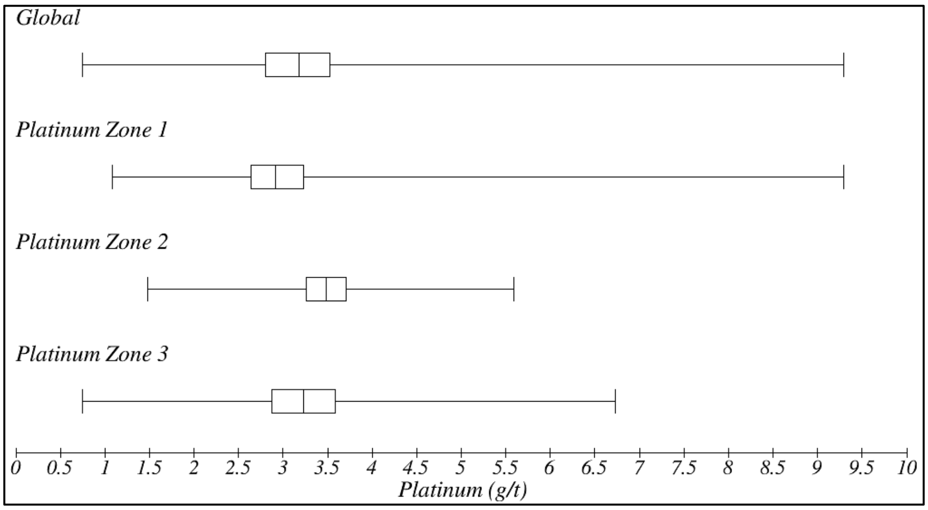

Figure 56: Platinum box plots for the various zone.

A comparison of the three zones using Q-Q plots Figure 57 also illustrate the differences in values in the three zones. For Pt-Zone 1 and Pt-Zone 2 the plots of their values is above the 45^0 line which proves that Pt-Zone 1 has a lower grade than Pt-Zone 2 similarly for the Pt-Zone 1 and Pt-Zone 3 plot. Pt-Zone 2 and Pt-Zone 3 plot show a higher grade for Pt-Zone 2 till at about 4.00g/t, from there on Pt-Zone 3 has a few higher-grade values than Pt-Zone 2.

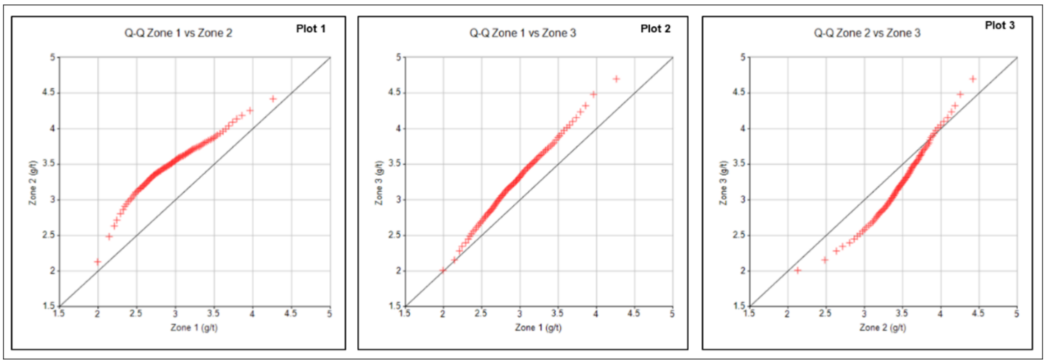

Figure 57: Q-Q plots of the platinum zones.

5.4.3 Influence of geology on the platinum grade

A plot of the geological structures with the platinum zones is shown on Figure 58. There is no obvious relation of the zones with the faults and dykes. The slumps and potholes show no relation to the grade distribution across the research area. A relation is evident when looking at the internal waste existence across the Amandelbult area. The lower grade zone i.e. Pt-Zone 1 is associated with the area with the most intersection of internal waste. Grade profiles of the PGE grade are shown in Figure 59 and clearly show that grade reduces within the internal waste pyroxenite in the reef.

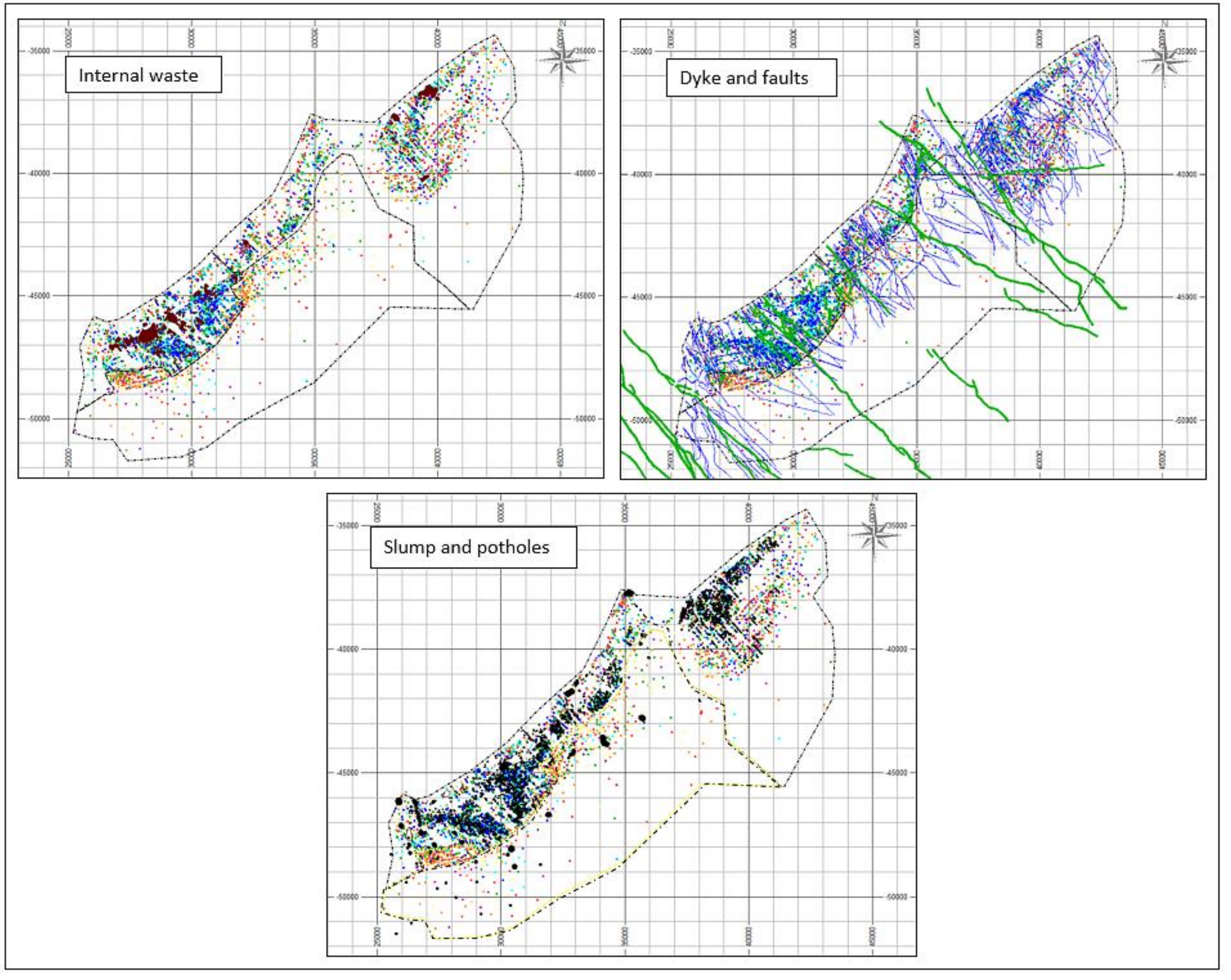

Figure 58: Platinum zones in comparison with geological structures

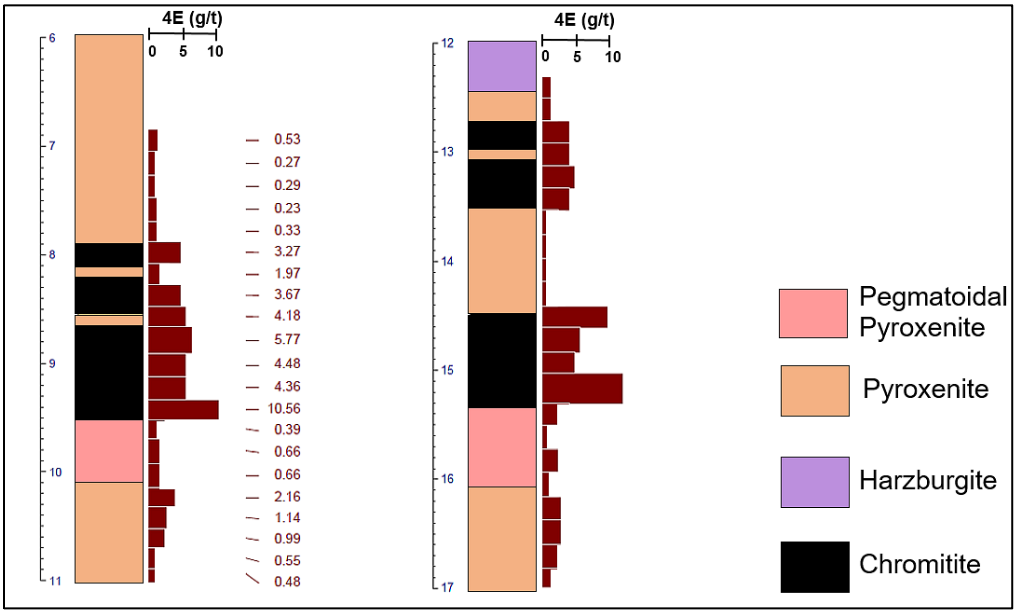

Figure 59: Grade profile comparison of two boreholes with one having minimal internal waste and the other extensive.

The thickness zones and platinum zones in as far as Pt-Zone 1 is concerned show an inverse correlation in that when the orebody is thicker, then the grade is lower than in all the zones. The thicker reef in Pt-zone 1 is as a result of an increased internal waste pyroxenite which has a lower grade and mineralization.

5.4.4 Platinum variography

The platinum variograms for the three zone identified all show clear structures (see Figure 60). The platinum variograms are well behaved in comparison to the thickness and density variograms. Filters were applied in Pt-Zone 1 and Pt-Zone 2.No filters were applied for Pt-Zone 3 and global zone when calculating the experimental variogram with two structures fitted to experimental variograms of Pt-Zones 1, 3 and global and 3 structures fitted to Pt-Zone 2 experimental variogram.

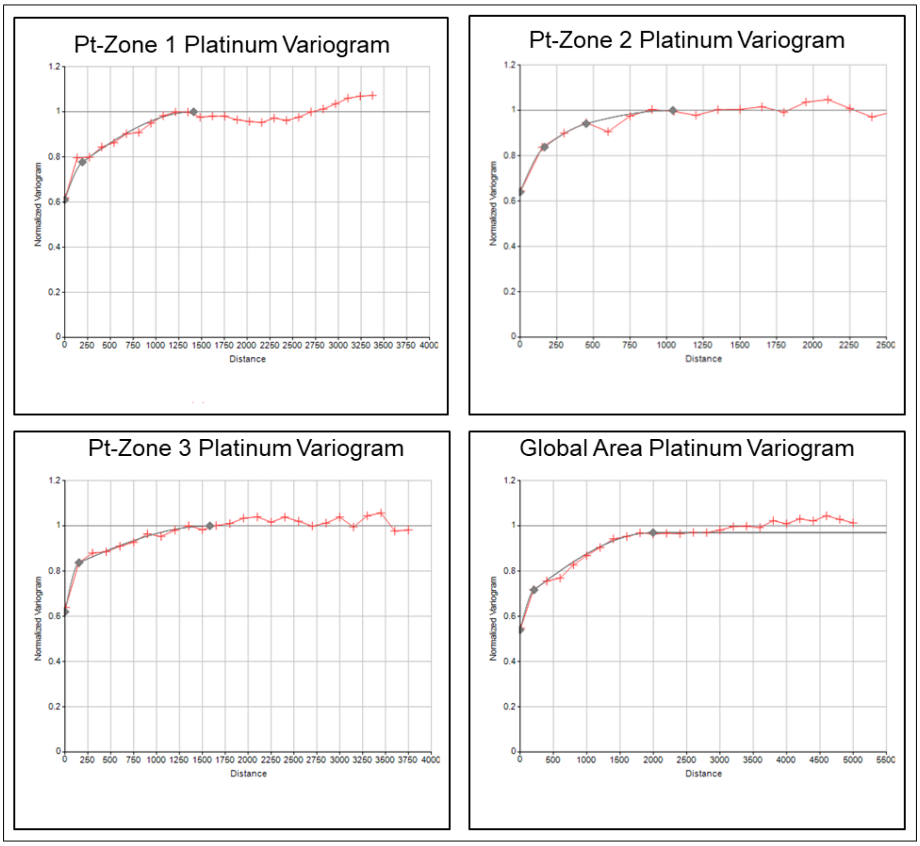

Figure 60: Experimental variograms of the Platinum and fitted models.

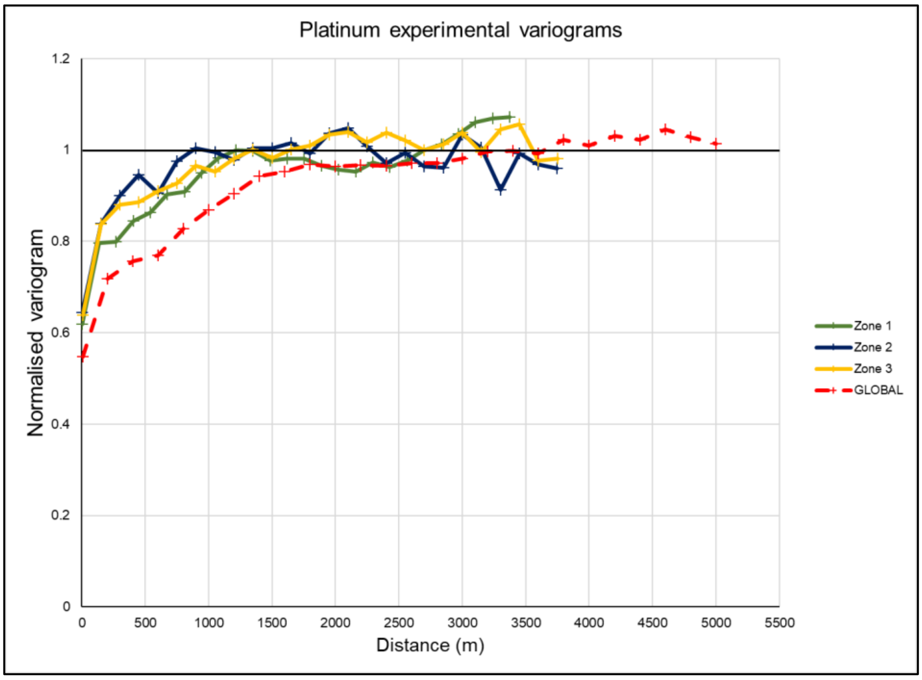

Figure 61: Stacked theoretical variograms of the Platinum grade.

All three zones including the global area show a high nugget effect of above 50% Figure 61. Lomberg (2014) states that this is usual and expected of platinum deposits. The global variogram has a longer range as compared to the variograms for the zones and also a slightly lower nugget. The input values used for the variogram calculation are shown in Table 11 and the model fitting parameters are in Table 12.

Table 11: Platinum experimental variogram data input values.

Zone	Lag (m)	Filter minimum (g/t)	Filter maximum (g/t)	No. of excluded samples	% excluded
1	135	2.0	4.0	82	3
2	150	2.5	4.5	46	3
3	150	-	-	-	-
Global	200	-	-	-	-

Table 12: Platinum variogram model parameter values.

		Structure 1		Structure 2		Structure 3	
Zone	**Nugget**	**Range**	**Variance**	**Range**	**Variance**	**Range**	**Variance**
1	0.61	194	0.11	1413	0.28	-	-
2	0.64	166	0.11	451	0.10	1042	0.15
3	0.62	153	0.19	1582	0.19	-	-
Global	0.54	208	0.13	1996	0.30	-	-
Global*	0.56	208	0.13	1996	0.31	-	-

*The sample variance and variogram sill are not equal. The variogram parameters have been adjusted to sum to one for the kriging exercise.

5.5 Optimum Block Size Determination Based on the Zone Variograms

Kriging is defined as the best linear unbiased estimator but Vann *et al* (2003) state that this is only so if the block size and neighbourhood are correctly defined when estimation is conducted as failing to do so can result in estimates that are conditionally bias. Rivoirard (1987) mention that the two parameters that can be used to determine an appropriate neighbourhood are the weight of the mean and the slope of regression which compares the true grade to the estimated grade. Deutsch and Deutsch (2012) mention also the kriging efficiency, kriging variance, block variance and slope of regression as some of the measures that can be used to measure the performance of kriged estimates.

According to Snowden Group (2017), an optimum block size is one yielding a SLOR of close to 1 and above 0.9, the kriging efficiency is above 80% and there are low numbers or no count of negative weights generated from solving the kriging solutions. Vann *et al*., (2003) suggest that testing of an appropriate block size should be carried out in three areas, a well-informed area (where data is abundant especially within the block being estimated). A less well informed (one where there is few data in the block and some data surrounding it) and a poorly informed block where the blocks have no data within them and no data in some direction.

The current block sizes used at Amandelbult are 250m x 250m for the areas where there is amble data available. For the areas where data is limited and sparse a 500 x 500m block size is used for estimation. The next section is to check and validate if the variograms for the zones, orebody thickness, density and platinum, constructed in the past chapters are still in agreement with the current block sizes in place. The process described by Vann *et al*., (2003) was used for this purpose. The Datamine ™ macro written by Stevenson (2010) by was used to test various block sizes and graphs of the results were constructed for interpretation.

5.5.1 Optimum block size for the orebody thickness study

In order to conduct an optimum block size study across the zones for the thickness, density and Platinum, three blocks were selected for analysis, the first block was selected in a well-informed area were data is abundant, the second in a moderately informed area and the third in a poorly informed are were data points are few around the test block. The blocks selected for running the study on various block sizes for the orebody thickness are shown in Figure 62. Three areas were selected in each zone, well informed (green block), moderately informed (blue blocks) and poorly informed (red blocks). The block size study resultant graphs are shown in Figure 63 , Figure 64 and Figure 65 and suggest that for the well informed area, a block size of between 100m x 100m and 150 x 150m will be suitable for estimation whilst a 250m X 250m block size will be suitable for the moderately informed area and 500 x 500m for the poorly informed areas.

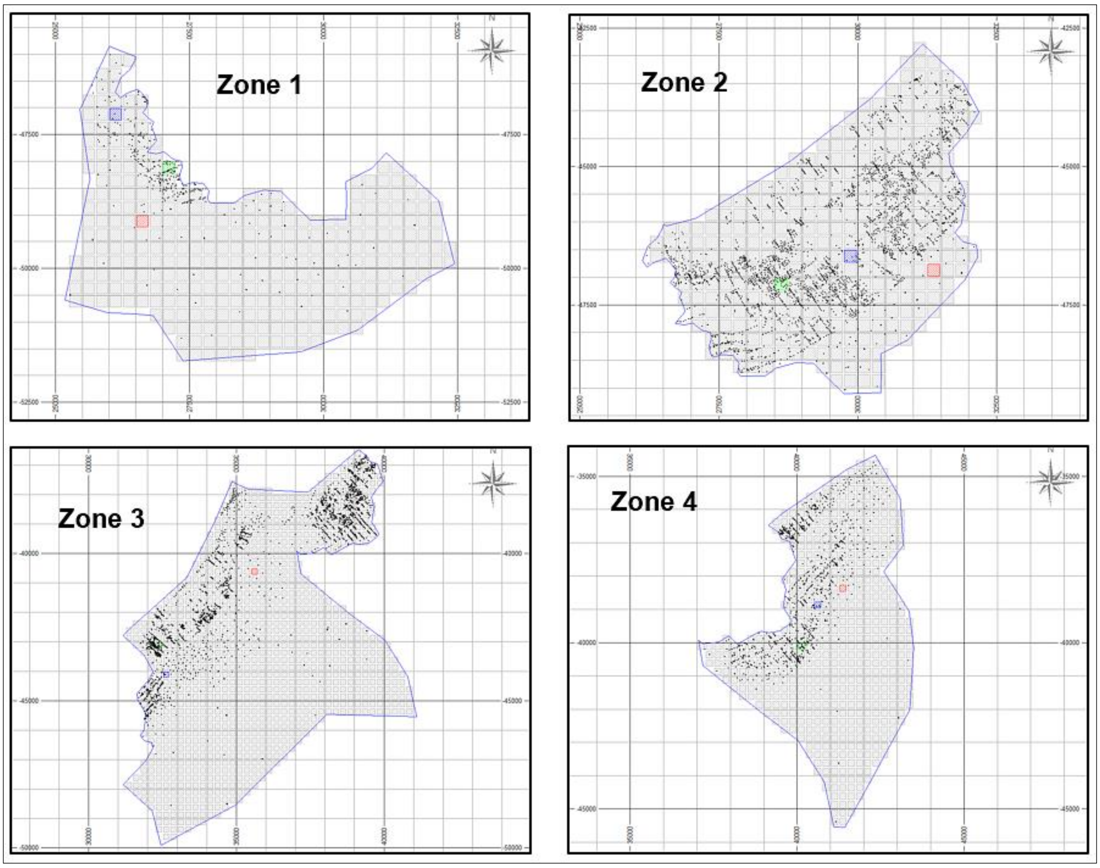

Figure 62: KNA test blocks with data distribution for the thickness zones.

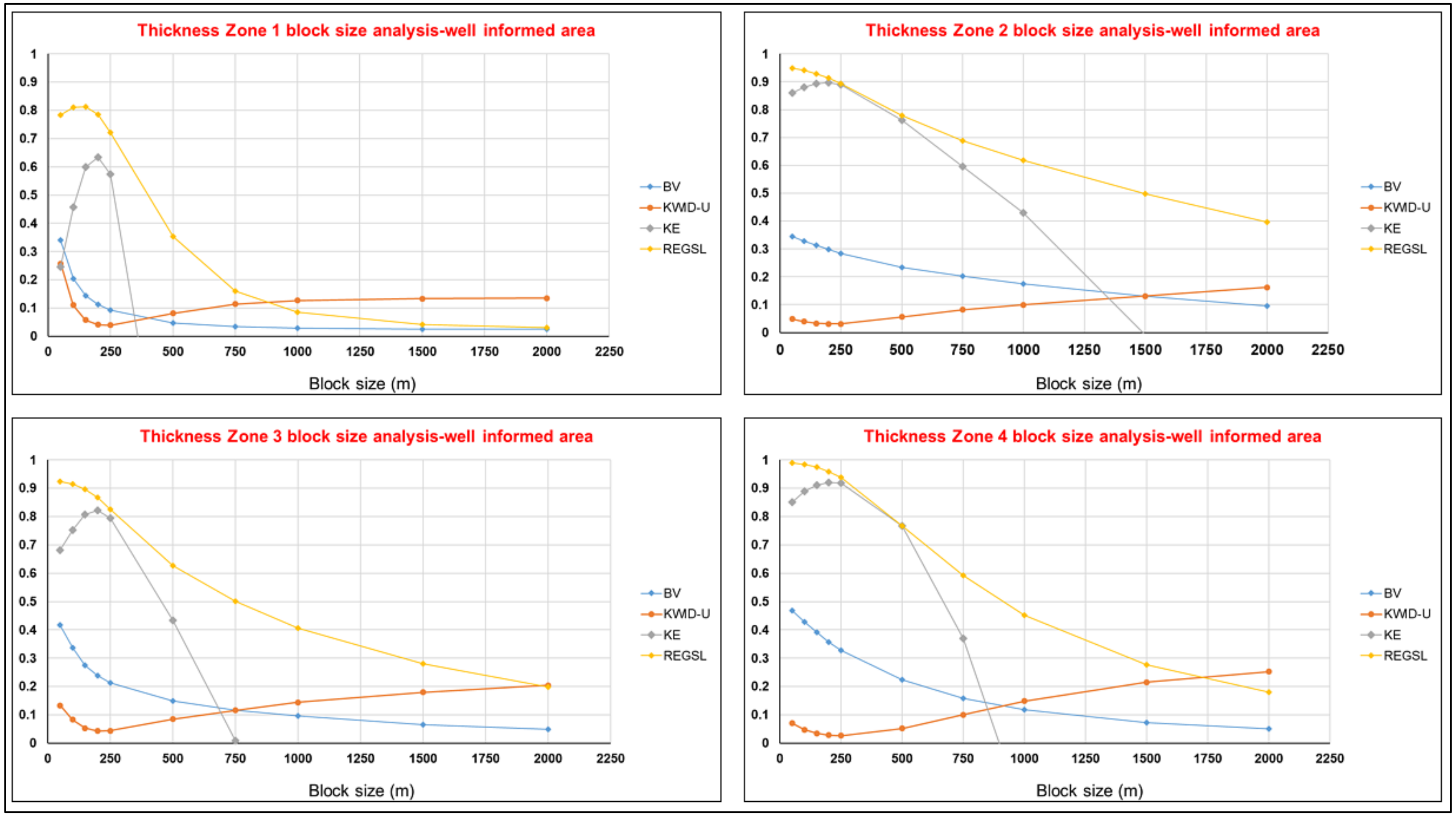

Figure 63: Results of the block size analysis for the well informed thickness areas.

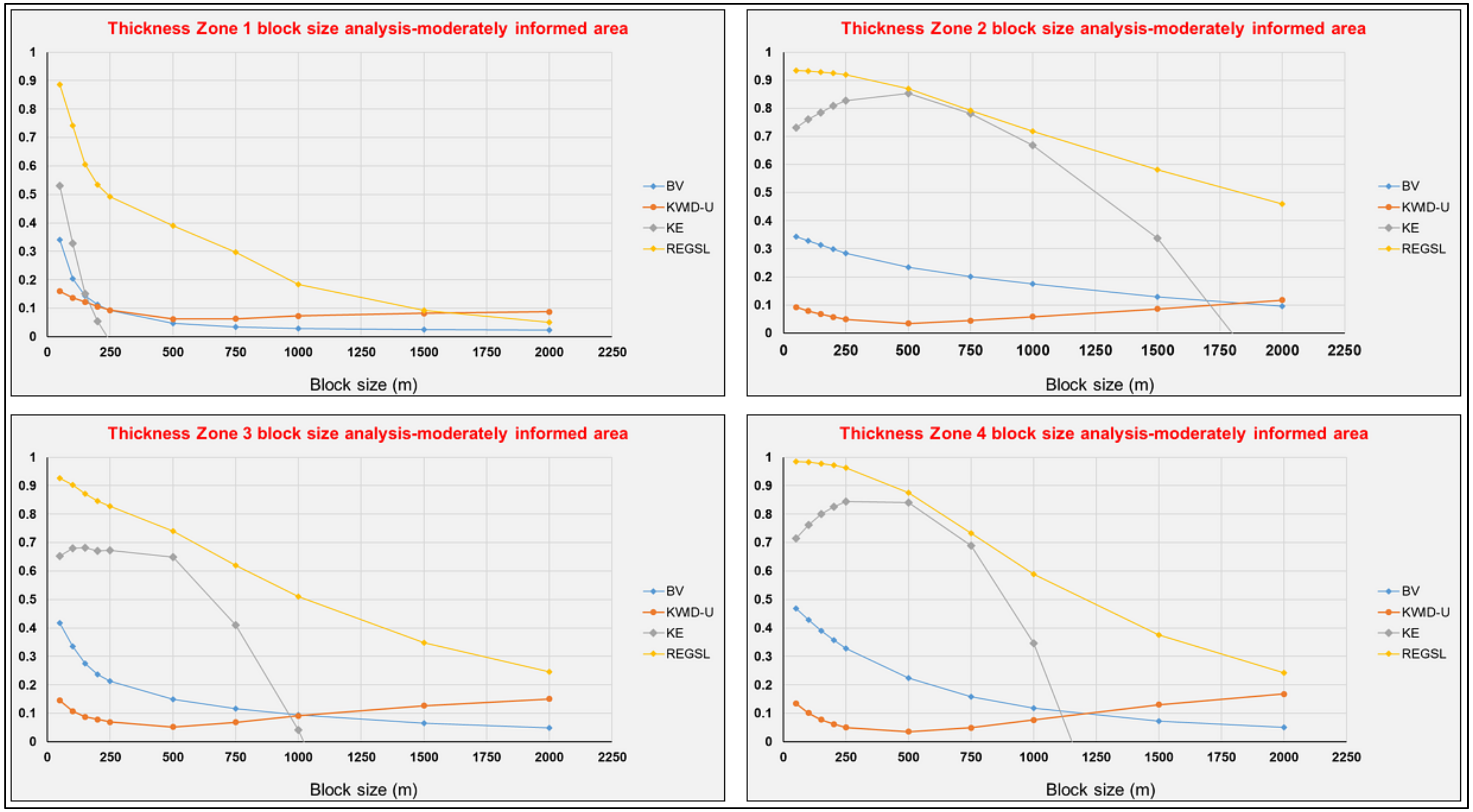

Figure 64: Results of the block size analysis for the moderately informed thickness areas.

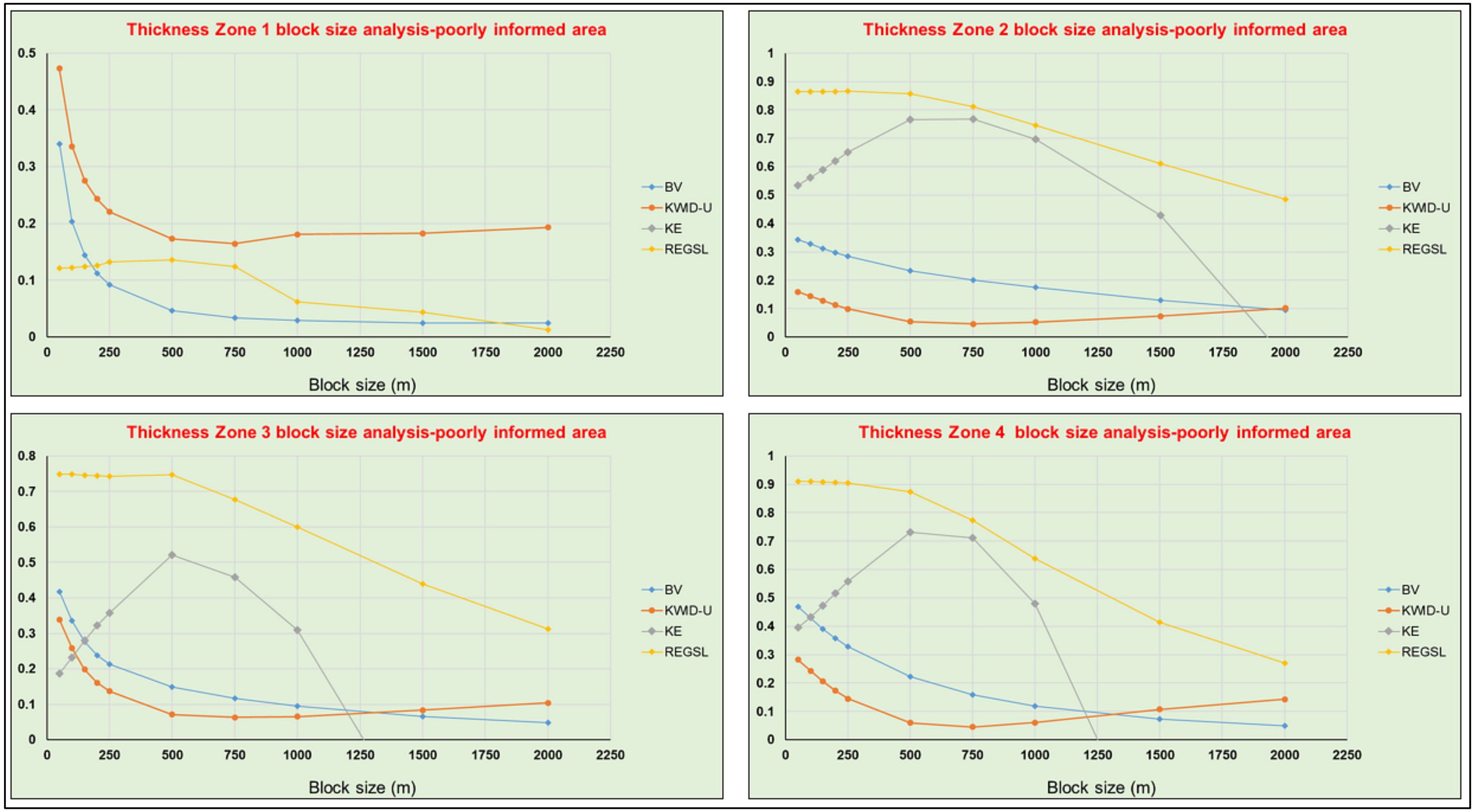

Figure 65: Results of the block size analysis for the poorly informed thickness areas.

5.5.2 Optimum block size analysis for the orebody density

The density Zones and respective selected blocks in the well, moderate and poorly informed areas for the block size analysis are shown in Figure 66 and similarly with the orebody thickness four zones were used to do the analysis.

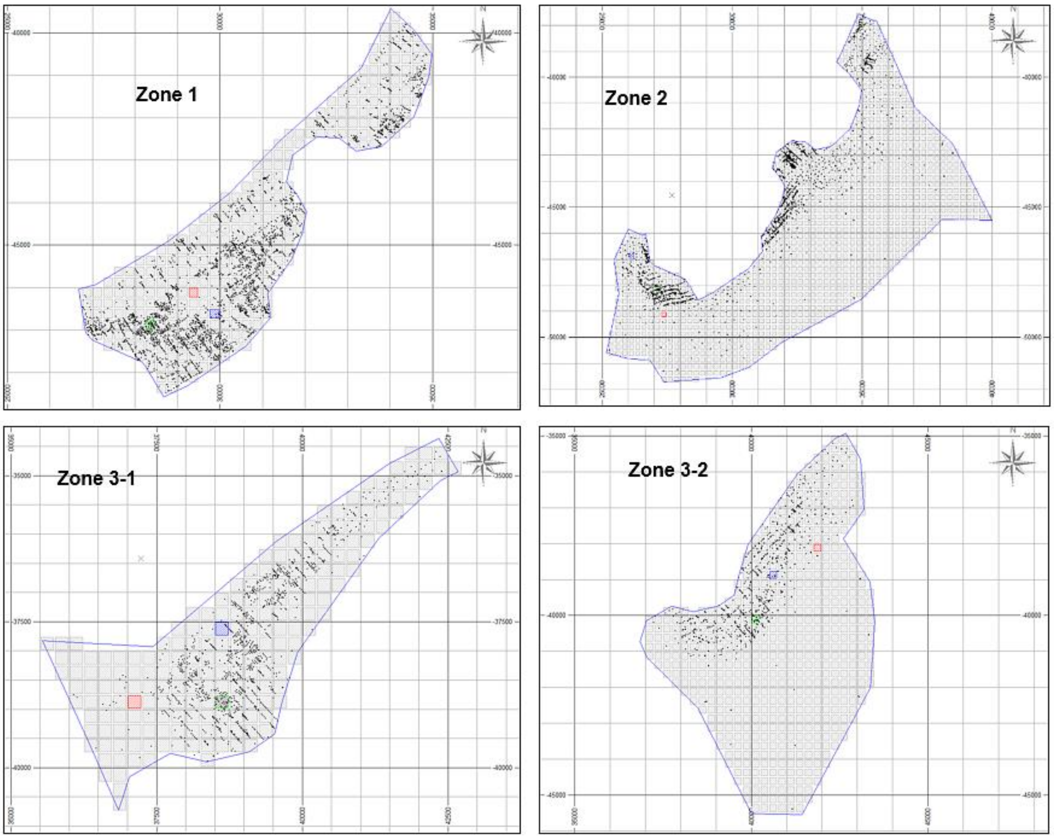

Figure 66: Selected test blocks with data distribution for the density zones.

A graphical representation of the results of the density block size analysis is shown in Figure 67, Figure 68 and Figure 69 for the various zones. For the well-informed area, a block size of between 100m x 100m and 150m X 150m indicates that it will be suitable for estimating areas were data is abundant. Moderately informed areas can be estimated using 250m x 250m size blocks whilst poorly informed areas indicate a suitable block size of 500m x 500m.

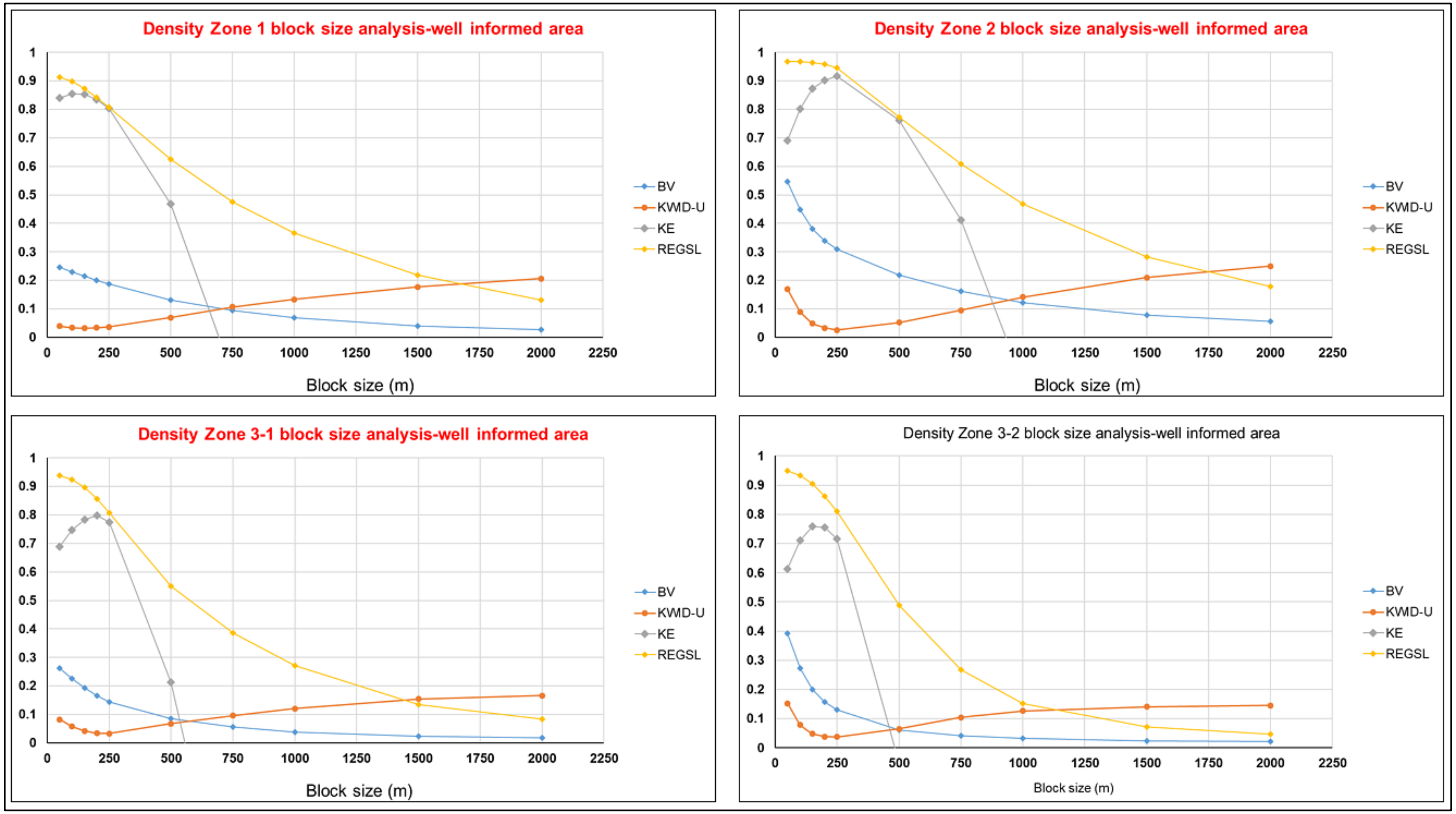

Figure 67: Results of the block size analysis for the well informed density areas.

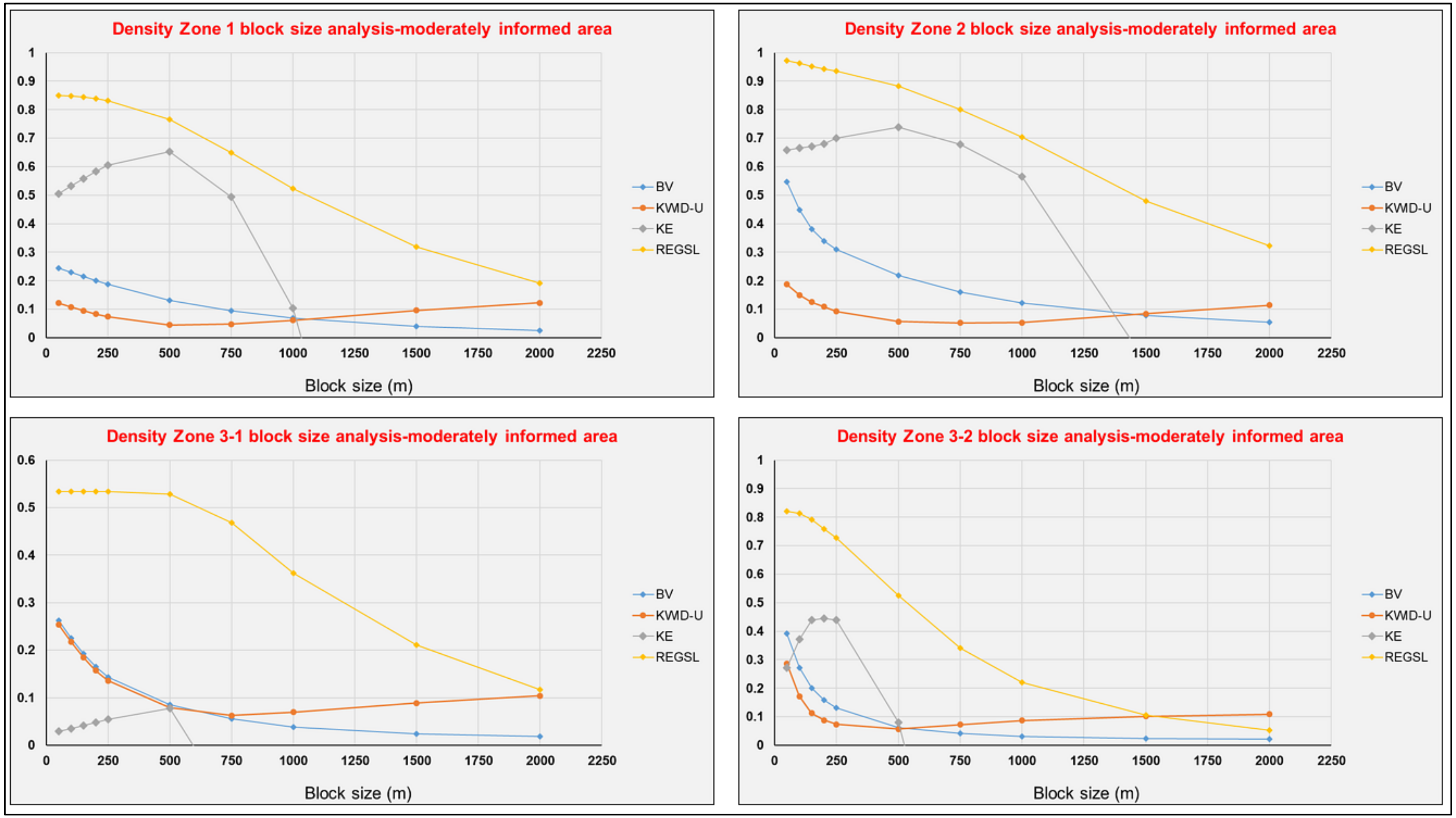

Figure 68: Results of the block size analysis for the moderately informed density areas.

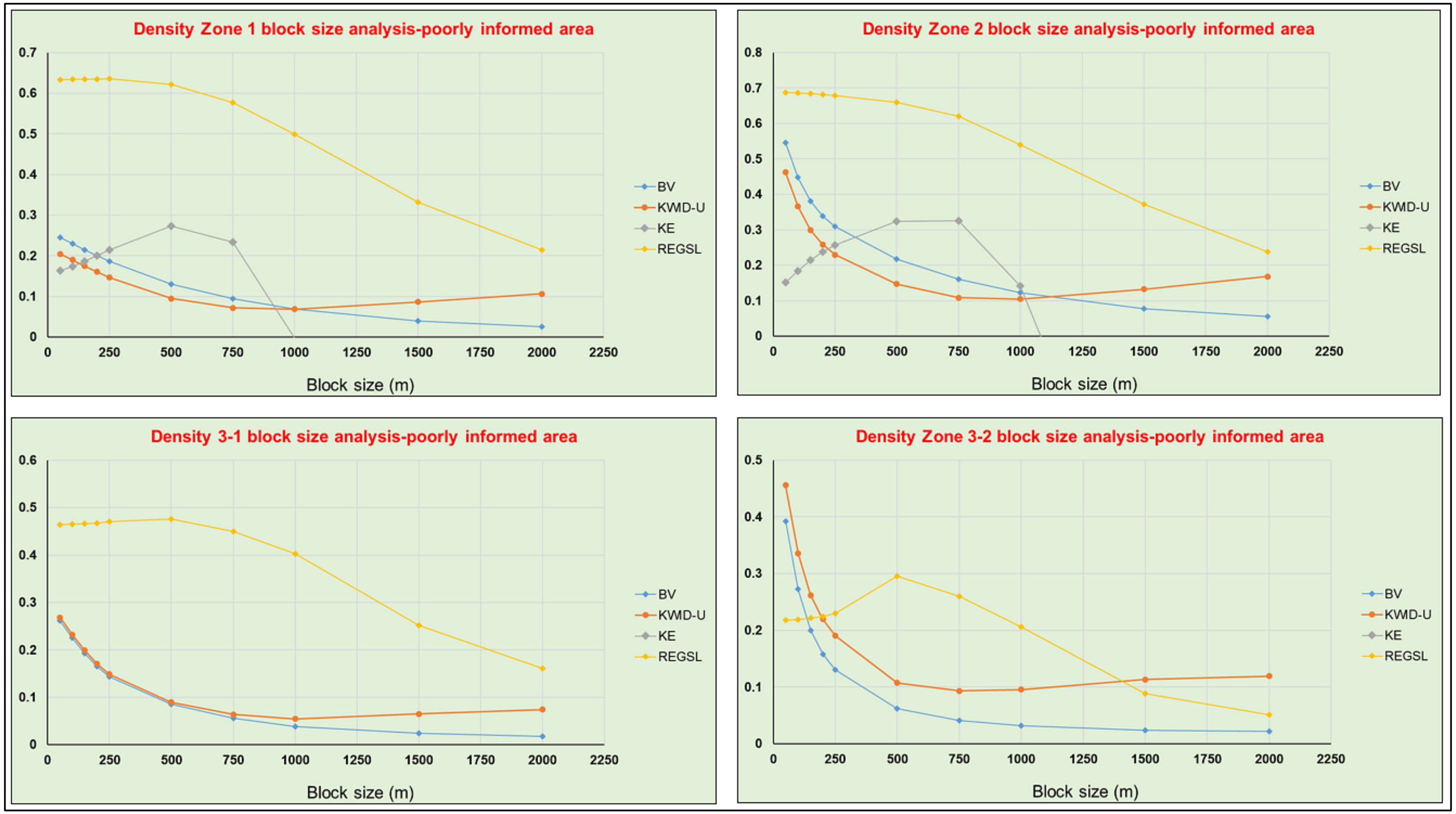

Figure 69: Results of the block size analysis for the poorly informed density areas.

5.5.3 Optimum block size analysis for the orebody platinum grade

The selected platinum grade blocks for the block size analysis are shown in Figure 70 for the well, moderately and poorly informed areas.

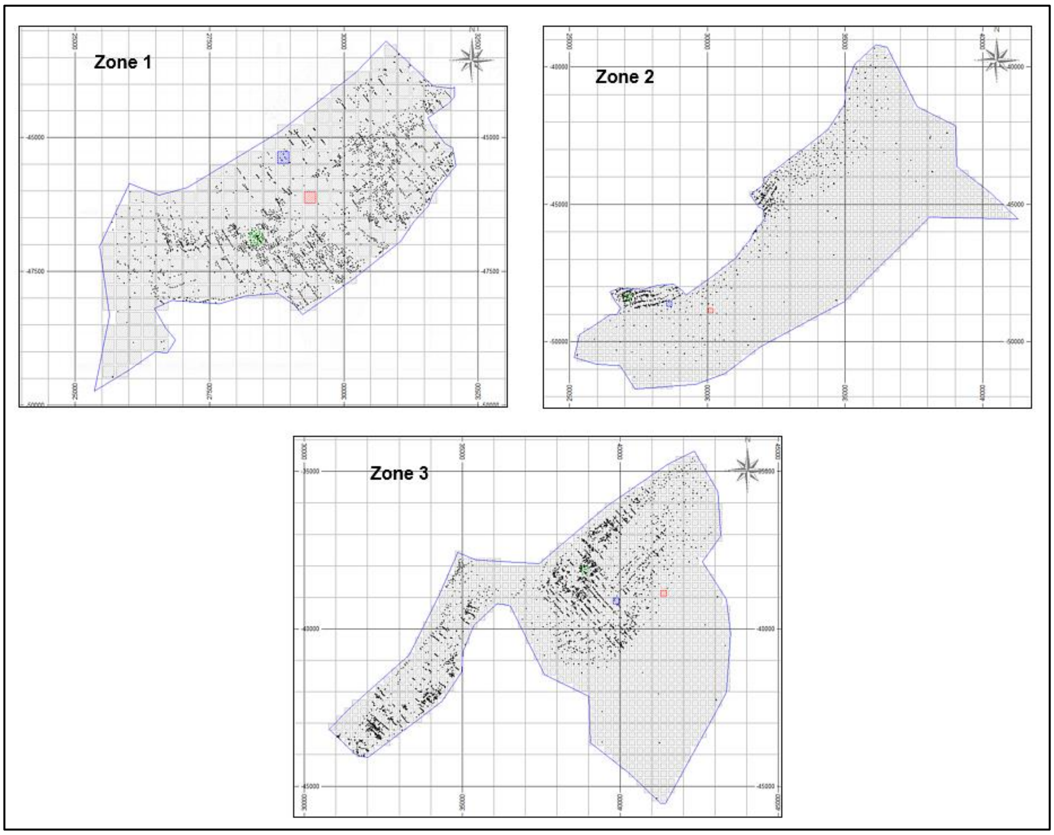

Figure 70: selected test blocks with data distribution for the Platinum grade zones.

The block size analysis graph results to determine suitable block sizes for estimation are shown in Figure 71 , Figure 72 and Figure 73 for the three platinum grade zones. A block size of 100m x 100m to 150m x 150m is suitable for the well-informed area, 250m x 250m for the moderately informed area and 500m x 500m for the poorly informed areas according to the graphs.

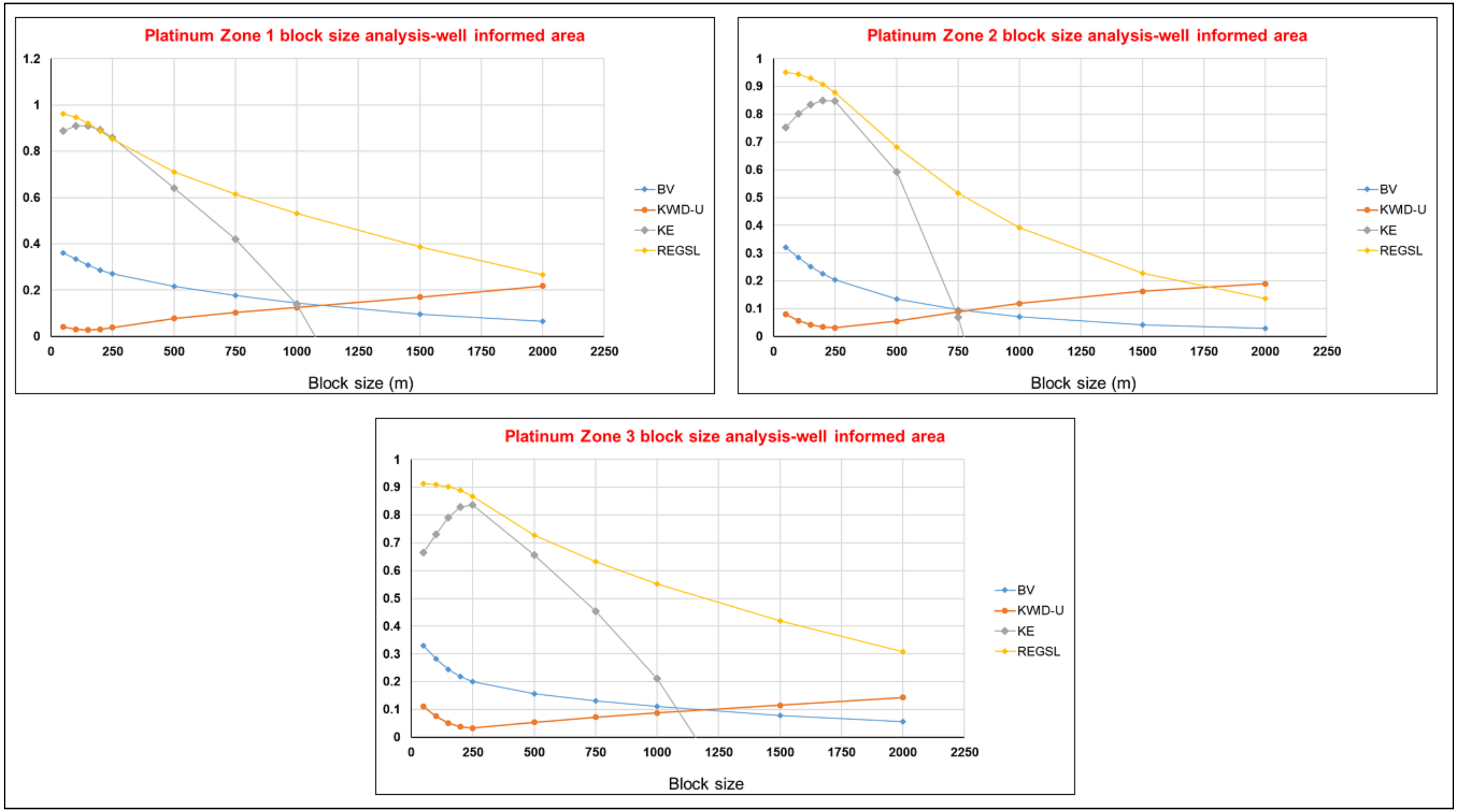

Figure 71: results of the block size analysis for the well informed platinum areas.

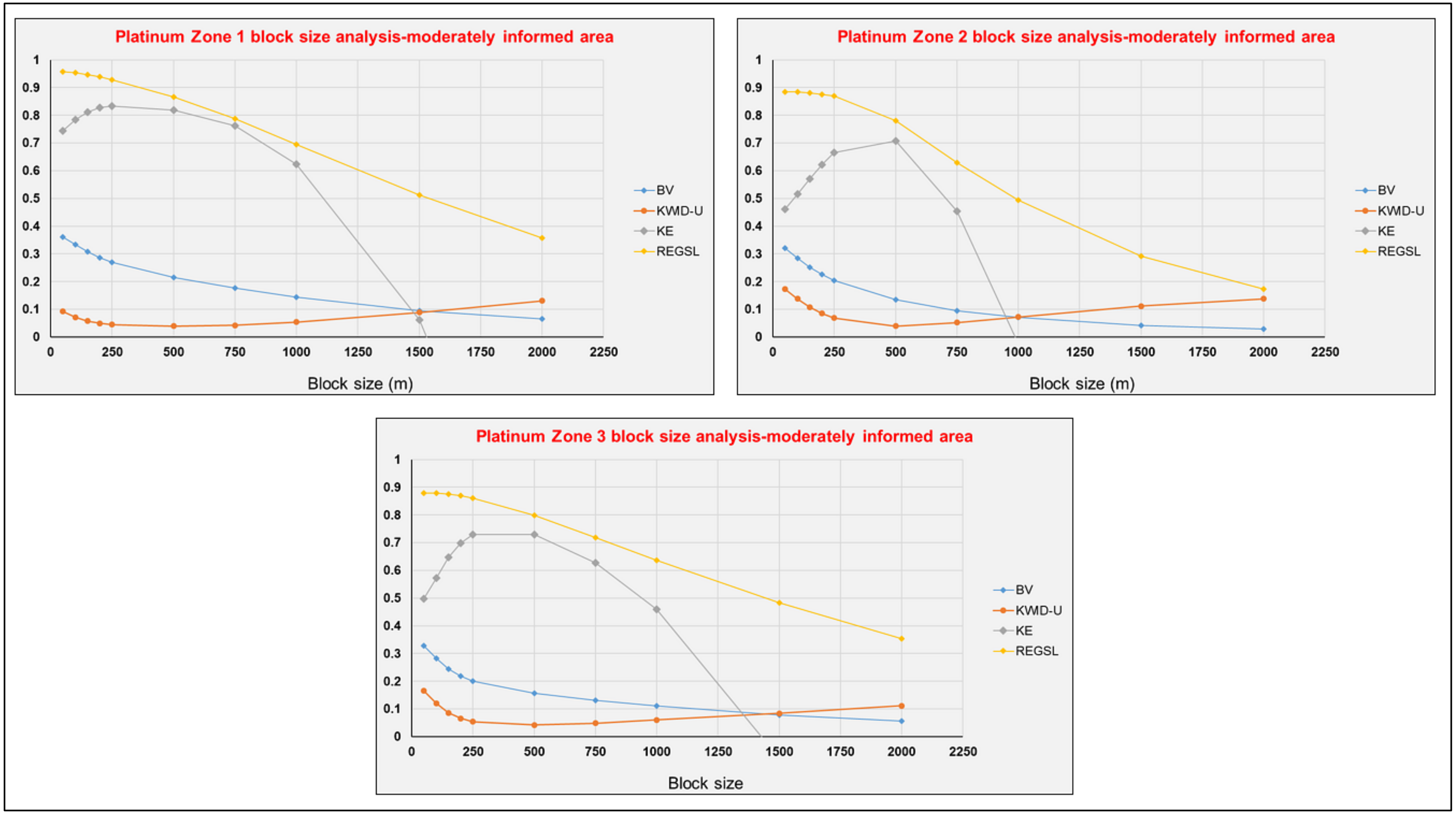

Figure 72: Results of the block size analysis for the moderately informed platinum areas.

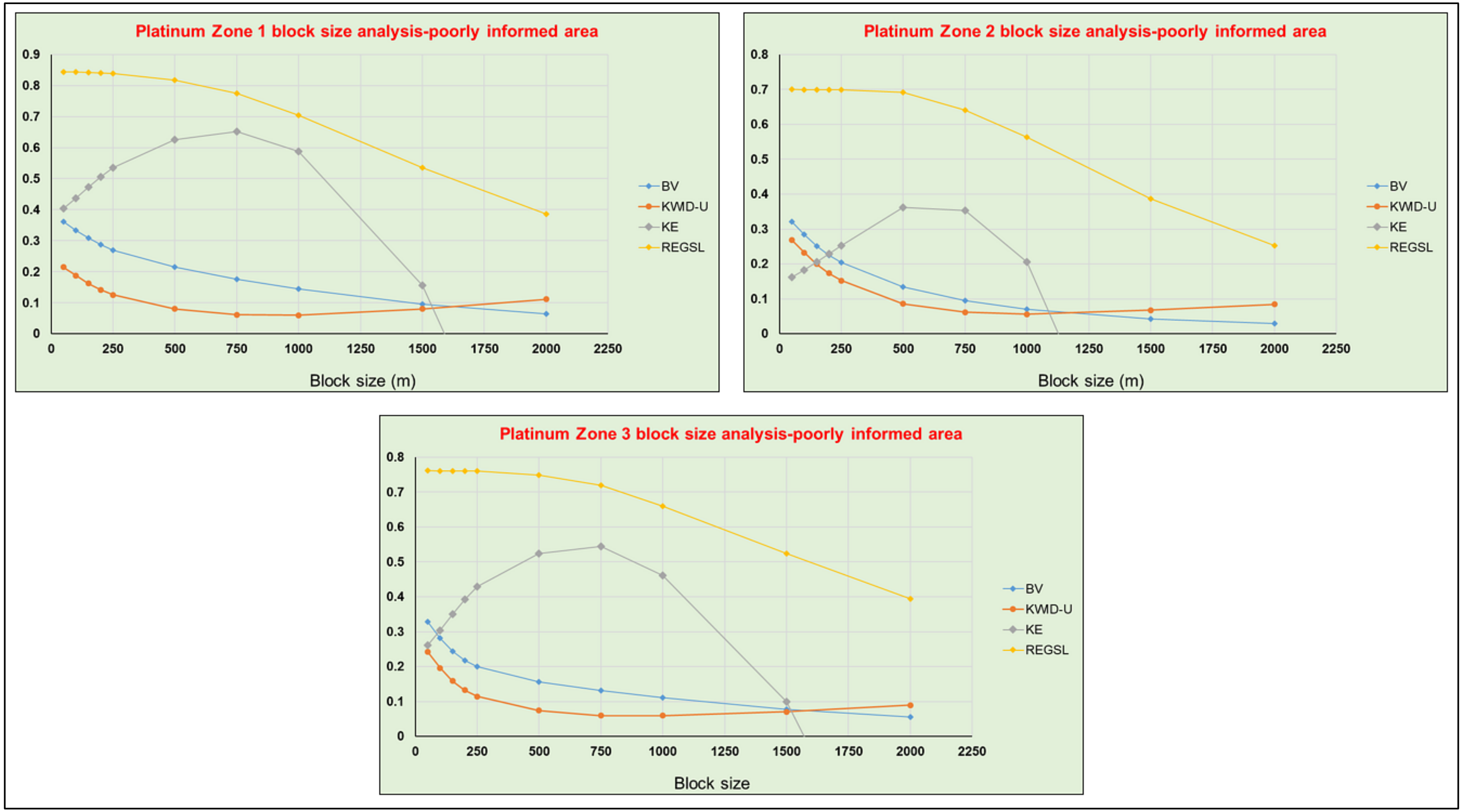

Figure 73: Results of the block size analysis for the poorly informed platinum areas.

5.5.5 Conclusion of the block size study

The block size analyses for the new variograms identified for the various zones agree with the currently used 250m x 250m blocks and 500m x 500m blocks at Amandelbult Complex. The analysis however did highlight that a smaller block size of less than 250m x 250m in the well-informed areas should be investigated as this may result in a higher resolution definition of the model in the areas where there is more information.

5.6 Block Estimation

Data collection for obtaining ore deposit grades or other properties of interest is usually accomplished using drilling and channel sampling for example which represent a minute portion of the orebody. Eventually for mining purposes this data needs to be converted to some form of usable format for mine planning purposes and to represent the orebody which is usually in the form of a block model.

According to Poniewierski (2019) block models are a simplified representation of an orebody volume and its associated rocks (waste) in a brick or cell like format, with each cell containing the estimated variables of the orebody such as the grade or density. An example of a block model is shown in Figure 74. Different colours are usually used to show the range of the variable value of each block for example the grade.

Depending on the extent of the orebody, a block model may be computer generated in 2 dimensions (2D) or 3 dimensions (3D). Rossi and Deutsch

(2014) suggest that 2D models may be suitable for tabular or vein-type deposits and stratigraphically controlled deposits for example, coal deposits or heavy sands deposits whilst massive deposits (for example massive sulphide deposits and skarn deposits) with pronounced development in the third dimension can be modelled in 3D.

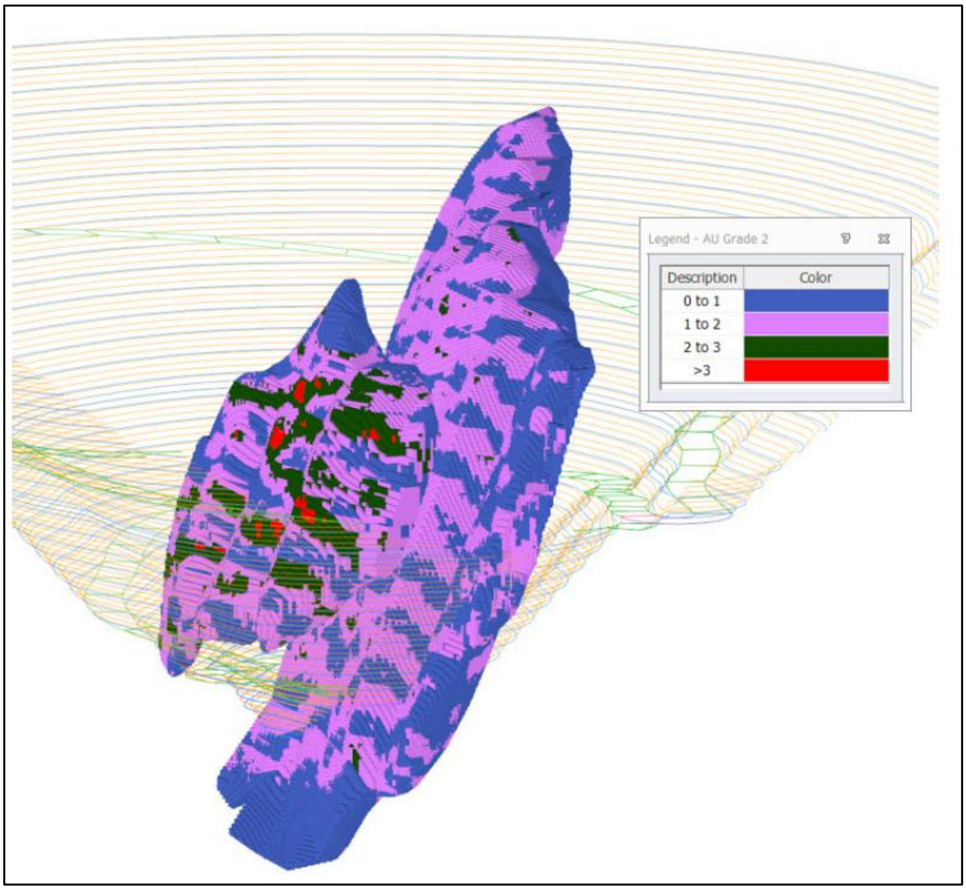

Figure 74: An example of a block model. Source: Poniewierski (2019).

The block estimation at Amandelbult is currently carried out in Datamine™ software using two sets of 2D block sizes, 250 x 250m for the well informed and moderately informed areas and 500m x 500m for the poorly informed areas where data is sparse (Figure 75) (Colquhoun, 2018). During the estimation run Datamine requires 4 files, the estimation parameter file (EPAR), search parameter file (SPAR), variogram parameter file (VARPAR) and the file with the data. The EPAR file specifies the estimation method, variables to be estimated and variogram reference number to be used in the estimation. The SPAR file specifies the search distance, number of minimum and maximum samples to use in the estimation. If the minimum number of samples is not reached within the first search a second search is used whereby the distance of the first search is multiplied by a factor of 1.5. If the minimum number of samples is still not achieved in the second search, the first search distance is multiplied by 30. The VARPAR file specifies the variogram parameters i.e. type of variogram, sill, range and nugget.

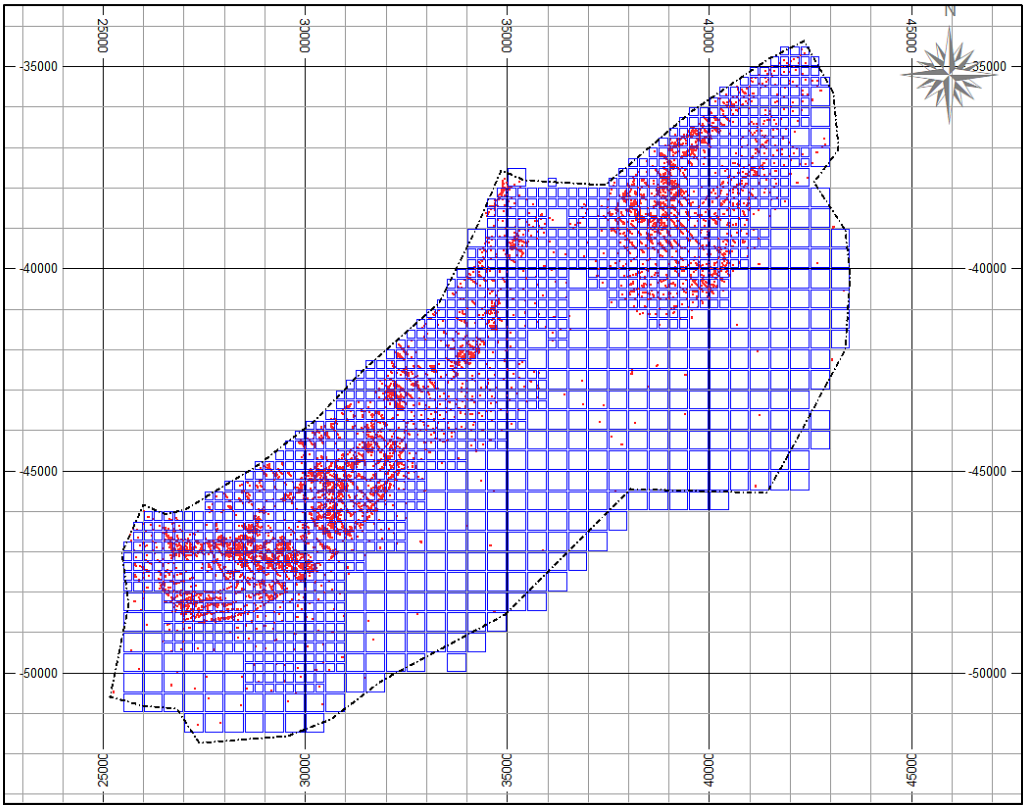

Figure 75: 2D 250m x 250m and 500 x 500m block model (blue blocks) over the study area with the data (red) location plot.

For this research study the variogram model parameters (Table 13) identified for the different zones for the orebody thickness, density and platinum in the previous sub-chapter will be checked against a global variogram. This is to check if there is an improvement in the estimation results from using a variogram for a zone and a global variogram. WID-GU refers to the orebody thickness variogram parameters for the Global area and WID-UZ1-UZ4 refers to the orebody thickness variogram parameters for T-Zones 1 to 4. This is the same for the density (SG) and the platinum (PT).

Table 13: Variogram parameter file.

Variogram reference number	**Description**	**Nugget**	**ST1**	**ST1**	**ST1**	**ST1**	**ST2**	**ST2**	**ST2**	**ST2**	**ST3**	**ST3**	**ST3**	**ST3**
NUM			PAR 1	PAR 2	PAR 3	PAR 4	PAR 1	PAR 2	PAR 3	PAR 4	PAR 1	PAR 2	PAR 3	PAR 4
1	WID-GU	0.48	295	295	295	0.14	1551	1551	1551	0.10	4773	4773	4773	0.28
2	PT-GU	0.56	208	208	208	0.13	1996	1996	1996	0.31	-	-	-	-
3	SG-GU	0.56	212	212	212	0.13	2004	2004	2004	0.41	-	-	-	-
4	WID-UZ1	0.39	42	42	42	0.15	81	81	81	0.33	348	348	348	0.13
5	WID-UZ2	0.64	318	318	318	0.09	1962	1962	1962	0.27	-	-	-	-
6	WID-UZ3	0.49	133	133	133	0.30	675	675	675	0.09	1568	1568	1568	0.12
7	WID-UZ4	0.49	207	207	207	0.12	614	614	614	0.25	1398	1398	1398	0.14
8	SG-UZ1	0.74	408	408	408	0.10	1053	1053	1053	0.16	-	-	-	-
9	SG-UZ2	0.34	117	117	117	0.31	714	714	714	0.22	1335	1335	1335	0.13
10	SG-UZ3-1	0.70	204	204	204	0.17	768	768	768	0.13	-	-	-	-
11	SG-UZ3-2	0.46	105	105	105	0.38	434	434	434	0.16	-	-	-	-
12	PT-UZ1	0.61	194	194	194	0.11	1413	1413	1413	0.28	-	-	-	-
13	PT-UZ2	0.64	166	166	166	0.11	451	451	451	0.10	1042	1042	1042	0.15
14	PT-UZ3	0.62	153	153	153	0.19	1582	1582	1582	0.19	-	-	-	-

5.6.1 Thickness estimation

The OK block estimates (Figure 76) of the orebody thickness were conducted firstly using the global variogram and secondly done using the T-Zone variograms for each zone. From a global visual perspective, the two estimates generally appear to be similar, although there are areas where the two estimates are different when doing a detailed comparison of the block estimates. The estimates both highlight the thin zone of T-Zone 1 and the thick reef zone of T-Zone 2 well. The high variability identified in T-Zone 4 is also captured by both estimates. For the interest of comparison, the zones boundaries are shown on both block estimates.

Estimation comparison of the thickness estimates

By looking at the true values, which is the average of the data values in an individual block, and estimated values of various estimation methods, (Isaaks and Srivastava, 1989) compare the performance of different estimation by comparing their statistics of the error residuals i.e. the difference between the true values and estimated values using the formulae:

$$error = r = \hat{V} - V \quad \text{Eq 14}$$

Where r is the error, $\hat{\mathrm{V}}$ is the estimated value and V the true value. According to (Isaaks & Srivastava, 1989), statistical analysis of the errors can assist is identifying which estimation method is best by constructing histograms of the residuals which can indicate bias by showing the distribution of the errors i.e. positive bias when the mean of the residual is < 0, negative bias when the mean of the residuals is > 0 and no bias when the mean of the errors is equal to 0 as shown on Figure 77.

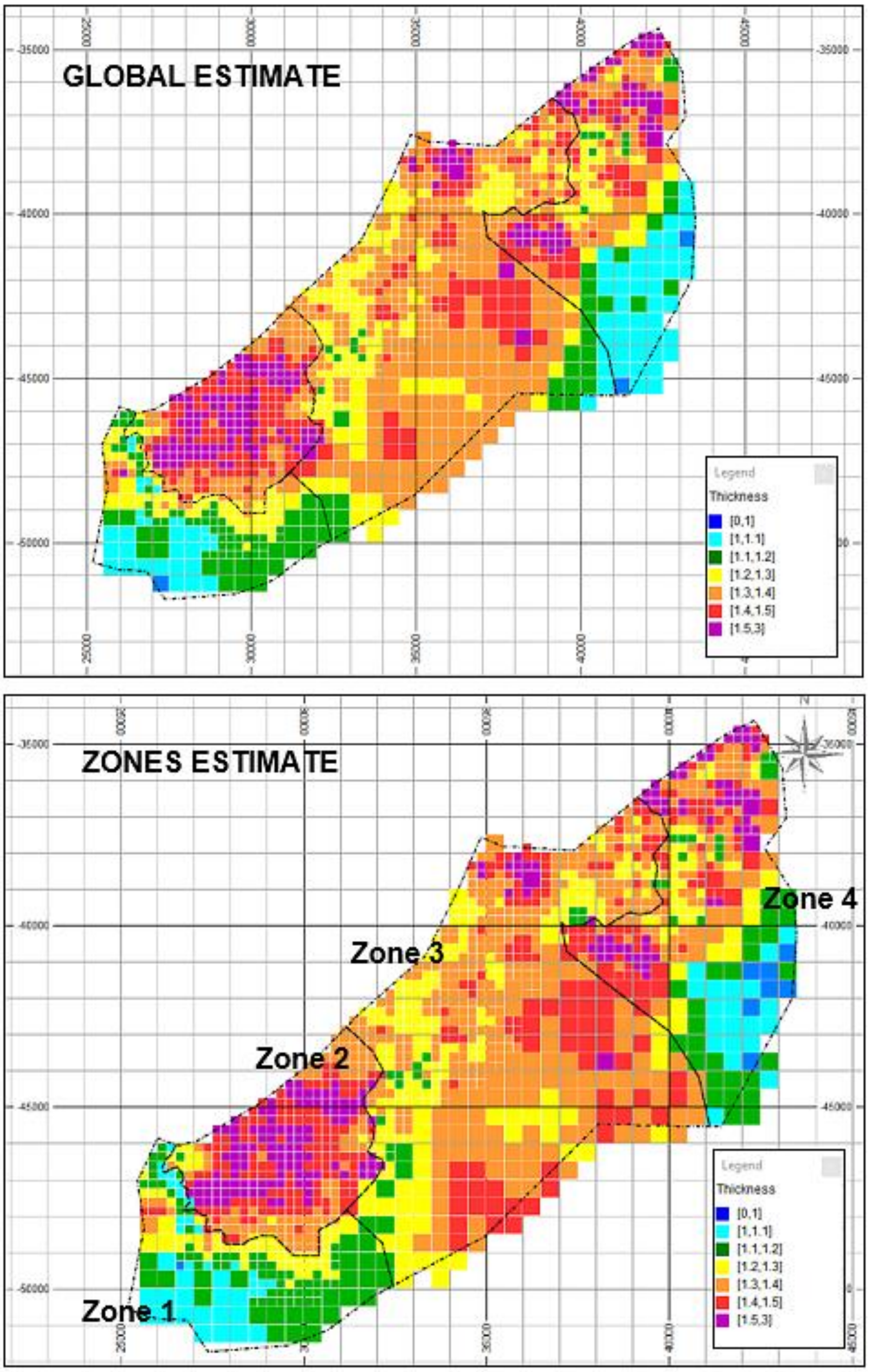

Figure 76: Thickness zones estimates for the global area and the zoned areas for 250x250m-500x500m blocks.

By determining the Mean Absolute Error (MAE) and Mean Square Error (MSE), a measure of the bias and spread of the error can be quantified and compared (Asli and Marcotte, 1995):

$$Mean\ Absolute\ Error = MAE = \frac{1}{n}\sum_{i=1}^{n}|r| \qquad \text{Eq 15}$$

$$Mean\ Squared\ Error = MSE = \frac{1}{n}\sum_{i=1}^{n} r^2 \qquad \text{Eq 16}$$

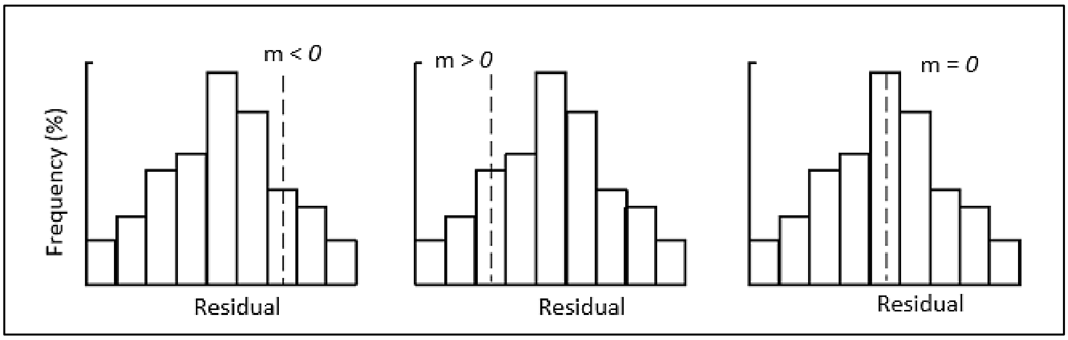

Figure 77: Histogram of residuals showing a case where there is negative bias, positive bias and no bias in the estimation errors. Source: Isaaks and Srivastava (1989).

A scatter plot of the true values (mean of sample data values in a block) versus the estimated values can indicate how the two match against each other and a plot closer to a 45^0 line of the scatter plot indicates the best estimate Figure 78. The correlation coefficient of the true values and estimated values can indicate how close the points on the scatter plot fall close to the 45^0 line. This gives a measure of the strength of similarity/dissimilarity between two variables using the formula:

$$\rho_{XY} = \frac{\sum_{i=1}^{n} X_i Y_i - \frac{1}{n}\left(\sum_{i=1}^{n} X_i\right)\left(\sum_{i=1}^{n} Y_i\right)}{\sqrt{\left\{\sum_{i=1}^{n} X_i^2 - \frac{1}{n}\left(\sum_{i=1}^{n} X_i\right)^2\right\}\left\{\sum_{i=1}^{n} Y_i^2 - \frac{1}{n}\left(\sum_{i=1}^{n} Y_i\right)^2\right\}}} \qquad \text{Eq 17}$$

Where n is the sample size, X_i, Y_i are the individual data values and $\frac{1}{n}\sum_{i=1}^{n} X_i$ is the sample mean, which is same for Y_i.

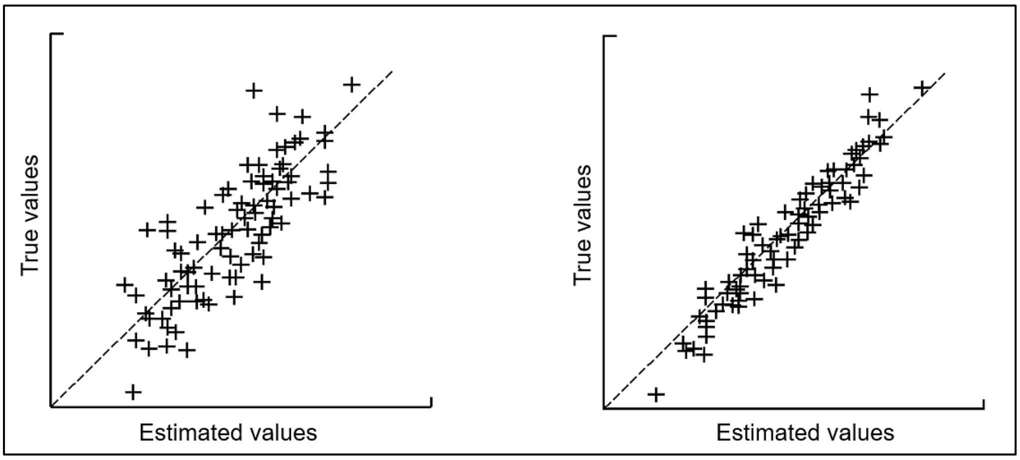

Figure 78: Scatter plot of true values and estimated values. A closer cloud of points is preferred (b) as opposed to a more spread of points (a). Source: Isaaks and Srivastava (1989).

As a guideline, Ratner (2009) suggest the following thresholds for interpreting the correlation coefficient:

1. If 0 then there is no linear relationship
2. Values of +1 and -1 indicate perfect linear relationships, with positive when one value increases the other variable also increases. This is reverse for negative.
3. Values of between 0 and 0.3 and 0 and -0.3, suggest a weak linear relationship.
4. Values between 0.3 and 0.7 and -0.3 and -0.7 indicate a moderate positive/negative linear relationship.
5. Values of between 0.7 and 1 and -0.7 and -1 suggest a strong positive/negative linear relationship.

To compare how the estimates, perform against each other a scatter plot of the true values and estimates were constructed in MS Excel. The plot compares how close the estimates are to the raw data used for the OK exercise. If the estimates and true values plot on a 45^0 line then there is good correlation between the estimates and the data and visa-versa if the scatter forms a cloud of points that do not plot close to the 45^0 line then there is poor correlation between the estimated values and the true values. The correlation coefficient of the true values and the estimated values was calculated in MS Excel to compare how close the two values are similar to each other. A high correlation coefficient indicates that the true value and estimated values are highly similar, whilst a lower correlation coefficient indicates that they are not so similar.

Interpretation of the scatter plots shown in Figure 79 do not indicate much difference in the global estimates and the T-Zone estimates. The point clouds look almost similar and this makes it difficult to identify which estimation matches the true values.

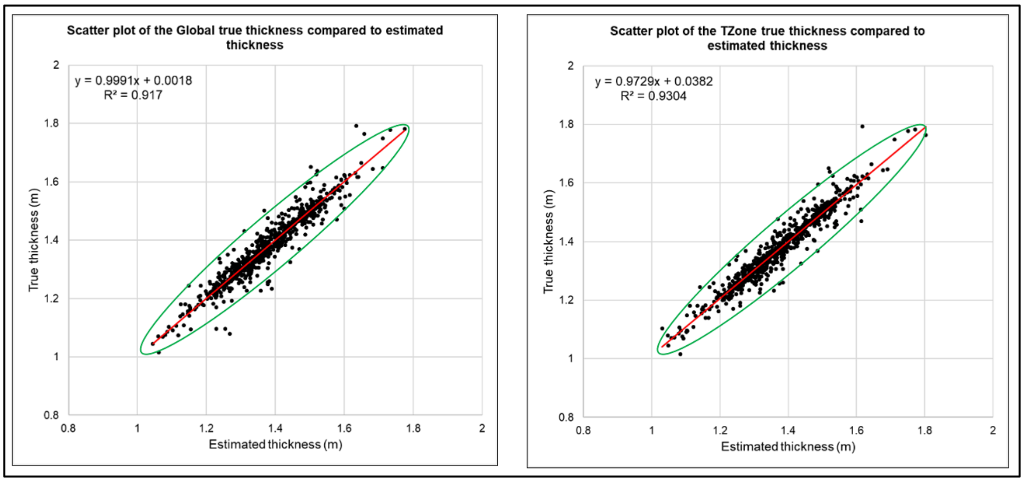

Figure 79: Scatter plots of the true value and estimates for the global and T Zones area.

The ellipse in green drawn around the cloud of points for both scatter plots indicates that the T-Zones estimates are closer to the 45^0 line in comparison to the Global scatter cloud. This is illustrated by the number of points outside the ellipse which are higher in the Global scatter plot.

The summary statistics in Table 14 indicate that the T-Zone estimates highlight a slight improvement compared to the global estimates when looking at the mean error, the MAE, MSE and correlation coefficient. The true thickness means are also more similar with the mean of the estimated thickness of the T-Zones area as opposed to the global estimates.

Table 14: Statistics of the estimation errors of the Global and T-Zone area estimates.

	Mean error (m)	MAE (m)	MSE (m)	True (m)	Estimated (m)	Correlation coefficient
Global	0.016	0.036	0.004	1.190	1.206	0.832
T-Zone1	-0.005	0.03	0.002	1.190	1.185	0.894
Global	-0.002	0.017	0.001	1.453	1.451	0.937
T-Zone2	0.001	0.013	0.0004	1.453	1.454	0.949
Global	0.001	0.019	0.001	1.328	1.329	0.784
T-Zone3	-0.001	0.019	0.001	1.328	1.327	0.864
Global	-0.004	0.033	0.002	1.390	1.386	0.852
T-Zone4	-0.002	0.035	0.002	1.390	1.388	0.857

5.6.2 Density estimation

The block estimate plans of the global and individual D-Zones are shown in Figure 80 and similarly as with the thickness estimates, a visual inspection of the two show that the estimates are more or less the same in general but when looking in detail there are areas where the estimates are different. A low-density area for the D-Zone 3-1 and 3-2 are highlighted by both estimates as observed in the post map of the density values.

Estimation comparison of the density estimates

The scatterplot of the true density values and estimated values is shown in Figure 81. The scatter plots look almost identical and their interpretation is difficult which is the same situation with the thickness scatter plot. This indicates that the estimates of both the global and D-Zones are not very different to each other however the ellipse around the cloud of points indicates a higher proportion of points outside the ellipse for the Global than for the Zones estimates.

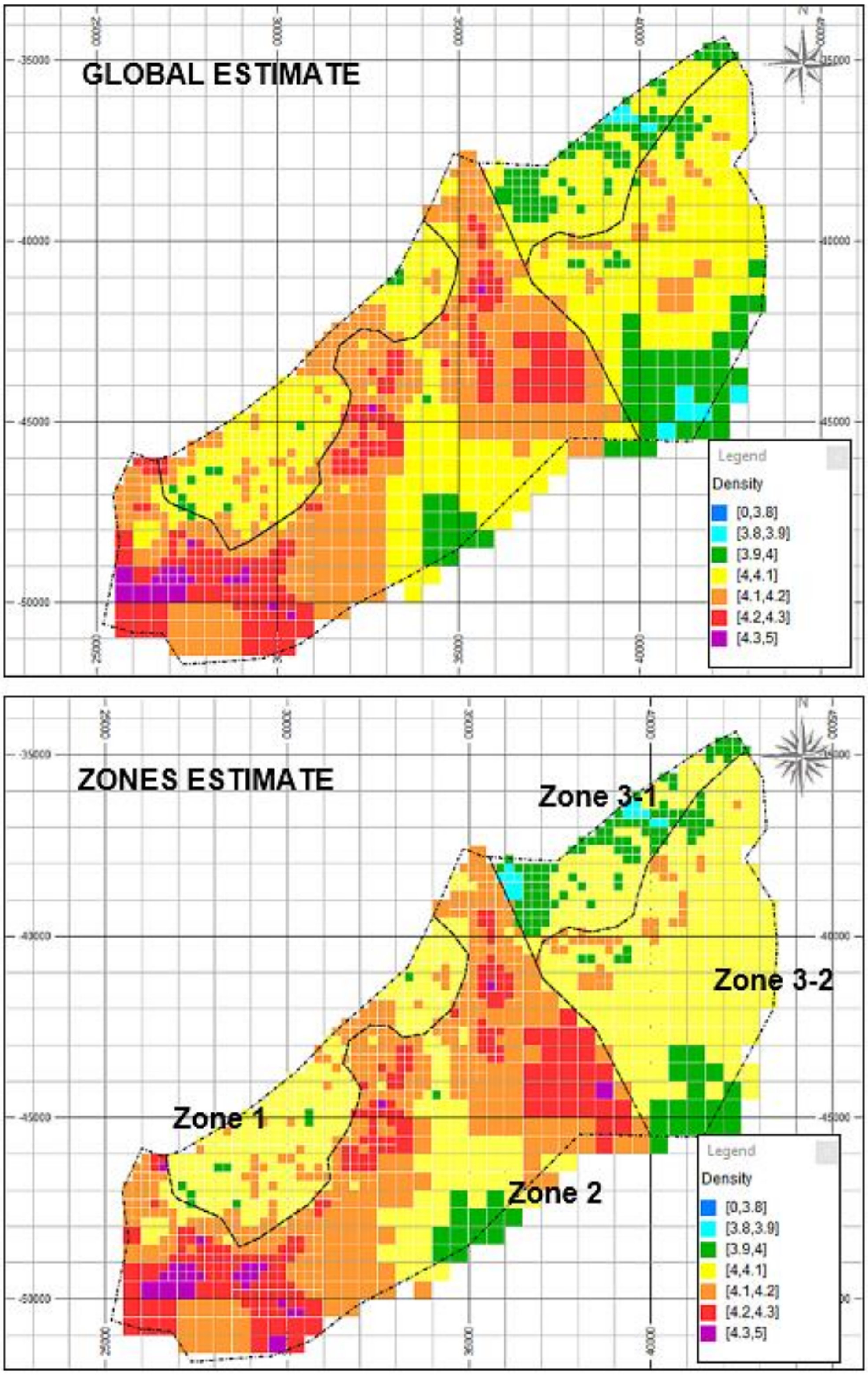

Figure 80: Block estimates of the density (t/m^3) for the global area and zone areas.

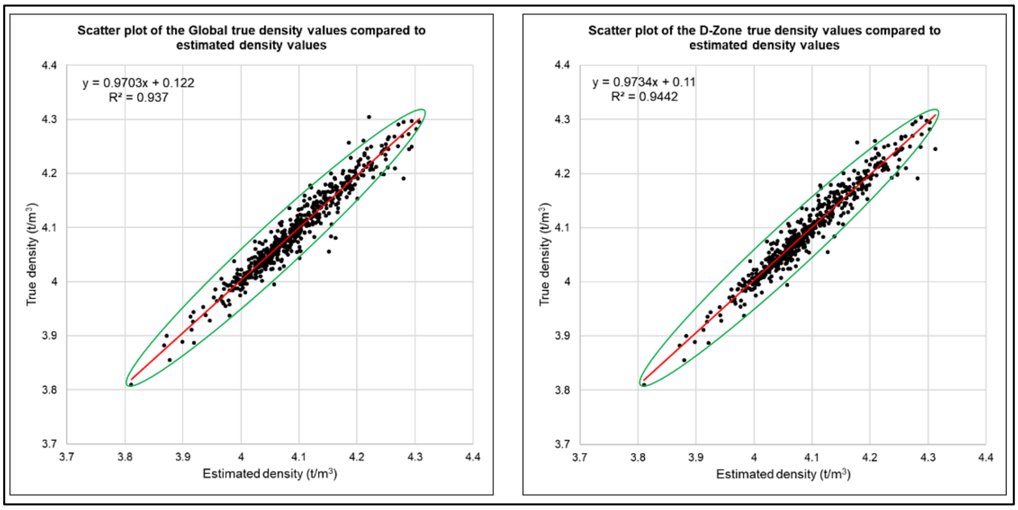

Figure 81: Scatter plots of the density true value and estimates for the global and D-Zone area.

Table 15: Comparison of the model results and the data of the density.

	Mean error (m)	MAE (t/m^3)	MSE (t/m^3)	True (t/m^3)	Estimated (t/m^3)	Correlation coefficient
Global	0.003	0.010	0.000	4.068	4.071	0.692
D-Zone1	0.001	0.006	1.0E-04	4.068	4.067	0.851
Global	-0.002	0.017	0.001	4.170	4.169	0.845
D-Zone2	-0.001	0.018	0.001	4.170	4.169	0.855
Global	-3E-04	0.010	0.000	4.008	4.008	0.913
D-Zone3-1	0.000	0.009	0.000	4.008	4.009	0.953
Global	-0.004	0.016	0.000	4.066	4.062	0.840
D-Zone 3-2	-0.005	0.017	0.000	4.066	4.061	0.910

The statistics of the errors in Table 15 do support the results of the scatter plot in that there is not a substantial difference in the mean error, MAE and MSE for the global estimates and the D-Zone estimates. The average of the estimates are also not considerably different to each other as well. When looking at the correlation coefficient of the two sets of estimates however, the D-Zone estimates have a high correlation coefficient compared to the global estimates which indicates an improvement in the estimates for the D-Zones.

5.6.3 Platinum estimation

The block estimates of the Platinum grade are shown on Figure 82 for the global and Zones areas. The estimates look similar when compared to each other when looking broadly across the area, but as with the observation made with the thickness and density estimates, a closer inspection show some dissimilarities in some areas. Both estimates are able to capture the lower grade area identified in the platinum post map analysis.

Comparison of the platinum estimates

As with the thickness and density scatter, the platinum scatter plots Figure 83 of the global and Pt-Zones true vs estimated, it is very difficult to identify which of the two has performed well as the scatter look almost identical as well as the proportion of points outside the ellipse around the scatter cloud. The statistics of the errors (Table 16) indicate that the global is outperformed by the D-Zone estimates when comparing them to the true values. For Pt-Zone 1 and 2 it is obvious that there is improvement in the estimates and for Pt-Zone-3, the global and Pt-Zone estimates are very similar. The correlation coefficient of the true and estimated values show that the Pt-Zones estimates are much similar to the true values and lesser for the global estimates which indicates that there is an improvement in using the individual variograms of the Pt-Zones rather than the global variogram.

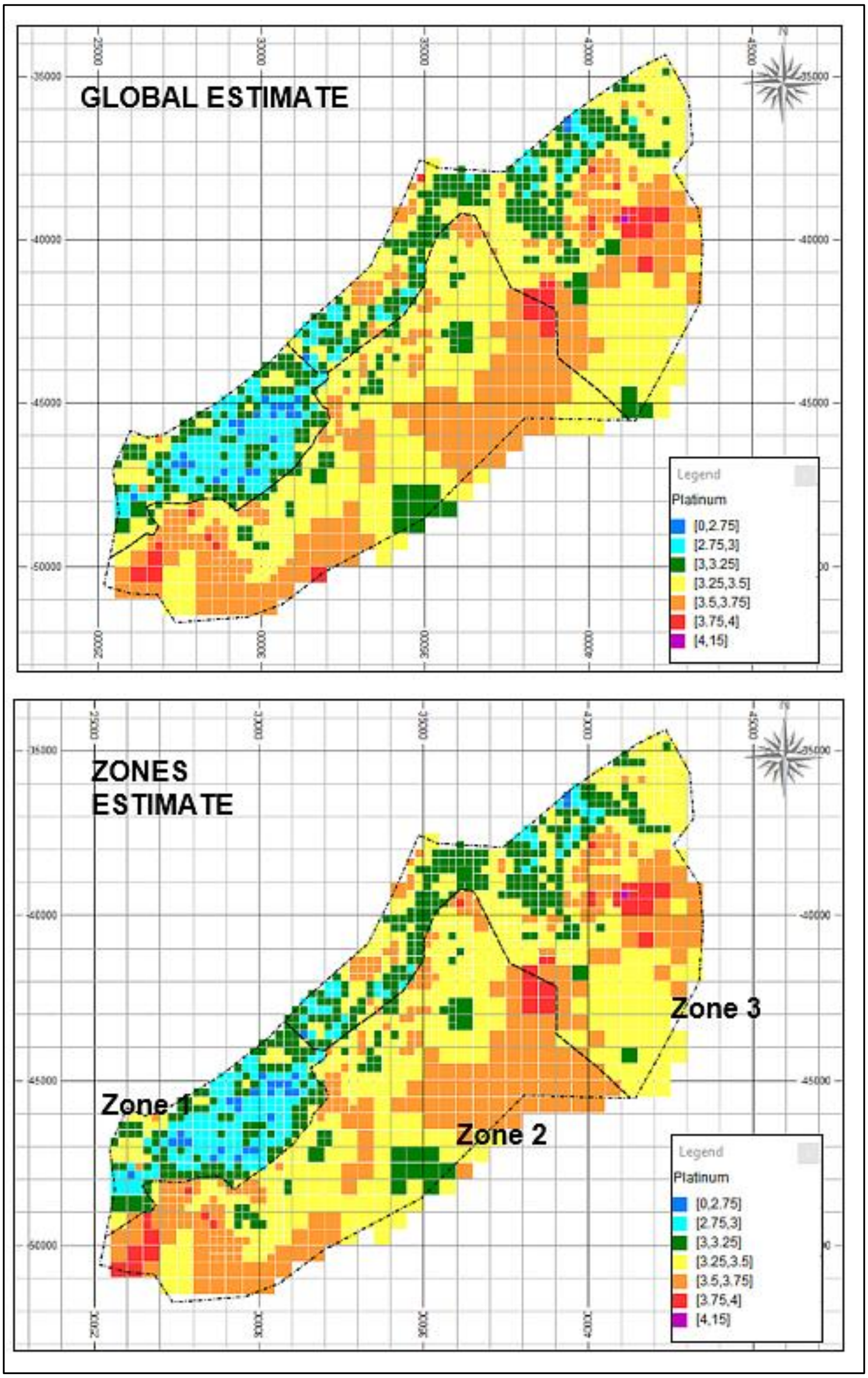

Figure 82: Platinum grade block estimates for the global and the Pt-Zones.

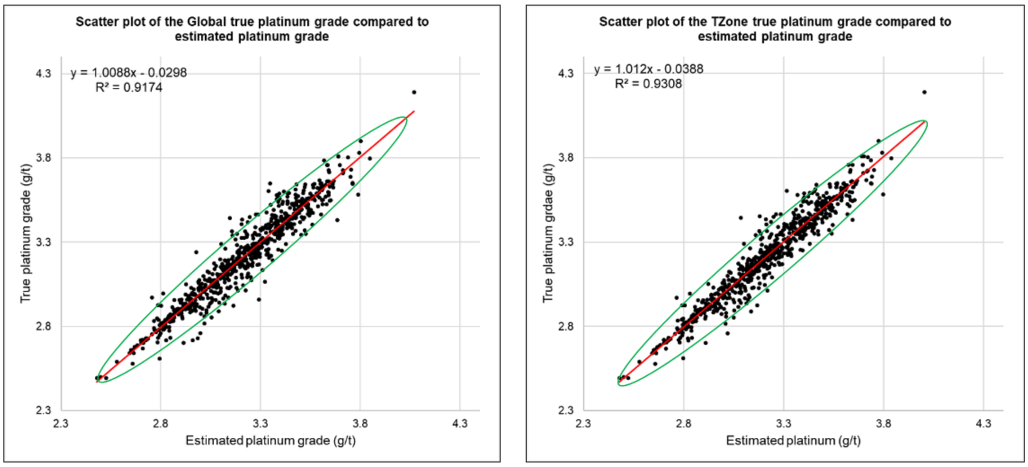

Figure 83: Scatter plots of the true value and estimates for the global and Pt-Zone area.

Table 16: Comparison of the model result and the data of the platinum grade.

	Mean error (m)	MAE (g/t)	MSE $(g/t)^2$	True (g/t)	Estimated (g/t)	Correlation coefficient
Global	0.014	0.055	0.014	2.989	3.003	0.916
Pt-Zone1	0.008	0.046	0.005	2.989	2.996	0.938
Global	-0.019	0.054	0.005	3.462	3.444	0.657
Pt-Zone2	-0.007	0.043	0.003	3.462	3.456	0.739
Global	0.0004	0.056	0.006	3.280	3.28	0.886
Pt-Zone3	-0.002	0.056	0.006	3.280	3.278	0.904

5.7 Conclusion

The data analysis of the of the orebody thickness, density and platinum grade of the UG2 from the borehole and channel sample was conducted using statistics and geostatistics. The geology in relation to the orebody thickness, density and platinum shows correlation with amount of internal waste between the main seam and the leaders. When looking at the dykes, faults and potholes no obvious relation is evident. By using the data posting of these three variables, areas showing homogeneity were identified and were confirmed by the various statistical tools used. The variography exercise also highlighted that the global variogram and zone variogram differ. This is because the data is now from a single population. The optimum block study indicated that a smaller block size might be suitable for well-informed area were data is abundant. The OK estimations of the global estimate and zone estimate showed that in general the zone estimates improved in quality and outperformed the global estimates. It is concluded that when considering domains when doing Mineral Resource estimate using kriging on the Amandelbult data, the confidence in the estimates increases.

6 RESULTS AND DISCUSSION

6.1 Introduction

The results of the study are captured in this chapter, a recollection and summary of the outcome of the methodology applied to finally arrive to the geozones identified is also given. A summary of the data posting, statistical analysis, geology, geostatistical analysis and kriging estimates follow.

6.2 Data Posting

Interpretation of the data posting of the orebody thickness, density and platinum highlighted areas various areas of high and low values exist. This allowed for the identification of the four zones for the thickness, four for the density and three for the platinum grade. The data posting of the values in different ranges provided an overall spatial view of the data. The advantage of the data post is that spatial variability can easily be identified across a large area containing a large amount of sample values.

6.3 Statistical Analysis

Statistical analysis using summary statistics, histograms, box plots and cumulative plots assisted in summarising and confirmation of the statistical properties of the zones identified using the data post maps. The exercise reinforced the homogeneity of the zones across the study area.

The global statistical calculations indicated that using all the data across the mine to some extent averages the statistical differences across the orebody. The influence of high values is reduced whilst that of low values is inflated when calculating the statistics of the global area. The comparative graphical summaries of the data i.e. histograms, box plots, cumulative distribution plots of individual zones with the global statistics of the UG2 all confirmed the spatial and non-spatial differences between the zones. The Q-Q plots also showed that a comparison of the zones amongst each other does not plot on the 45^0 line which again reinforced a difference in populations for all the three variables investigated.

6.4 Geology

Unlike for sedimentary and metamorphic originated ore deposits, mineralisation in igneous deposits is influenced at the time of the deposition of magma and cooling thereof. This is illustrated by the little influence of faults and dykes on the orebody characteristics as this are later events. There is a strong correlation between the presence of internal waste with the thickness, density and grade. The fact that the internal waste occurs within the reef itself, results in a thicker reef when the internal waste is increased. The internal waste is usually a pyroxenite with interstitial chromitite and has less density than chromitite on its own.

The lower density in D-Zone 1 is thus related to a thicker reef which is thickened by the internal waste which results in the lower density. Areas of thick reef are in close association with a lower density whilst thinner reef are associated with area of higher orebody density. The platinum grade is also influenced by the thickness of the reef. The T-Zone 1 area of the platinum grade has a lower grade compared to the other two platinum grade zones.

As with the density, the internal pyroxenite has a lower grade and when it is thicker it reduces the overall grade of the reef. The presence of slumps and potholes show no distinctive correlation with the zones of the thickness, density and platinum on a large scale. In conclusion the thicker the reef the lower the density and also the platinum grade where the internal waste has been increased. When looking at the geology, the internal waste has the highest influence on the character of the reef in terms of the density and grade.

6.5 Geostatistical Analysis

The thickness variograms show a clear structure which was easily modelled for T-Zone 2, 3, and 4. For T-Zone 1 the variography did not show a good structure and this largely attributed to the limited data in the zone with a short range. Since this area is also on the flanges of the mine and not much mining has occurred this is was to be expected.

The density zones 1 and 2 variography revealed a clear variogram. D-Zone 3 variography did not show a clear structure and indicated a trend in the variogram but this was improved after the zone was split even further into two zone, D-Zone 3-1 and 3-2.

Of the three variables, the platinum variograms were the best behaved. The ranges of the zones variograms are all shorter than the global variogram which is obviously due to the data limits imposed on the zones.

6.6 Optimum Block Size Analysis

This exercise was carried out to confirm the appropriateness of the current block sizes used in the resource estimation. The results of the optimum block size study conducted with the variograms of the zones identified for the thickness, density and thickness confirmed that the 250 X 250m and 500m X 500m block size are adequate for estimation in the moderate and poorly informed areas, however a smaller block size in the region of 100m X 100m to 150m X 150m in the well informed areas is envisaged to provide more robust estimates with an improved resolution and definition.

6.7 Kriging Estimation Results

The estimation results comparison of the global variogram and the Zone variograms for the thickness, density and platinum, show that the MAE is much lower when estimation is carried out using the Zone variogram as opposed to the global variogram. The same is true for the MSE. The correlation coefficient calculated for the global and Zone estimates, show that it is higher for the Zone estimates which indicates that the Zone estimates are closer to reality and more representative of the available data.

7 CONCLUSIONS

The UG2 data base used for resource estimation at Amandelbult has increased over the years and this has allowed for an assessment to be conducted to see if the UG2 orebody within the lease area can be split into separate homogenous regions using statistical and geostatistical properties.

In conclusion the summary statistics generated from the data set successfully highlighted different geo-zones of the orebody thickness, density and platinum grade. Graphical statistics such as histograms, cumulative probability plots and box plots aided in justifying the zones identified from the data posting. The respective variograms identified for the various zones outperformed the global variograms for the thickness, density and platinum. The comment made by Guibal (2001) that orebody domaining is justified if it results in improved variography holds true for the UG2 case of the Amandelbult data.

Observations made by Davey (1992) are similar to what has been observed with the Amandelbult data. The thickness, density and grade of the UG2 are correlated in that an increased thickness is associated with a lower grade and lower density whilst a reduced thickness is associated with a higher grade and higher density.

Estimation using OK did show improvement in quality of the estimates when comparing the MAE, MSE and correlation coefficient of the global estimates and the Zone estimates. The study has shown that statistics and geostatistics can be used to identify different homogenous geo-zones in a deposit which can ultimately result in improved estimates.

It is further concluded that the objectives of the research study have been achieved through a detailed assessment of the literature and appropriate application of available techniques supported by validation evidence.

8 RECOMMENDATIONS

Based on the results achieved with this research study, the following recommendations are put forward:

Since the statistics calculated in the zones and the global area for the thickness, density and platinum show differences, it is recommended that for future planning purposes the statistics for the individual zones be used rather than applying a global as this may result in an over or underestimation of either the thickness, density or platinum grade.

As more information is acquired, the statistics should be reviewed to see if the additional data can assist in confirming the zones identified and to check that the zones are valid.

When considering the geology indication is that the thickness, density and platinum grade are more related to the thickness of the internal pyroxenite separating the leaders from the main seam, as such a detailed study of this relationship is recommended and should focus on scrutinizing the borehole and channel sample grade profile of the UG2 at Amandelbult to determine the distribution of the density or platinum grade across the reef. Upon completion of this exercise, the zones identified in this research can be checked if they correspond to the grade profile and this will also assist in justifying the zones identified if there is a link between the grade profile and the zones.

Due to time constraints, not all the elements/variables available could be studied. It is recommended that all the available information undergo the same process as the variable investigated in this study as this will aid in checking for a relationship with the zones that have been identified. Eventually after all the variables have been studied, all the zones for all the variables can be superimposed and a decision can be made for a final UG2 geozone delineation for Amandelbult.

As a result of the large amount of data available the mean can be calculated with much more confidence, estimation using simple kriging should be investigated for areas with scare data within in the respective zones identified. The results can be compared to the OK results to see if there is a need to change the estimation method based on the increased data available.

Since there was improvement in the estimate when using the zone variograms and comparing it to the global variogram, estimation is recommended to be conducted using the zone variogram rather than the global variogram. Using the global variogram can result in smoothed estimates and may not be representative of reality. Over and under estimation can be introduced as well as a result of using a global variogram.

The optimum block size study exercise showed that a smaller block size might be suitable in the well informed areas, an investigation needs to be carried out to confirm which small block size can be used which is less than the current 250m X 250m block size. This has the potential of enhancing the resolution of the block estimates and further improving the estimates when using OK for the deposit. A suggestion would be to logically use 125m X 125m blocks as this is half the currently used 250m X 250m blocks.

Since there is always some uncertainty with boundaries of domains, a contact analysis study is recommended for the orebody thickness, density and platinum domains to determine whether the boundaries are hard or soft. A simulation study can also be done to aid in this verification.

RERERENCES

Anglo American Plc (2018) ‘Ore Reserves and Mineral Resources Report 2018’.

Appleyard, G. (2001) ‘An Overview and Outline’, in Edwards, A. C., *Mineral Resource and Ore Reserve Estimation - The AusIMM Guide to Good Practice*. Melbourne: Australasian Institute of Mining and Metallurgy (Monograph, 23), pp. 3–11.

Asli, M. and Marcotte, D. (1995) ‘Comparison of approaches to spatial estimation in a bivariate context’, *Mathematical Geology*, 27(5), pp. 641–658.

AvRuskin, G. A., Jacquez, G. M. and Meliker, J. R. (2004) ‘Visualization and exploratory analysis of epidemiologic data using a novel space time information system’, *International Journal of Health Geographics*, 3(1), p. 26. doi: 10.1186/1476-072X-3-26.

Caldwell, S. (2012) *Statistics Unplugged*. Cengage Learning. Available at: https://books.google.co.za/books?id=YfkKAAAAQBAJ.

Cawthorn, R. (2011) ‘Geological interpretations from the PGE distribution in the Bushveld Merensky and UG2 chromitite reefs’, *The Journal of The Southern African Institute of Mining and Metallurgy*, 111(no2), pp. 67–79.

Cawthorn, R. (2015) ‘The geometry and emplacement of the Pilanesberg Complex, South Africa’, *Geology Magazine, Cambridge University Press*, 12 January, pp. 802–812. doi: 10.1017/S0016756814000764.

Chilès, J. P. and Desassis, N. (2018) ‘Fifty years of kriging’, in *Handbook of Mathematical Geosciences: Fifty Years of IAMG*. Switzerland: Springer, pp. 589–612.

Clark, I. (1979) *Practical geostatistics*. London: Elsevier Applied Science.

Clark, I. (2015) ‘Regression revisited (again)’, *The Journal of The Southern African Institute of Mining and Metallurgy*. (Danie Krige Commemorative Edition), 115(1), pp. 45–50.

Coertze, F. J. (1958) ‘Intrusive relationship and ore-deposits in the Western part of the Bushveld Igneous Complex’, *Trans. The Geological Society of South Africa*, 61(No1), pp. 387–400.

Colquhoun, I. (2018) ‘Amandelbult UG2 Reef Resource Modelling Report’. Anglo American Plc.

Coombes, J. (1997) ‘Handy tips on variography’, in *AusIMM national conference on Ironmaking resource and reserve estimation*. Melbourne: The Australasian Institute of Mining and Metallurgy, pp. 127–130.

Coombes, J. (2008) *The art and science of resource estimation: a practical guide for geologists and engineers*. Subiaco, W.A.: Coombes Capability.

Cousins, C. A. and Feringa, G. (1964) 'The chromitite deposits of the western belt of the Bushveld Complex', in *The geology of some ore deposits in Southern Africa*. Haughton SH. Johannesburg, South Africa: Geological Society or South Africa, pp. 183–202.

Davey, S. R. (1992) 'Lateral variations within the upper Critical Zone of the Bushveld Complex on the farm Rooikoppies 297 JQ, Marikana, South Africa', *South African Journal of Geology*, 95(no(3/4)), pp. 141–149.

David, M. (1977) *Geostatistical ore reserve estimation*. Amsterdam: Elsevier (Developments in geomathematics, 2).

Deutsch, C. (2007) *The Slope of Regression for Kriging Estimators*. Annual Report 09, 311. University of Alberta: Center for Computational Geostatistics, Department of Civil Engineering and Environmental Engineering, pp. 311-1-311–4. Available at: http://www.ccgalberta.com/resources/reports/.

Deutsch, J. L. and Deutsch, C. V. (2012) *Kriging, stationarity and optimal estimation: Measures and suggestions.* Annual Report 14. Canada: University of Alberta, pp. 306-1-306–8. Available at: http://www.ccgalberta.com/ccgresources/report14/2012-306_kriging_measures_and_suggestions.pdf.

Deutsch, J. L., Szymanski, J. and Deutsch, C. V. (2014) 'Checks and measures of performance for kriging estimates', *The Journal of The Southern African Institute of Mining and Metallurgy*, 114, pp. 233–230.

Dewing, K. (2007) 'Are Your Data Good Enough: A Checklist for Mining Prospects', *Geoscience Canada*, 34(no2), pp. 65–69.

Dishaba Mine (2019) 'Geology of Amandelbult Complex'. Dishaba Mine, Thabazimbi: Anglo American Plc.

Doane, D. and Seward, L. (2011) 'Measuring skewness: A forgotten statistic?', *Journal of Statistics Education*, 19(2), pp. 1–18. doi: 10.1080/10691898.2011.11889611.

Dodge, Y. (2008) 'Histogram', in *The Concise Encyclopedia of Statistics*. New York, NY: Springer New York, pp. 242–244. doi: 10.1007/978-0-387-32833-1_178.

Dohm, C. (2003) 'Application of simulation techniques for combined risk assessment of both geological and grade model-an example', *South African Institute of Mining and Metallurgy*, (Application of Computers and Operations Research in the Mineral Industries), pp. 351–354.

Dohm, C. (2018a) 'Course notes for Geostatistical valuation of ore reserves'. University of the Witwatersrand, South Africa.

Dohm, C. (2018b) 'Course notes for Statistical Valuation of Ore Reserves'. University of the Witwatersrand, South Africa.

Eales, H. V. (1996) ‘The Bushveld Complex’, *Elsevier*. Edited by R. G. Cawthorn. (Layered Intrusions), 15, pp. 181–229.

Eales, H. V. (ed.) (2001) *A first introduction to the geology of the Bushveld Complex and those aspects of South African geology that relate to it: the story of one of the great events in the geological history of Southern Africa, told in informal language to show what geology is about*. Pretoria, South Africa: The Council for Geoscience (Popular geoscience series, 2).

Eales, H. V., Botha, W. J. and Hattingh, P. J. (1993) ‘The mafic rocks of the Bushveld complex: a review of emplacement and crystallization history, and mineralization, in the light of recent data’, *Geology and Development in Southern Africa*, 16(1), pp. 121–142. doi: 10.1016/0899-5362(93)90163-K.

Eales, H. V., de Klerk, W. J. and Teigler, B. (1990) ‘Evidence for magma mixing processes within the Critical and Lower Zones of the northwestern Bushveld Complex, South Africa’, *Chemical Geology*, 88(3), pp. 261–278. doi: 10.1016/0009-2541(90)90093-M.

Emery, X. and Ortiz, J. (2005) ‘Estimation of mineral resources using grade domains: Critical analysis and a suggested methodology’, *The Journal of The Southern African Institute of Mining and Metallurgy*, 105, pp. 247–255.

Emery, X. and Ortiz, J. (2006) ‘Geostatistical estimation of mineral resources with soft geological boundaries: A comparative study’, *The Journal of The Southern African Institute of Mining and Metallurgy*, 106, pp. 577–584.

Glacken, I. M. and Snowden, D. V. (2001) ‘Mineral Resource Estimation’, in *Mineral Resource and Ore Reserve Estimation-The AusIMM Guide to good practice*. A C Edwards. Melbourne: The Australasian Institute of Mining and Metallurgy, pp. 189–198.

Glass, H. J. (2003) ‘Method for assessing quality of the variogram’, *The Journal of The South African Institute of Mining and Metallurgy*, 103, pp. 43–51.

Goovaerts, P. (1997) *Geostatistics for natural resources evaluation*. New York: Oxford University. Press (Applied geostatistics series).

Gringarten, E. and Deutsch, C. V. (2001) ‘Teacher’s Aide Variogram Interpretation and Modeling’, *Mathematical Geology*, 33(4), pp. 507–534. doi: 10.1023/A:1011093014141.

Guibal, D. (2001) ‘Variography, a tool for the Resource Geologist’, in *Mineral resource and Ore Reserve Estimation - The AusIMM Guide to Good Practice*. Melbourne: The Australasian Institute of Mining and Metallurgy, pp. 85–90.

Gy, P. (2004) ‘Sampling of discrete materials - A new introduction to the theory of sampling: I. Qualitative approach’, *Chemomotrics and intelligent laboratory systems*, 74(no74), pp. 7–24. doi: 10.1016/j.chemolab.2004.05.012.

Hatton, C. J. and Gruenewaldt, G. von (1985) *The geological setting and petrogenesis of the Bushveld chromitite layers.* Pretoria: Institute for Geological Research on the Bushveld Complex, University of Pretoria (57).

Heuvelink, G. and Pebesma, E. (2002) 'Is the ordinary kriging variance a proper measure of interpolation error?', in *Fifth International Symposium on Spatial Accuracy Assessment in Natural Resources and Environmental Sciences*. *Accuracy 2002 Symposium*, Amsterdam, the Netherlands: Institute for Biodiversity and Ecosystem Dynamics, University van Amsterdam, pp. 179–187.

Irvine, T. N. (1975) 'Crystallization sequences in the Muskox intrusion and other layered intrusions—II. Origin of chromitite layers and similar deposits of other magmatic ores', *Geochimica et Cosmochimica Acta*, 39(6), pp. 991–1020. doi: 10.1016/0016-7037(75)90043-5.

Isaaks, E. H. and Srivastava, R. M. (1989) *Applied Geostatistics*. New York, NY: Oxford Univ. Pr.

Journel, A. G. and Huijbregts, C. J. (1991) *Mining geostatistics*. 2003.Repr. of the 5th. printing. 1991. Caldwell, NJ: Blackburn.

Junge, M., Oberthür, T. and Melcher, F. (2014) 'Cryptic variation of chromite chemistry, platinum group element and platinum group mineral distribution in the UG-2 chromitite: An example from the karee mine, western Bushveld complex, South Africa', *Economic Geology*, 109(no3), pp. 795–810. doi: 10.2113/econgeo.109.3.795.

Karykowski, B. T. and Maier, W. D. (2017) 'Microtextural characterisation of the Lower Zone in the western limb of the Bushveld Complex, South Africa: evidence for extensive melt migration within a sill complex', *Contributions to Mineralogy and Petrology*, 172(8), p. 60. doi: 10.1007/s00410-017-1380-y.

Kestin, I. (2015) 'Statistics in medicine', *Neurointensive Care/Intensive Care*, 16(4), pp. 200–207. doi: 10.1016/j.mpaic.2015.01.007.

Khakestar, M. S., Madani, H. and Hassani, H. (2013) 'Determining the best search neighbourhood in reserve estimation, using geostatistical method: A case study anomaly No 12A iron deposit in central Iran', *Journal of the Geological Society of India*, 81(4), pp. 581–585. doi: 10.1007/s12594-013-0074-y.

Kinnaird, J. A. (2005) 'The Bushveld Large Igneous Province. Review Paper. The University of the Witwatersrand, Johannesburg'.

Krige, D. G. (1976) 'Some basic considerations in the application of geostatistics to the valuation of ore in South African gold mines.', *The Journal of The South African Institute of Mining and Metallurgy*, 76, pp. 383–391.

Krige, D. G. (1997) 'A practical analysis of the effects of spatial structure and of data available and accessed, on conditional biases in ordinary kriging.', in. *Geostatistical Wollongong '96, Fifth international Geostatistics Congress*, Wollogong, Australia: Kluwer, Dordrecht, pp. 799–810.

Krige, D. G. and Ueckermann, H. (1963) 'Value contours and improved regression techniques for ore reserve valuations', *South African Institute of Mining and Metallurgy*, 63, pp. 429–452.

Kumari, M., Singh, C. K. and Basistha, A. (2017) 'Clustering Data and Incorporating Topographical Variables for Improving Spatial Interpolation of Rainfall in Mountainous Region', *Water Resources Management*, 31(1), pp. 425–442. doi: 10.1007/s11269-016-1534-0.

Langwieder, G. (2018) 'Underground Sampling Standard'. Anglo American Platinum Group Standard, Mineral Resource Management, Geosciences.

Larrondo, P. and Deutsch, C. V. (2005) 'Accounting for Geological Boundaries in Geostatistical Modeling of Multiple Rock Types', in Leuangthong, O. and Deutsch, C. V. (eds) *Geostatistics Banff 2004*. Dordrecht: Springer Netherlands, pp. 3–12. doi: 10.1007/978-1-4020-3610-1_1.

Latha, C. and V Shribharathi, S. (2017) 'Q-Q Plot representation of feature extraction algorithms with recent network models for facial emotional recognition', *Journal of Advanced Research in Dynamical and Control Systems*, 9, pp. 423–443.

Lomberg, K. (2014) 'Best practice sampling methods, assay techniques, and quality control with reference to the platinum group elements (PGEs)', *The Journal of The Southern African Institute of Mining and Metallurgy*, Vol. 114(no1), pp. 53–62.

Maier, W. D. and Barnes, S. J. (2008) 'Platinum-group elements in the UG1 and UG2 chromitites, and the Bastard reef at Impala platinum mine, western Bushveld Complex, South Africa: Evidence for late magmatic cumulate instability and reef constitution', *South African Journal of Geology*, 111(no2-3), pp. 159–176.

Makgato, R. and Chingobo, O. (2019) *Technical Support Document, Tumela Mine*. TSD-TUM-GL-2019. Tumela Mine, Thabazimbi, p. 133.

Makgato, R. and Laubscher, J. (2018) 'Competent Persons Resource and Reserves Report 2018-Merensky and UG2 Reef, Dishaba Mine'. Anglo American Plc.

Matheron, G. (1963) 'Principles of geostatistics', *Economic Geology*, 58, pp. 1246–1266.

Mathez, E. A. and Mey, J. L. (2005) 'Character of the UG2 Chromitite and host rocks and petrogenesis of its pegmatoidal footwall, Northeastern Bushveld Complex', *Economic Geology*, 100, pp. 1617–1630.

McArthur, G. J. (1988) 'Using geology to control geostatistics in the Hellyer deposit', *Mathematical Geology*, 20(4), pp. 343–366. doi: 10.1007/BF00892983.

McCarthy, T. and Rubidge, B. (2005) *The story of earth & life: a southern African perspective on a 4,6-billion-year journey*. Cape Town, South Africa: Struik Publishers.

McLaren, C. and Villiers, J. (1982) 'The platinum-group chemistry and mineralogy of the UG-2 chromitite layer of the Bushveld Complex', *Economic Geology*, 77(no6), pp. 1348–1366. doi: 10.2113/gsecongeo.77.6.1348.

Miller, R. L. and Kahn, J. S. (1962) *Statistical analysis in the geological sciences*. University of California: Wiley. Available at: https://books.google.co.za/books?id=S4jZAAAAIAAJ.

Mitchell, A. and Scoon, R. (2012) 'The Platreef of the Bushveld Complex, South Africa: A new hypothesis of multiple, non-sequential magma replenishment based on observations at the Akanani Project, North-West of Mokopane', *South African Journal of Geology*, 155, p. no4.

Mosobalaje, O. O., Orodu, O. D. and Ogbe, D. (2019) 'Descriptive statistics and probability distributions of volumetric parameters of a Nigerian heavy oil and bitumen deposit', *Journal of Petroleum Exploration and Production Technology*, 9(1), pp. 645–661. doi: 10.1007/s13202-018-0498-4.

Moyo, M. (2012) *3/55 to 4/55 Internal Waste-Updates*. Note for Record DM-GEO_02-12_MGM_05. Dishaba Mine, Thabazimbi, p. 2.

van der Neut, M. (2018) 'QAQC Investigation of Assay Results Reported Between 6 July 2010 and 27 September 2017'. Anglo American Platinum Internal Report.

Noble, A. (2011) 'Mineral Resource Estimation', in *SME mining engineering handbook*. 3rd ed. Englewood, Colo.: Society for Mining, Metallurgy, and Exploration, pp. 203–217.

Pierce, R. and Chick, H. (2012) 'Workplace statistical literacy for teachers: interpreting box plots', *Mathematics Education Research Journal*, 25(2), pp. 189–205. doi: 10.1007/s13394-012-0046-3.

Poniewierski, J. (2019) 'Block model knowledge for mining engineers-An introduction'. Deswik.

Ratner, B. (2009) 'The correlation coefficient: Its values range between +1/−1, or do they?', *Journal of Targeting, Measurement and Analysis for Marketing*, 17(2), pp. 139–142. doi: 10.1057/jt.2009.5.

Rivoirard, J. (1987) 'Two key parameters when choosing the kriging neighborhood', *Mathematical Geology*, 19(8), pp. 851–856. doi: 10.1007/BF00893020.

Rossi, M. E. and Deutsch, C. V. (2014) *Mineral resource estimation*. Dordrecht, London: Springer.

SACS (1980) *South African Committee of Stratigraphy (SACS)-Lithostratigraphy of the Republic of South Africa, South West Africa/Namibia, and the republics of Bophuthatswana, Transkei, and Venda*. Pretoria: Republic of South Africa, Dept. of Mineral and Energy Affairs, Geological Survey (Stratigraphy of South Africa, pt. 1).

Schaeben, H. (1988) ‘Geology and mathematics: Progressing mathematization of geology’, *Geologische Rundschau*, 77(2), pp. 591–607. doi: 10.1007/BF01832400.

Schouwstra, R., Kinloch, E. D. and Lee, C. A. (2000) ‘A Short Geological Review of the Bushveld Complex’, *Platinum Metals Review*, 44(no1), pp. 33–39.

Scoates, J. S. and Friedman, R. M. (2008) ‘Precise age of the platiniferous Merensky Reef, Bushveld Complex, South Africa, by the U-Pb Zircon chemical abrasion ID-TIMS technique’, *Economic Geology*, 103(3), pp. 465–471. doi: 10.2113/gsecongeo.103.3.465.

Scoon, R. N. and Mitchell, A. A. (2012) ‘The Upper Zone of the Bushveld Complex at Roossenekal, South Africa: Geochemical stratigraphy and evidence of multiple episodes of magma replenishment’, *South African Journal of Geology*, 115(4), pp. 515–534. doi: 10.2113/gssajg.115.4.515.

Scoon, R. and Teigler, B. (1994) ‘Platinum-group element mineralization in the critical zone of the western Bushveld Complex: I. Sulfide poor-chromitites below the UG-2’, *Economic Geology*, 89(no5), p. 1121. doi: 10.2113/gsecongeo.89.5.1094.

Scott, D. (2008) ‘Histograms: Theory and Practice’, in *Multivariate density estimation: Theory, practice and visualization*. Houston, Texas: John Wiley & Sons (Wiley series in Probability and Statistics), pp. 47–94. doi: 10.1002/9780470316849.ch3.

SGS (2019) *Au, Pt, Pd by Fire Assay*. Available at: https://www.sgs.co.za/en/mining/analytical-services/geochemistry/precious-metals/au-pt-pd-by-fire-assay (Accessed: 29 July 2019).

Shand, S. (1932) ‘The geology of Pilansberg in the Western Transvaal: A study of Alkaline Rocks and Ring intrusions’, *Trans. The Geological Society of South Africa*, 31, pp. 97–156.

Sibiya, B. (2017) ‘Stratigraphy of Amandelbult Complex’. Anglo American Platinum, Dishaba Mine.

Snowden Group (2017) *Supervisor 8.7 - Multi-block kriging neighbourhood analysis*, *Software, Supervisor*. Available at: https://snowdengroup.com/news/supervisor-8-7-multi-block-kriging-neighbourhood-analysis/ (Accessed: 10 January 2019).

Snyman, Q. (2002) ‘Preliminary evaluation of the Lower Pseudo Reef as a potential Ore Body’. Anglo American Platinum Internal Report.

Stegman, C. (2001) 'How domains envelopes impact the resource estimate-Case studies for the Cobar Gold Field, NSW, Australia', in *Mineral resource and Ore Reserve Estimation - The AusIMM Guide to Good Practice*. Melbourne: The Australasian Institute of Mining and Metallurgy, pp. 221–236.

Stevenson, P. C. A. (2010) 'Anglo American Platinum Datamine Core Menu System'. Anglo American Platinum Internal Report.

Surfer (2016) 'Surfer software help document'. Golden Software, LLC, Golden, Colorado 80401-1866.

Teigler, B. and Eales, H. V. (1993) 'Correlation between chromite composition and PGE mineralization in the Critical Zone of the western Bushveld Complex', *Mineralium Deposita*, 28, pp. 291–302.

Tukey, J. W. (1977) *Exploratory data analysis*. Reading, Mass: Addison-Wesley Pub. Co (Addison-Wesley series in behavioral science).

Vann, J., Jackson, S. and Bertoli, O. (2003) 'Quantitative kriging neighbourhood analysis for the mining geologist - A description of the method with worked case examples', *The Australasian Institute of Mining and Metallurgy*, (5th International Mining Geology Conference, Melbourne), pp. 215–223.

Vermaak, C. (1985) 'The UG2 layer - South Africa's Slumbering Chromitite Giant', *Chromium Review*, (5), pp. 9–22.

Viljoen, M. J., Theron, J. and Underwood, B. (1986) 'The Amandelbult Section of the Rustenburg Mines Limited, with reference to the Merensky Reef', *Mineral Deposits of Southern Africa*, 1 and 2, pp. 1041–1061.

Von Gruenewaldt, G. (1973) 'The Main and Upper Zones of the Bushveld Complex in the Roossenekal area, eastern Transvaal', *Geological Society of South Africa*, 76, pp. 207–227.

Wilson, J. R., Cawthorn, R. and Kruger, F. (1994) 'Intrusive origin for the unconformable Upper Zone in the Northern Gap, western Bushveld Complex', *South African Journal of Geology*, 97(no4), pp. 462–472.

Zapata-Rios, X., Rivero, R. and Goovaerts, P. (2012) 'Spatial and temporal phosphorus distribution changes in a large wetland ecosystem', *Water Resources Research*, 48, pp. 1–15. doi: 10.1029/2011WR011421.

Zientek, M., Causey, D. and Parks, H. (2014) *Platinum-Group Elements in Southern Africa-Mineral Inventory and an Assessment of Undiscovered Mineral Resources*. Scientific Investigations Report 2010-5090-Q. USA: U.S. Geological Survey, p. 126. Available at: http://dx.doi.org/10.3133/sir20105090Q.

APPENDIX

Appendix A: Plan of the orebody thickness, density and platinum Zones

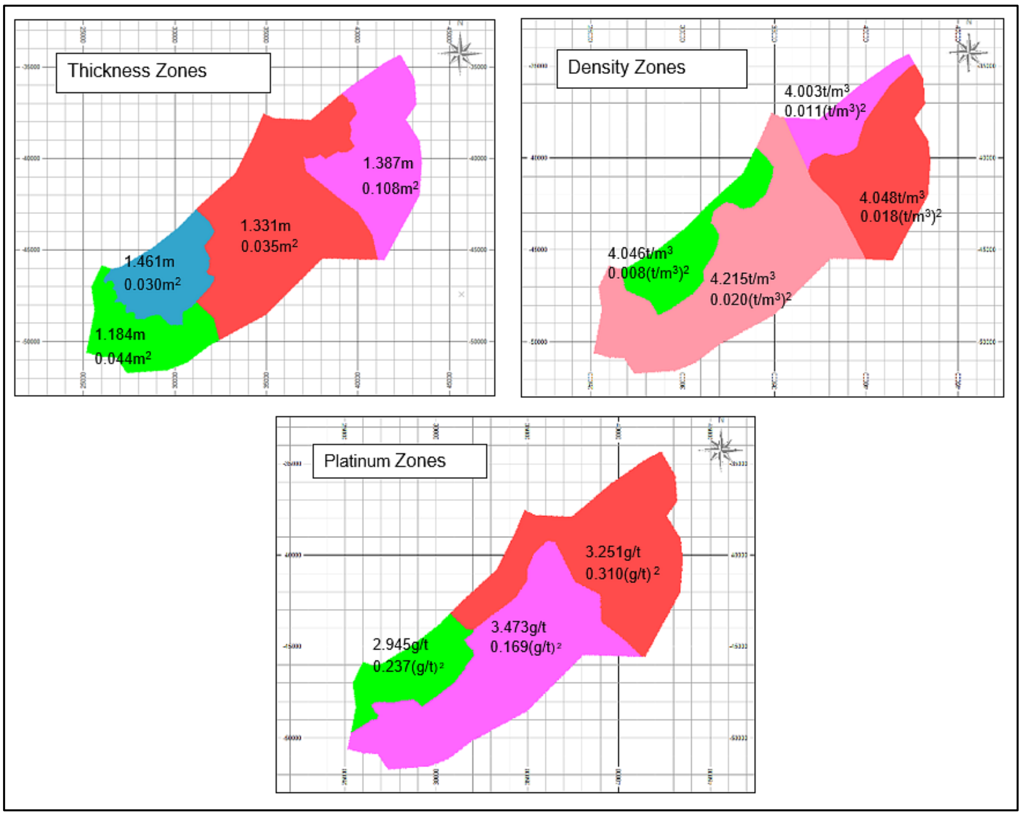

Figure 84: Zones identified for the orebody thickness, density and platinum grade with the respective mean (m) and variance (m^2) of each zone.

Appendix B: Post map plots

Thickness (m)

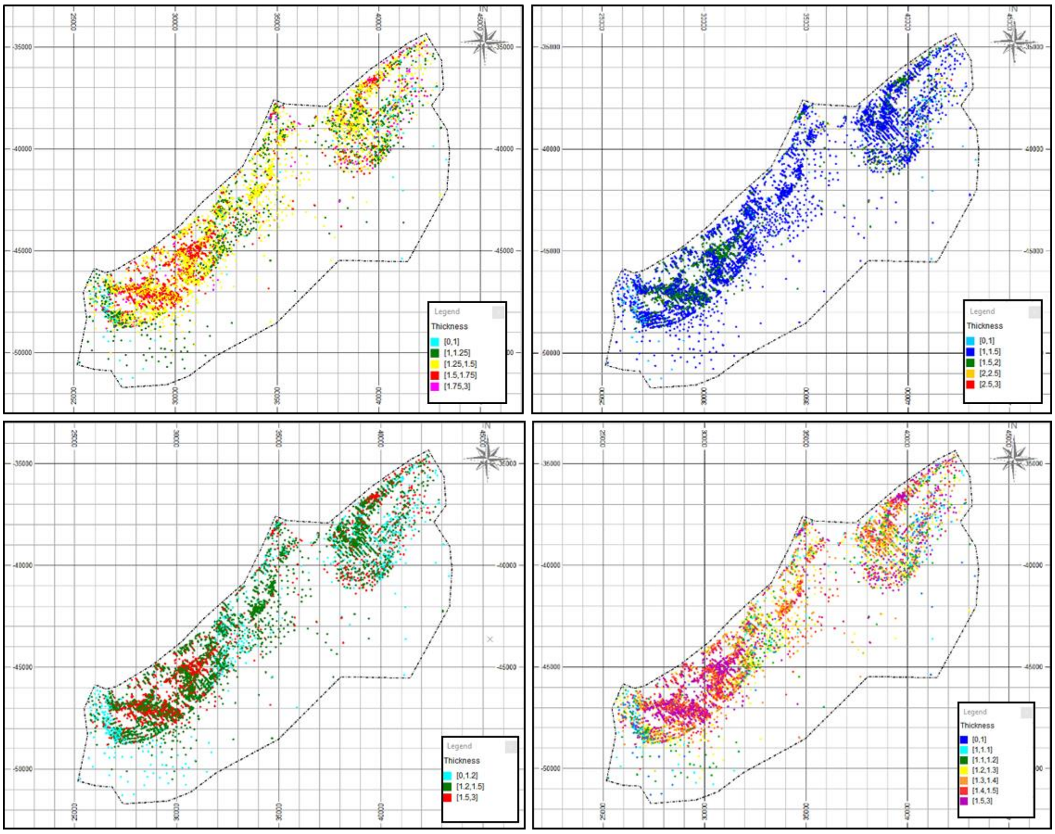

Figure 85: Post maps of the orebody thickness (m) at various intervals.

Density (t/m³)

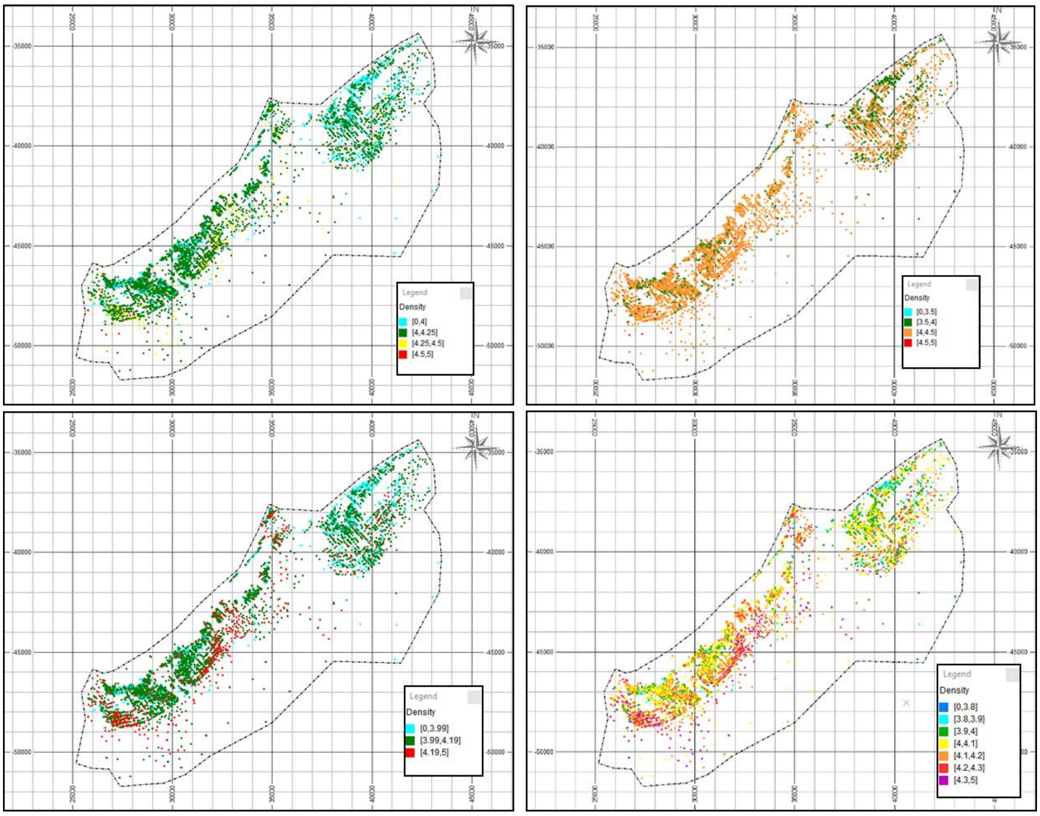

Figure 86: Post maps of the density (t/m³) at various intervals.

Platinum grade (g/t)

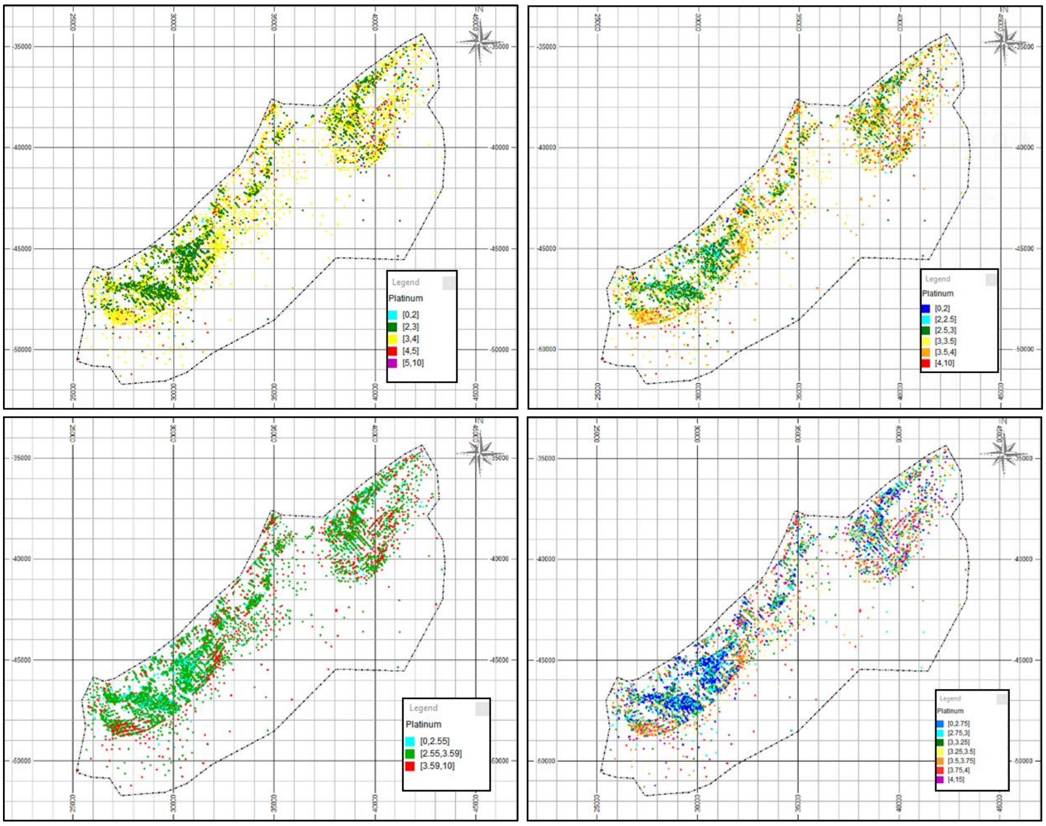

Figure 87: Post maps of the platinum grade (g/t) at different intervals.

Appendix B: True values versus estimated values scatter plots for individual zones

Thickness Zones

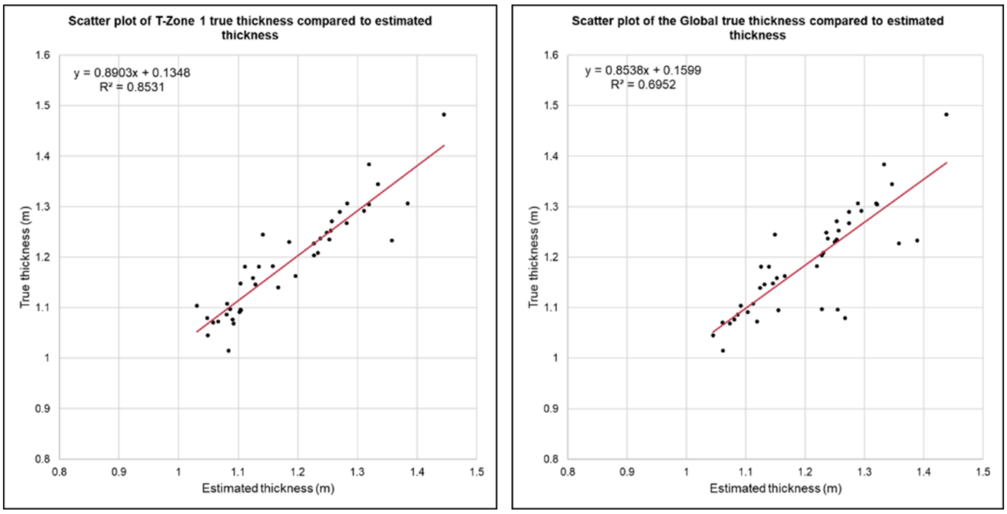

Figure 88: Scatter plot of the true values and estimated values using T-Zone 1 variogram (a) and Global variogram (b).

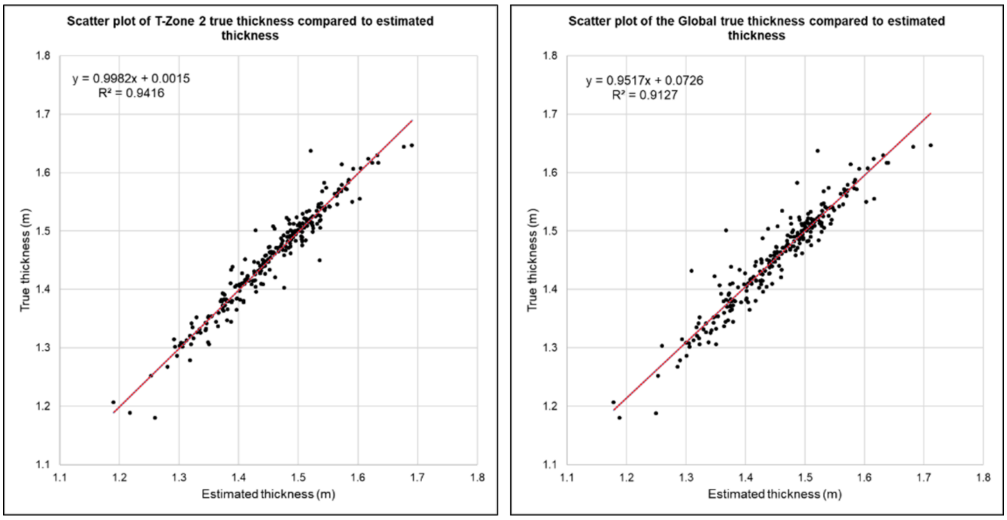

Figure 89: Scatter plot of the true values and estimated values using T-Zone 2 variogram (a) and using the Global variogram (b).

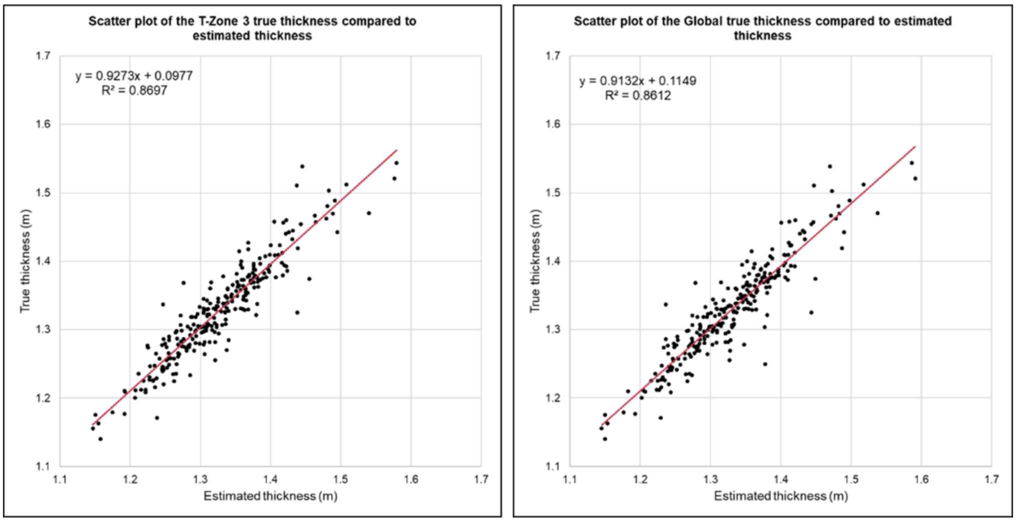

Figure 90: Scatter plot of thickness the true values and estimated values using T-Zone 3 variogram (a) and using the Global variogram (b).

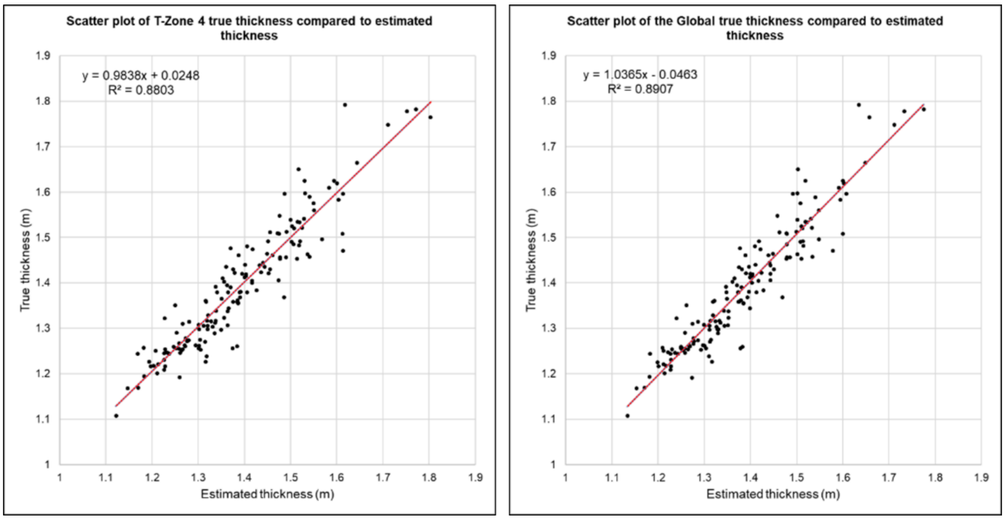

Figure 91: Scatter plot of the thickness true values and estimated values using T-Zone 4 variogram (a) and using the Global variogram (b).

Density Zones

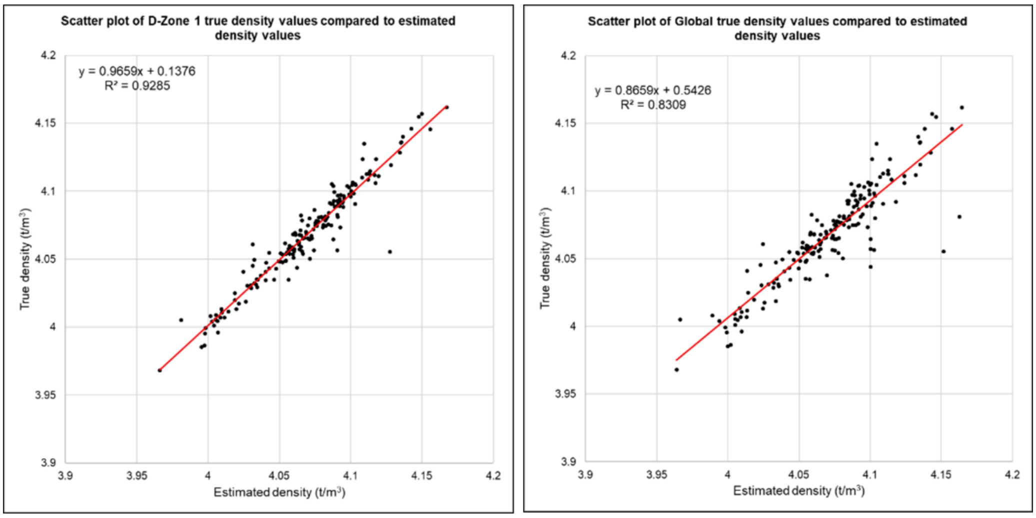

Figure 92: Scatter plot of the density true values and estimated values using D-Zone 1 variogram (a) and using the Global variogram (b).

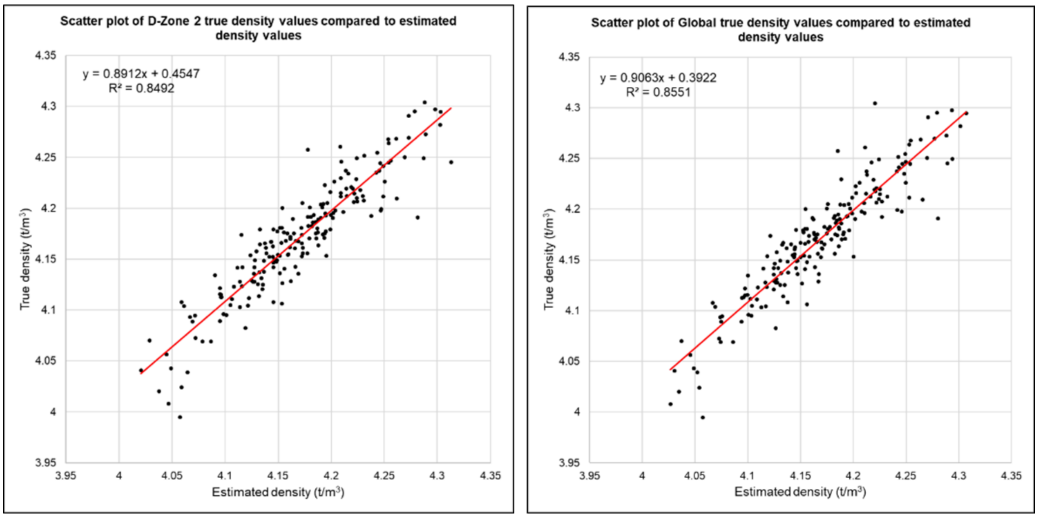

Figure 93: Scatter plot of the density true values and estimated values using D-Zone 2 variogram (a) and using the Global variogram (b).

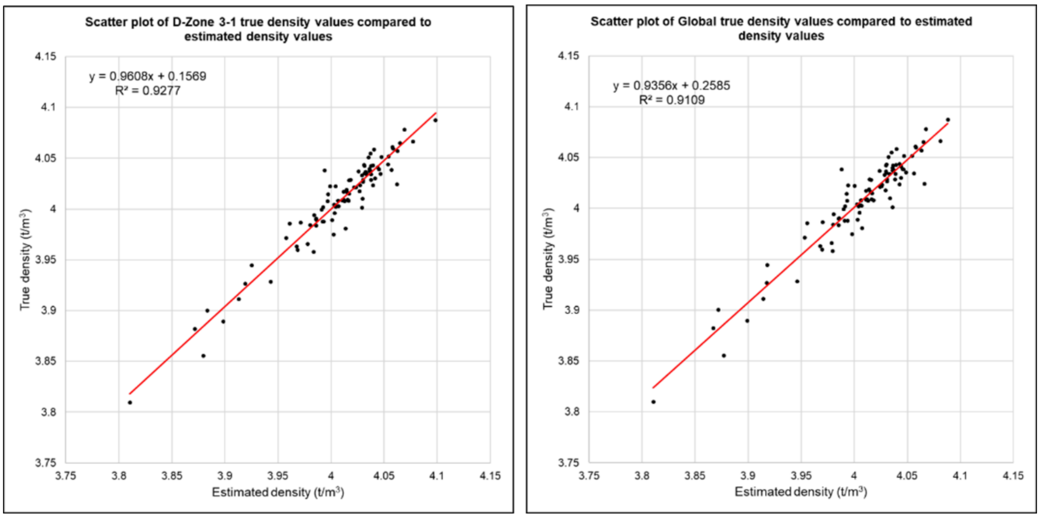

Figure 94: Scatter plot of the density true values and estimated values using D-Zone 3-1 variogram (a) and using the Global variogram (b).

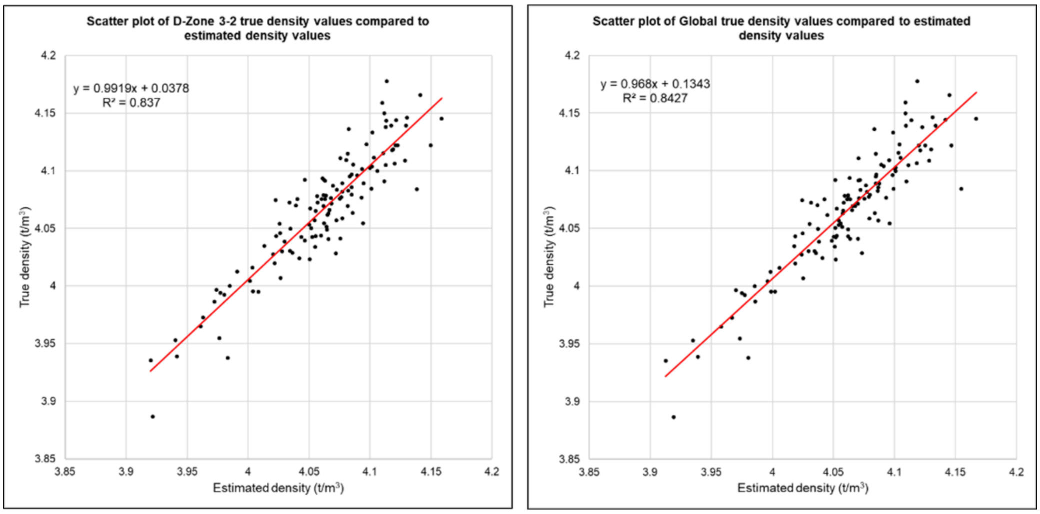

Figure 95: Scatter plot of the density true values and estimates values using D-Zone 3-2 variogram (a) and using the Global variogram (b).

Platinum Zones

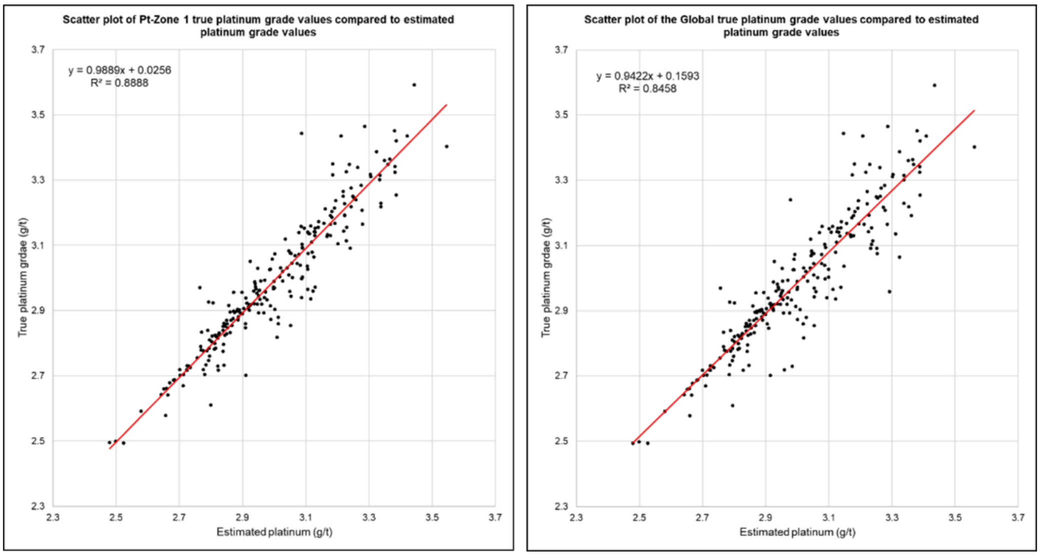

Figure 96: Scatter plot of the platinum grade true values and estimated values using Pt-Zone 1 variogram and using the Global variogram (b).

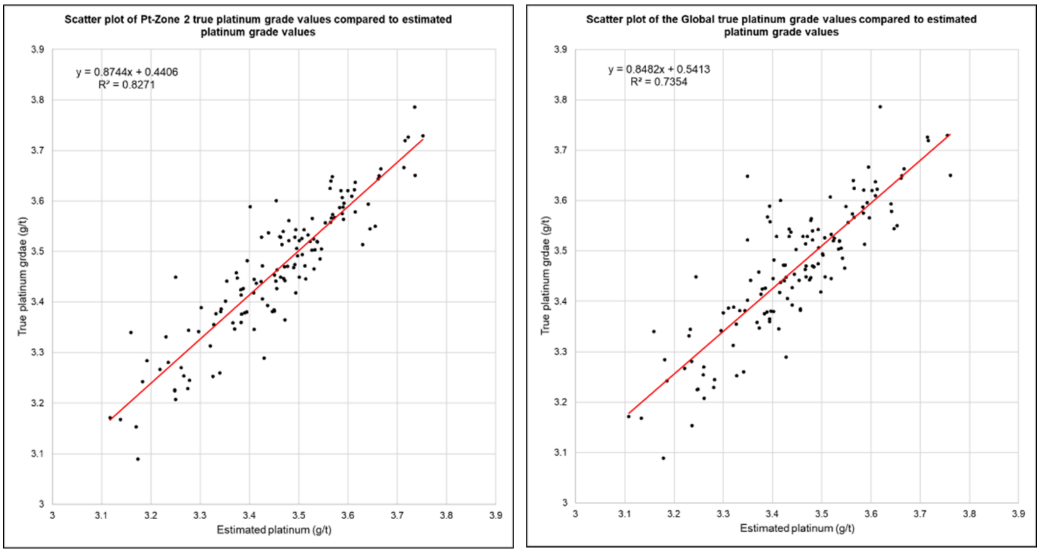

Figure 97: Scatter plot of the platinum grade true values and estimated values using Pt-Zone 2 variogram and using the Global variogram (b).

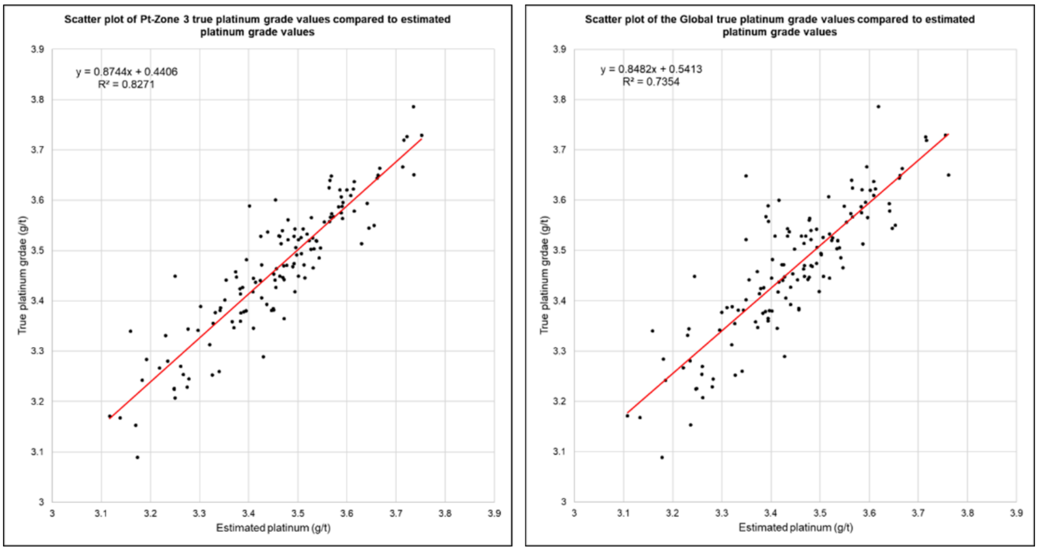

Figure 98: Scatter plot the platinum grade true values and estimated values using Pt-Zone 3 variogram and using the Global variogram.